CMB -II

(3K radiation)

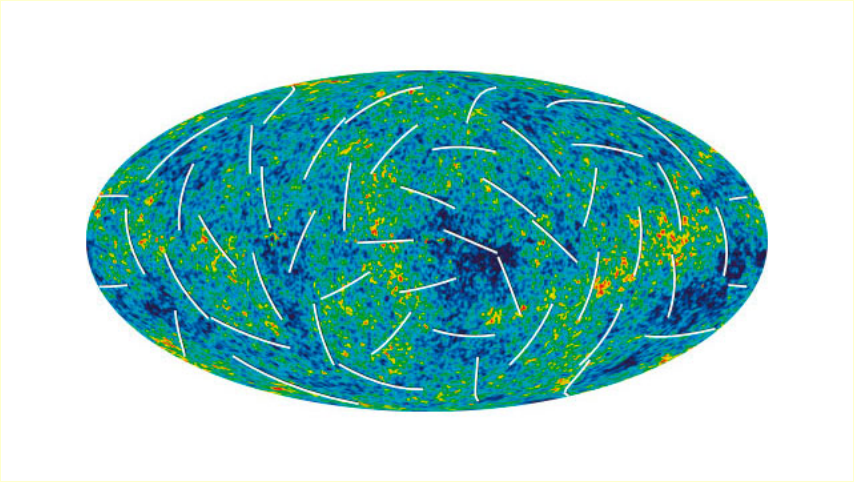

- Polarization

  [plots+idea: Hu&White (1997) New Astronomy, 2, 323]

- Secondary anisotropy

Electron scattering

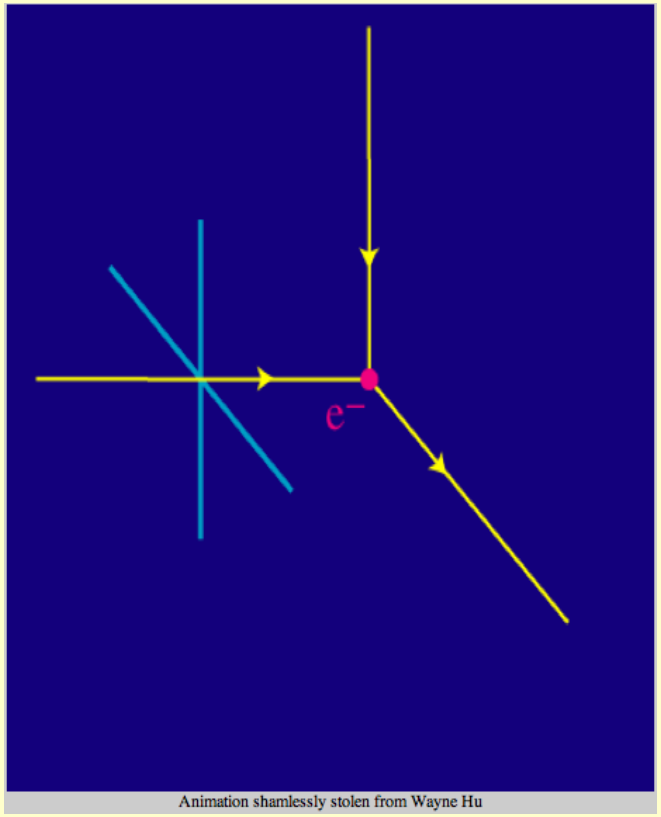

Unpolarized radiation

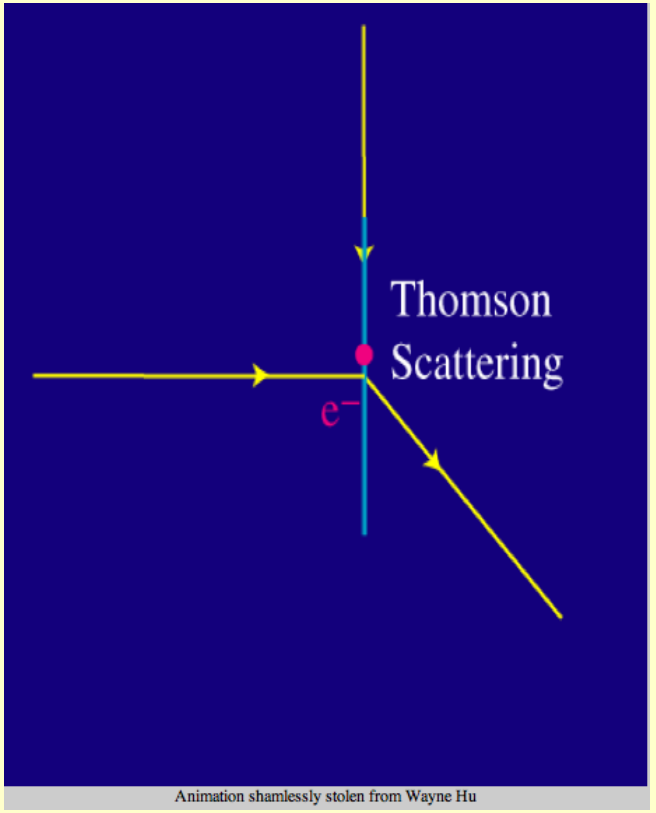

excited electron

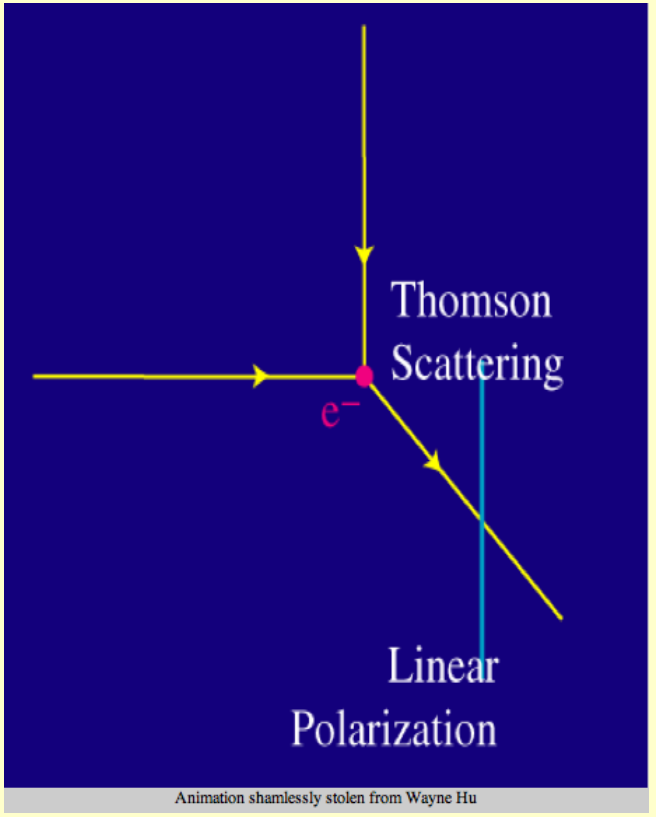

perpendicular scaterring

Line of sight (LOS) is perpendicular to the original direction of wave propagation → only the component perpendicular to the LOS can propagate toward the observer (EM waves are transverse)

(Schematic: the amplitude of scattered wave is much lower than the original)

Electron scattering

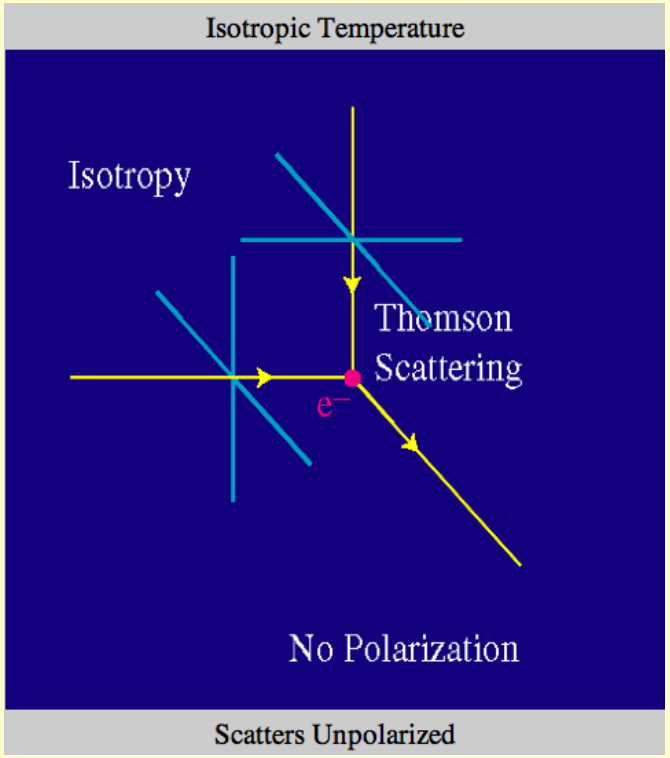

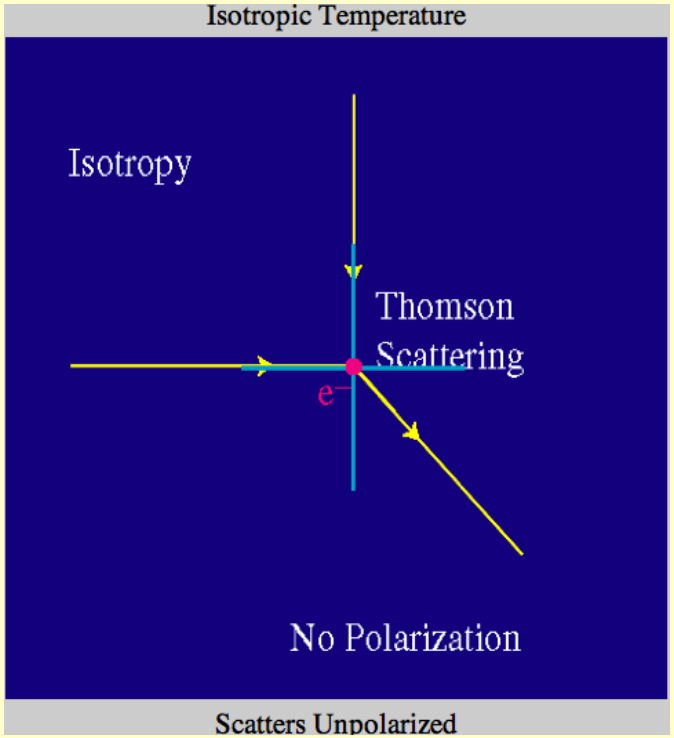

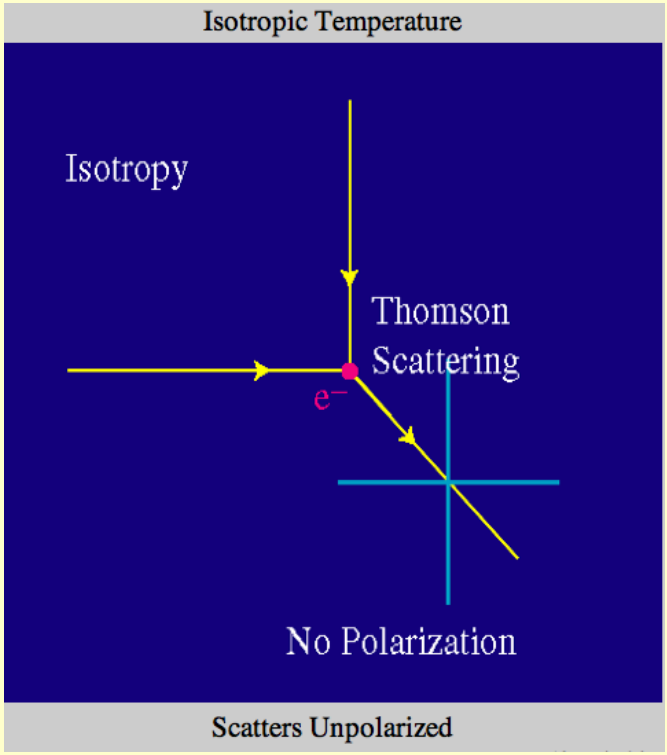

Two unpolarized waves excited electron scattered: half + half

Wave from the left "supplies" vertically polarized radiation, wave from the top "supplies" horizontally polarized radiation.
Incident radiation is isotropic → both scattered components have equal amplitudes → scattered radiation is not polarized

Electron scattering

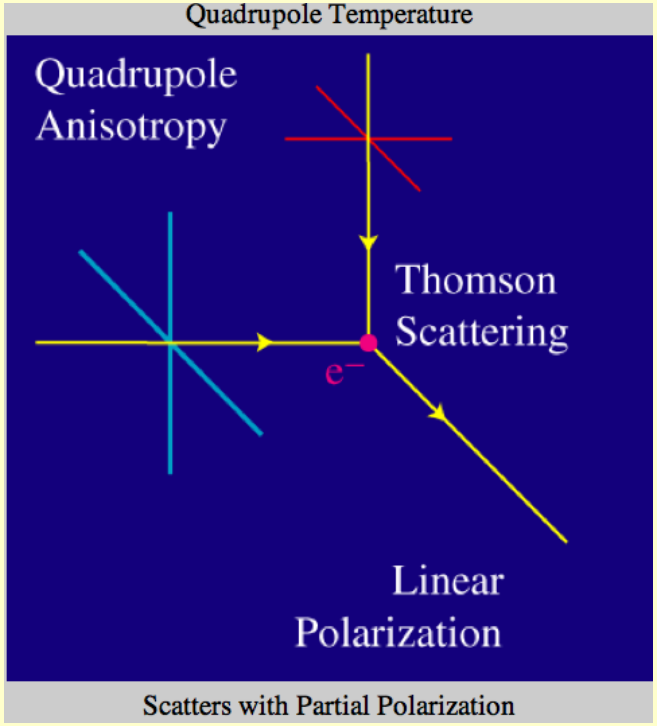

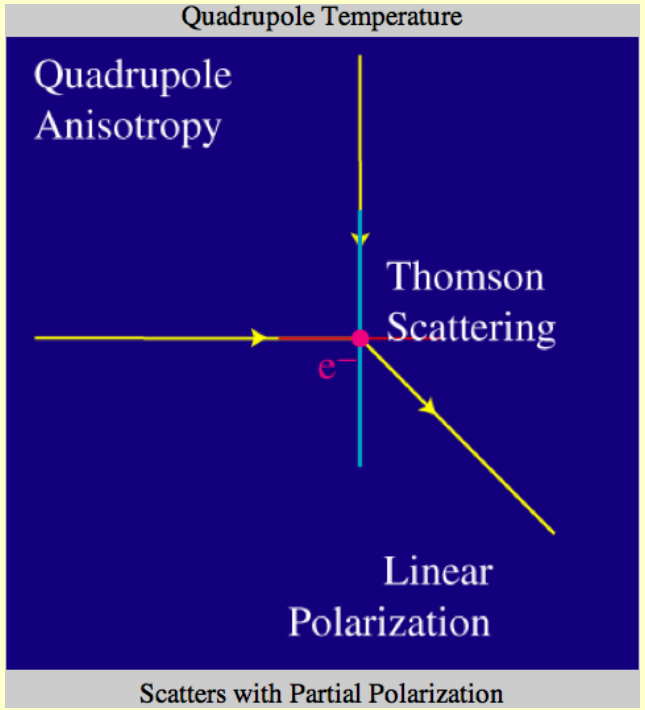

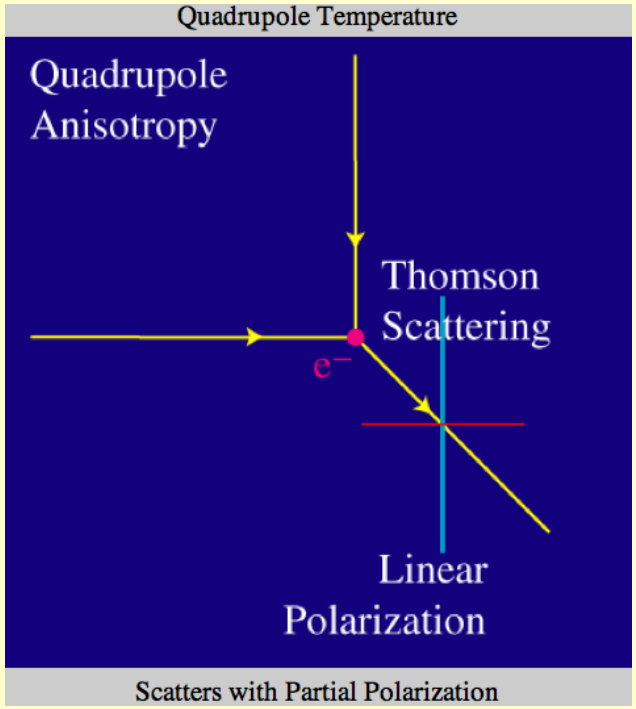

Two unpolarized waves excited electron scattered: unequal

Wave from the left "supplies" vertically polarized radiation, wave from the top "supplies" horizontally polarized radiation.
Wave from the top has lower amplitude → horizontal component of scattered radiation is weaker → scattered radiation is partially polarized

Scalar perturbation

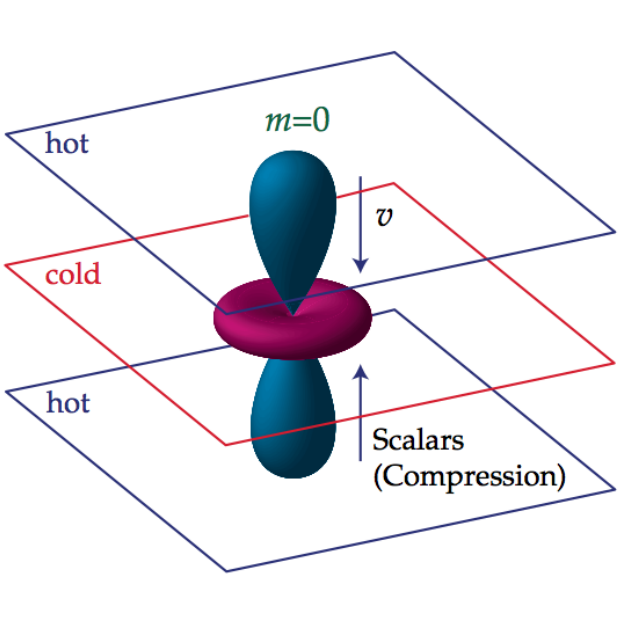

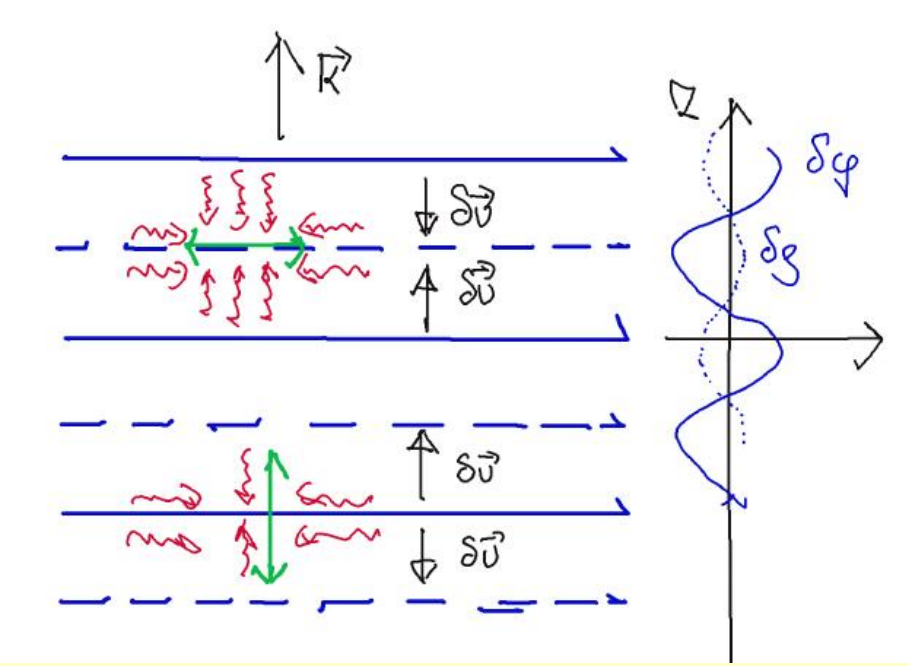

We consider a long wave perturbation, so the amplitude of potential perturbations is higher than for the density → at potential minima matter is denser than in the surroundings, and a local termometer would say the temperature is higher then elsewhere. Distant observer would say the region is colder than its surroundings; a local observer would also say the surroundings are hotter. This is due to the prevailing effect of gravitational redshift. So: on the wave-front of potential minimum there are more photons coming from the directions of potential maxima (along the wave-vector) than from perpendicular directions → emitted radiation is partially polarized in the direction perpendicular to the stronger flux of photons, or in direction perpendicular to the wave-vector. And opposite: polarization is perpendicular to wavefronts of potential maxima.

Scalar perturbations

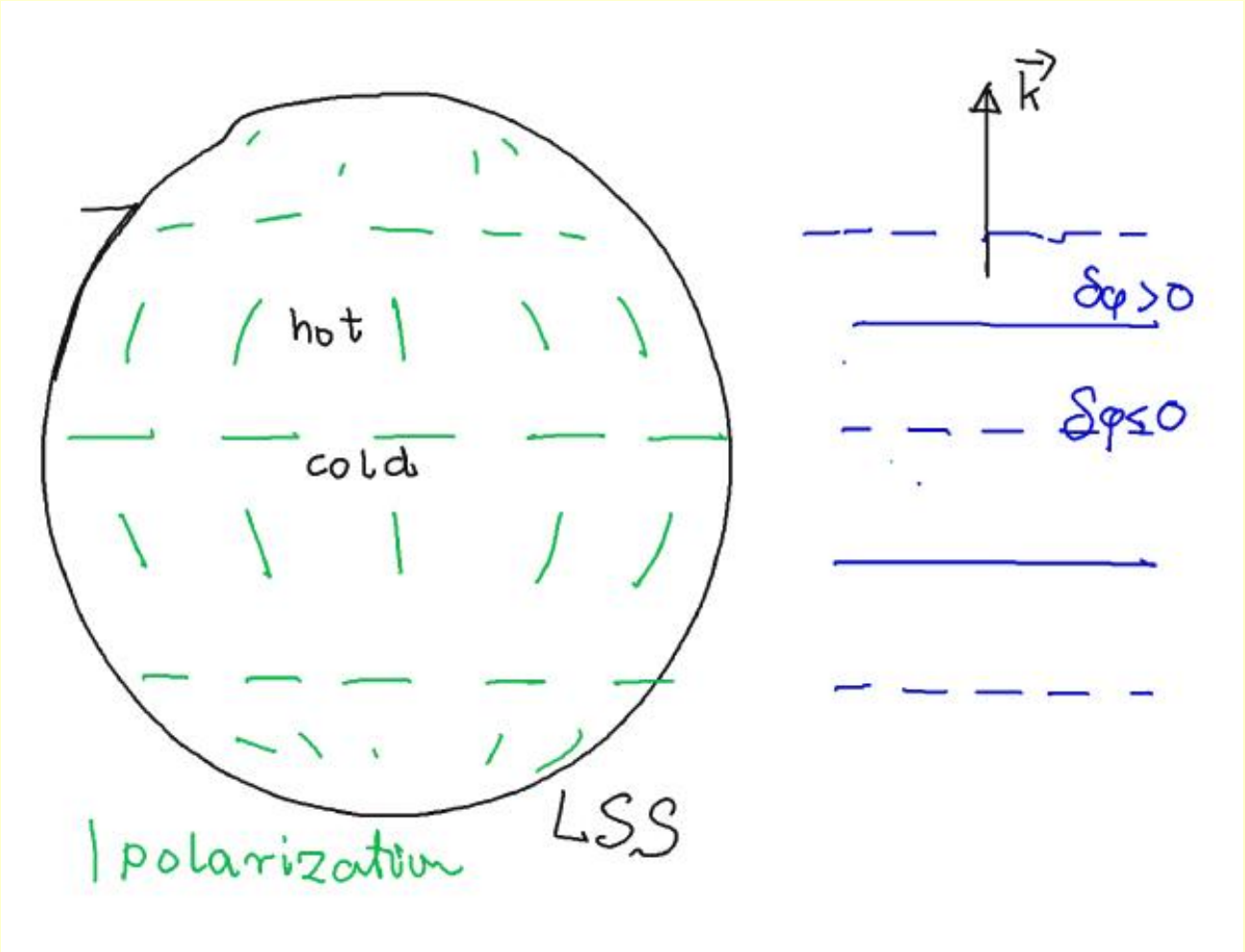

Direction of polarization on the sky due to a single long scalar wave (in green). On the side: positions of the potential wave fronts (in blue). (There is only ONE plane component, cold/hot places have a form of long stripes and it is easy to say what is parallel/perpendicular. On real CMB sky it is more complicated.

Scalar perturbations

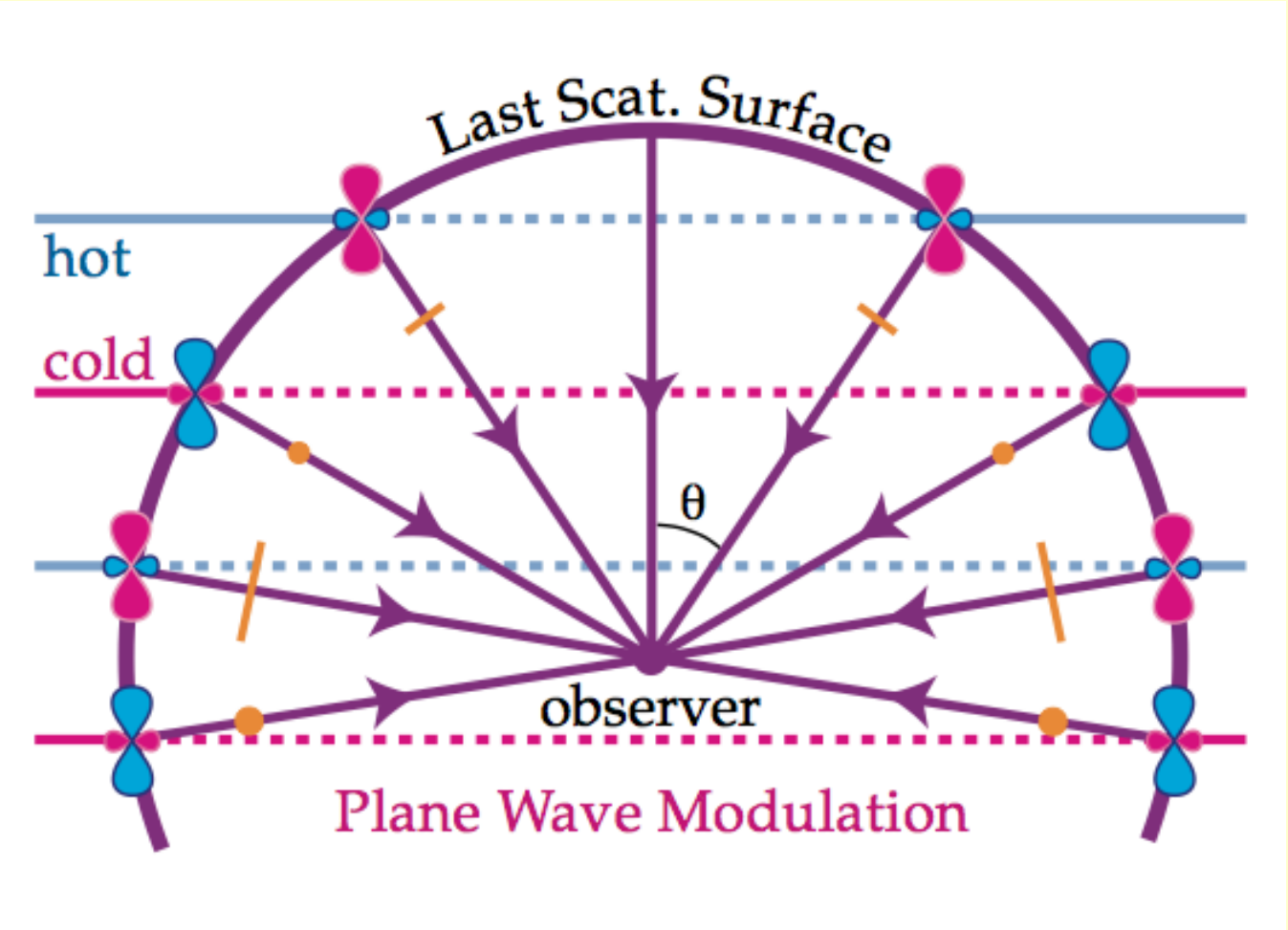

Single scalar plane wave with *lambda*=1/3 of the LSS diameter. Polarization is constant along each parallel and changes in the same way along meridians: its direction changes between E-W and N-S depending on the wave phase. The amplitude depends on sin *theta* due to the projection effects.

Single scalar wave

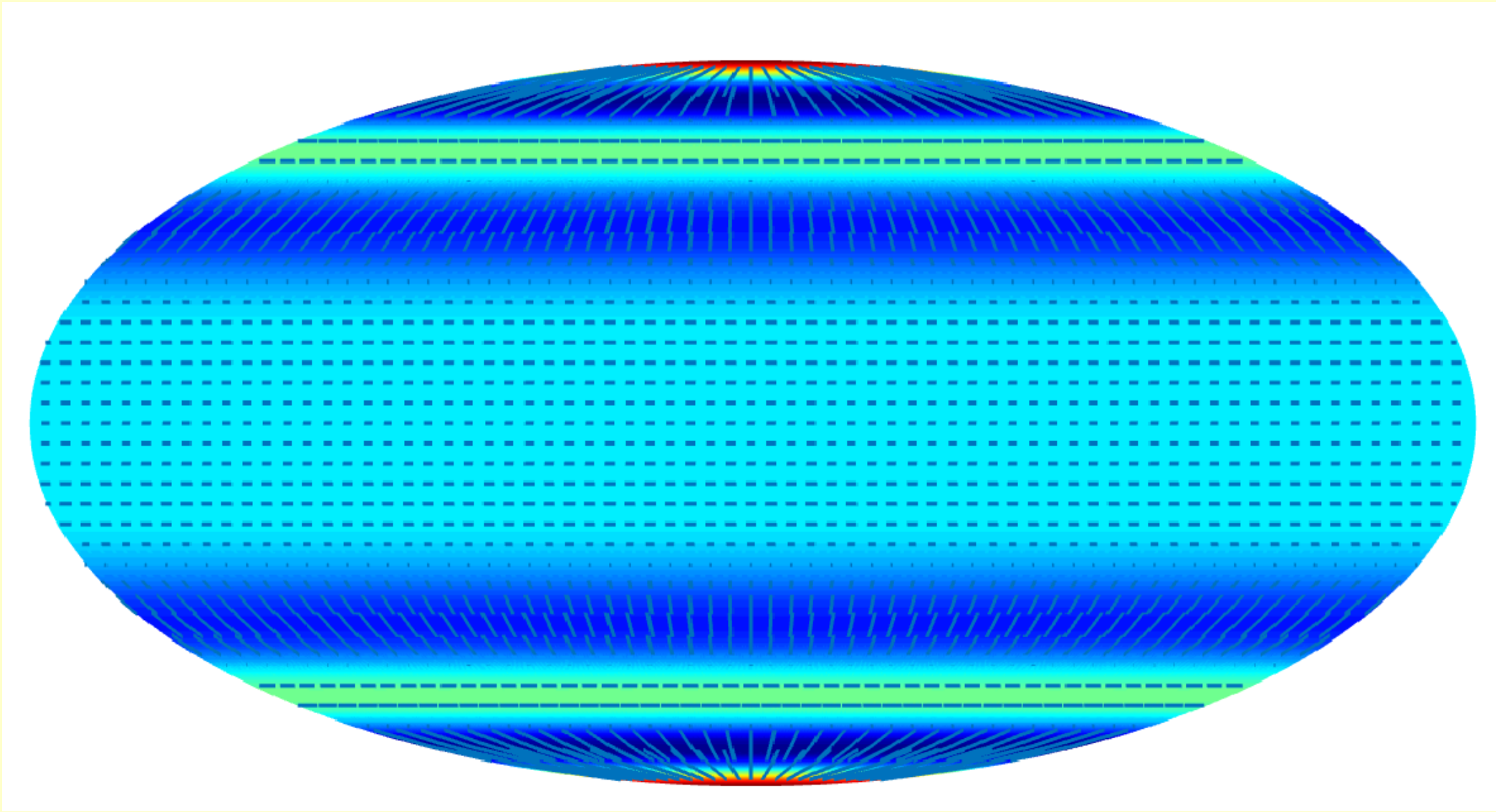

[Kamionkowski & Kovetz, arXiv:1510.06042]

Vector perturbations (vortices)

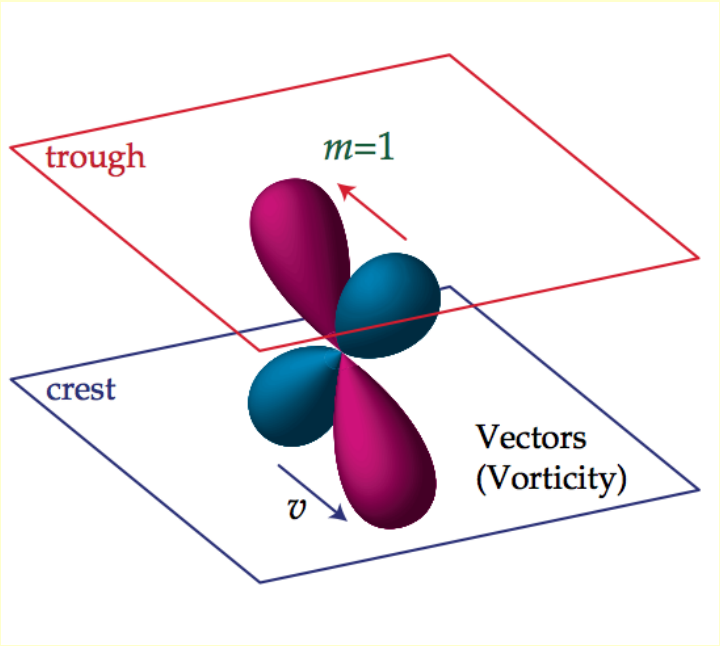

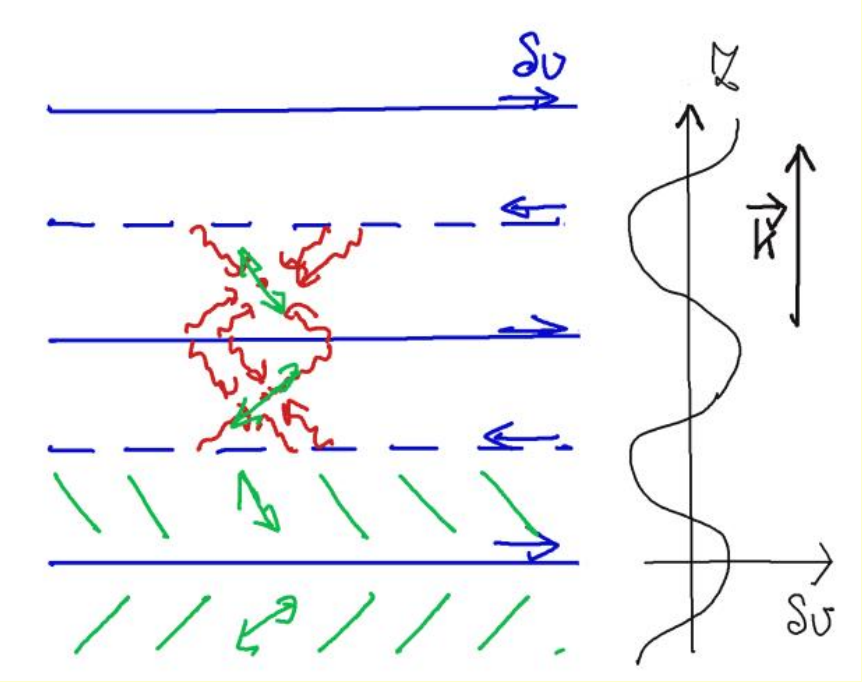

Vector perturbations are possible. If they existed during the recombination they might be imprinted in CMB fluctuations ...

There are more photons coming from places approaching the scattering region than from places receding. Direction of polarization is perpendicular to the direction of maximal photon intensity as shown.

In the picture line of sight is perpendicular to the wave-vector and to the velocity vector.

Vector perturbations (vortices)

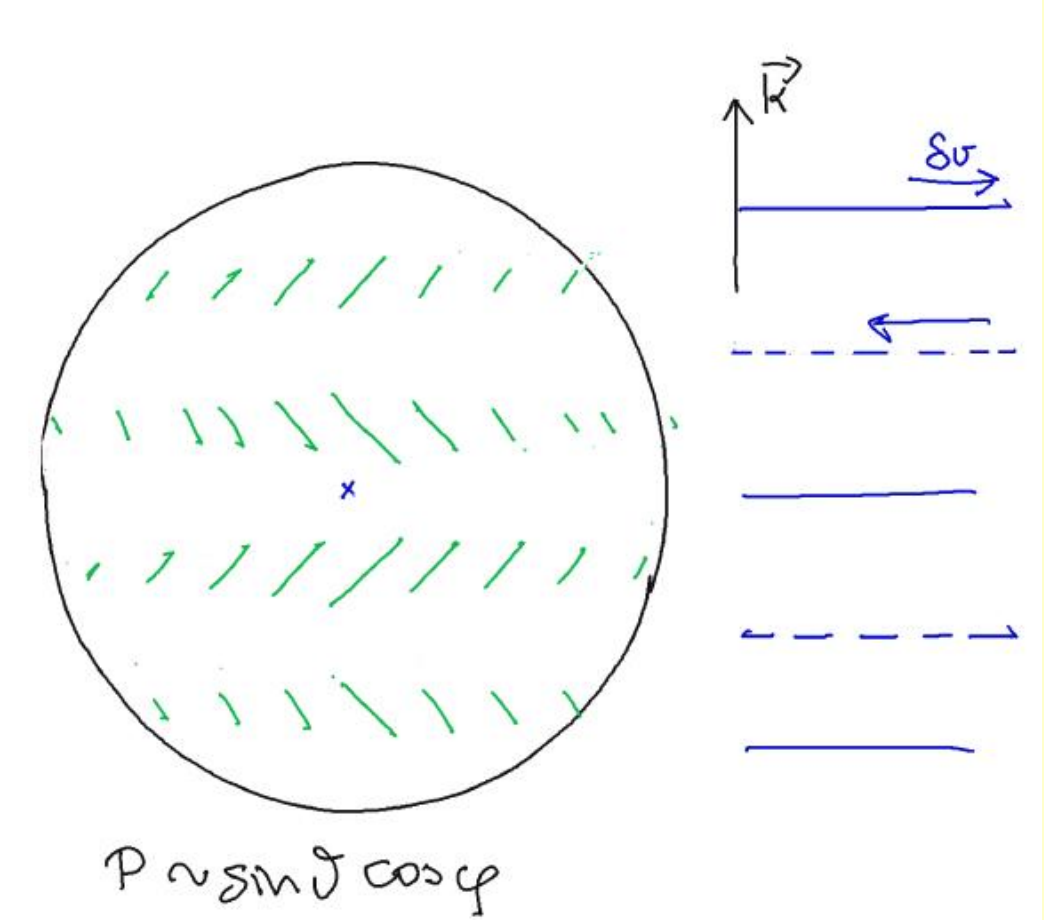

Maximum polarization is possible for observers looking from a direction perpendicular to the wave-vector and to the velocity vector (above: close to the center of the picture). Velocity projection introduces ~cos *phi* dependence. Wave vector projection introduces ~sin *theta* dependece. (There is also wave-phase modulation ~exp(i*k**chi***mu*) .)

Tensor perturbations (gravitational waves)

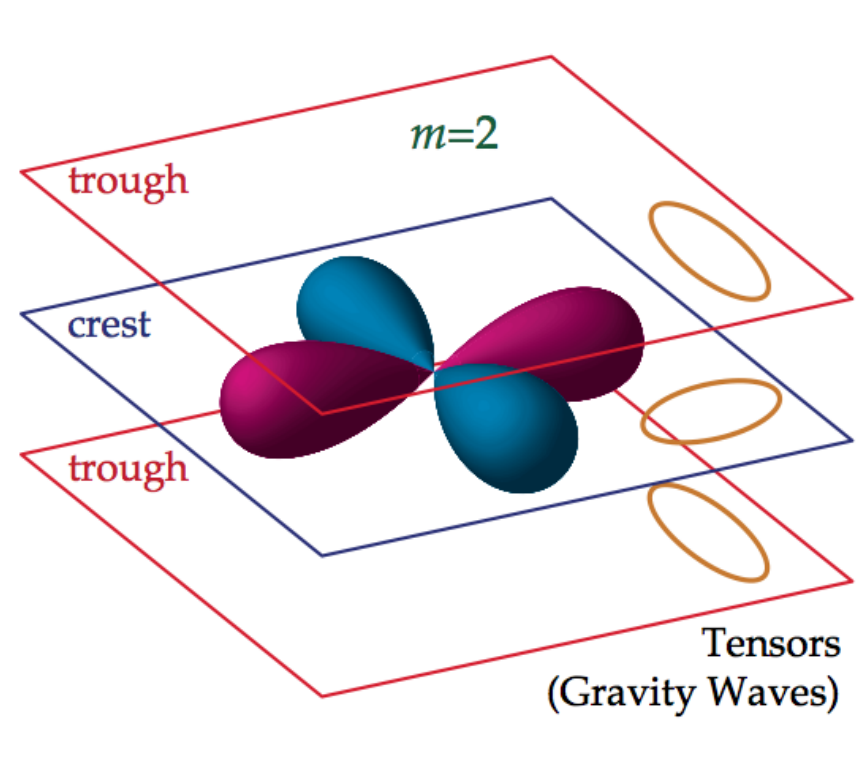

If such perturbations existed during the recombination they might leave their imprint in CMB polarization pattern ...

A tensor wave induces motion of matter in plane perpendicular to its wave vector. Suppose **k** is along z-axis and at the crest matter moves toward increasing $|x|$ and decreasing $|y|$. As a consequence there is a quadruple moment in photon gas, more of them coming from both directions along the y-axis and less coming along the x-axis. The number of photons approaching any location along the z-axis is everywhere the same. Depending on the location on the LSS that may produce polarization with different directions and amplitudes.

Tensor perturbations (gravitational waves)

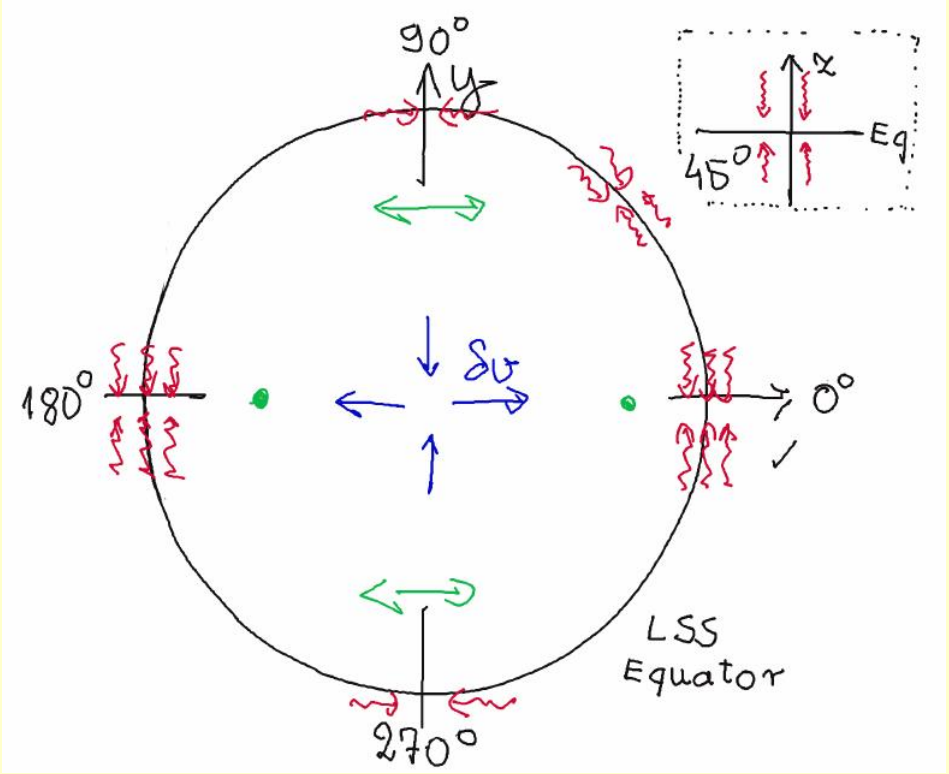

A tensor wave induces motion of matter in plane perpendicular to its wave vector. Suppose **k** is along *z*-axis and at the crest matter moves toward increasing |*x*| and decreasing |*y*|. Above the case when the wave crest plane is also equatorial plane of the observer. At 0 deg and 180 deg on the LSS there is enhanced flux of photons from E-W directions as compared to N-S (shown schematically at the upper right corner) → polarization is perpendicular to the direction of enhanced flux or N-S.
When moving toward 45 deg the enhancment in E-W direction goes to zero and there is no polarization at this point. Between 45-90 deg there is E-W polarization with maximum amplitude at 90 deg. Longitude dependence ~cos 2*phi* .

Single tensor wave

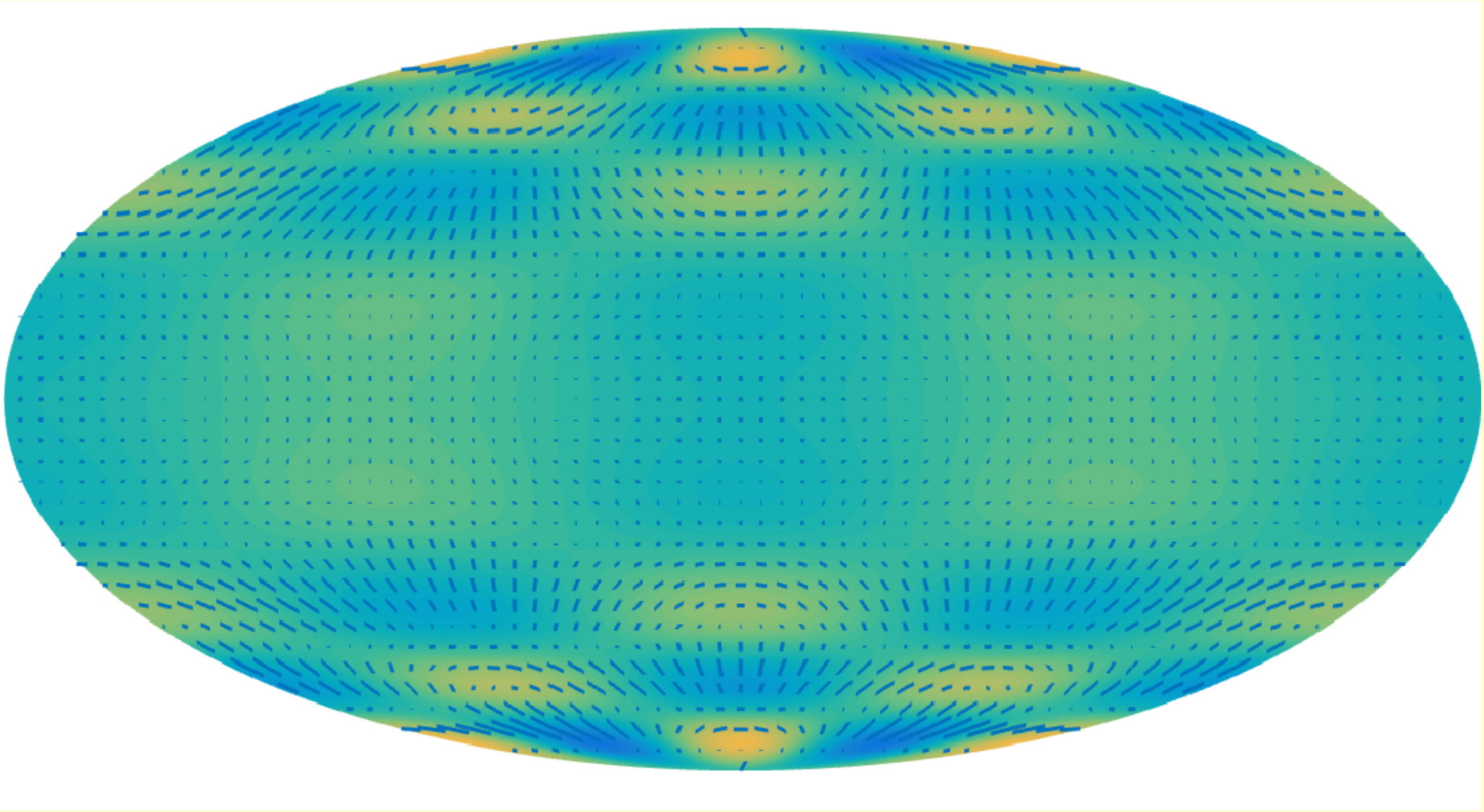

Tensor perturbation. Polarization changes along parallels and along meridians.
Both E-mode and B-mode are present

[Kamionkowski & Kovetz, arXiv:1510.06042]

Single hot spot (long waves)

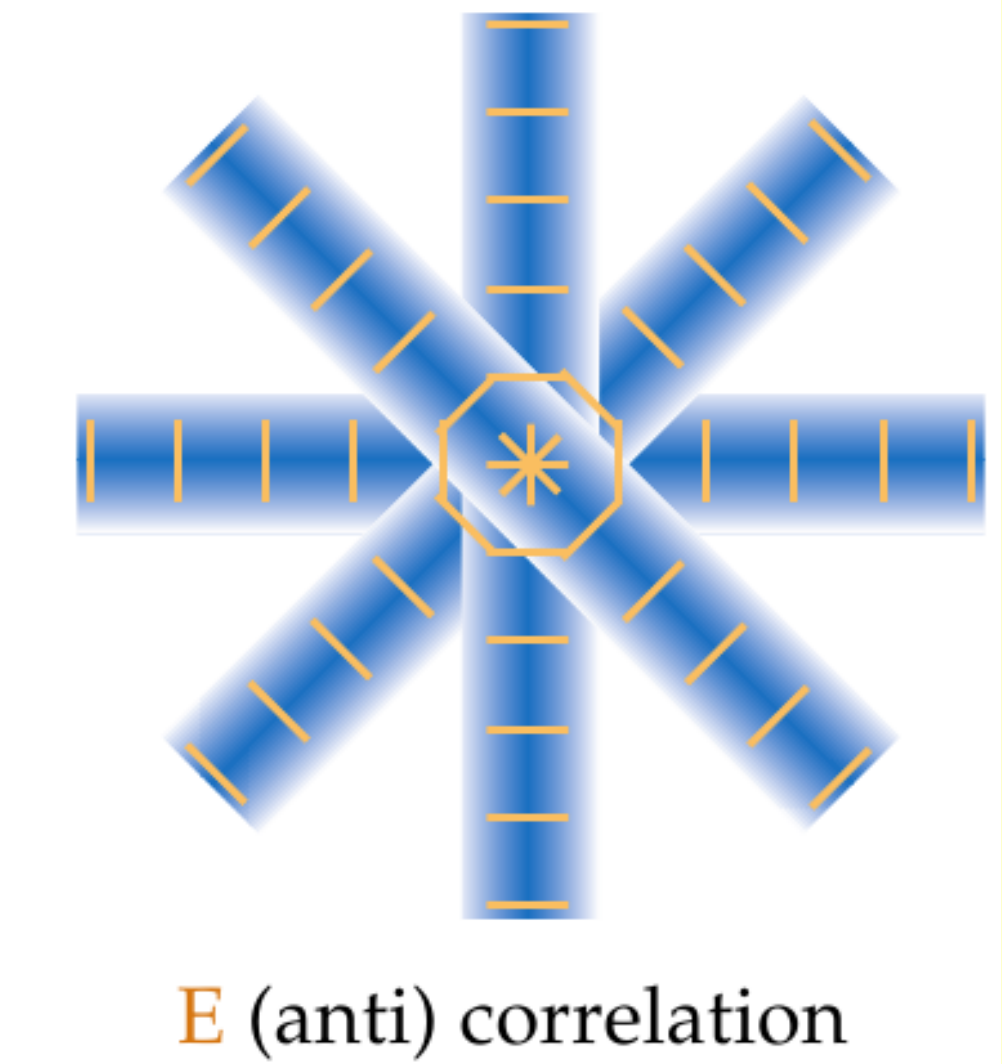

Hot spot constructed from 4 crossing crests of scalar waves.
Polarization makes characteristic pattern around the spot.

E-mode around a cold/hot spot

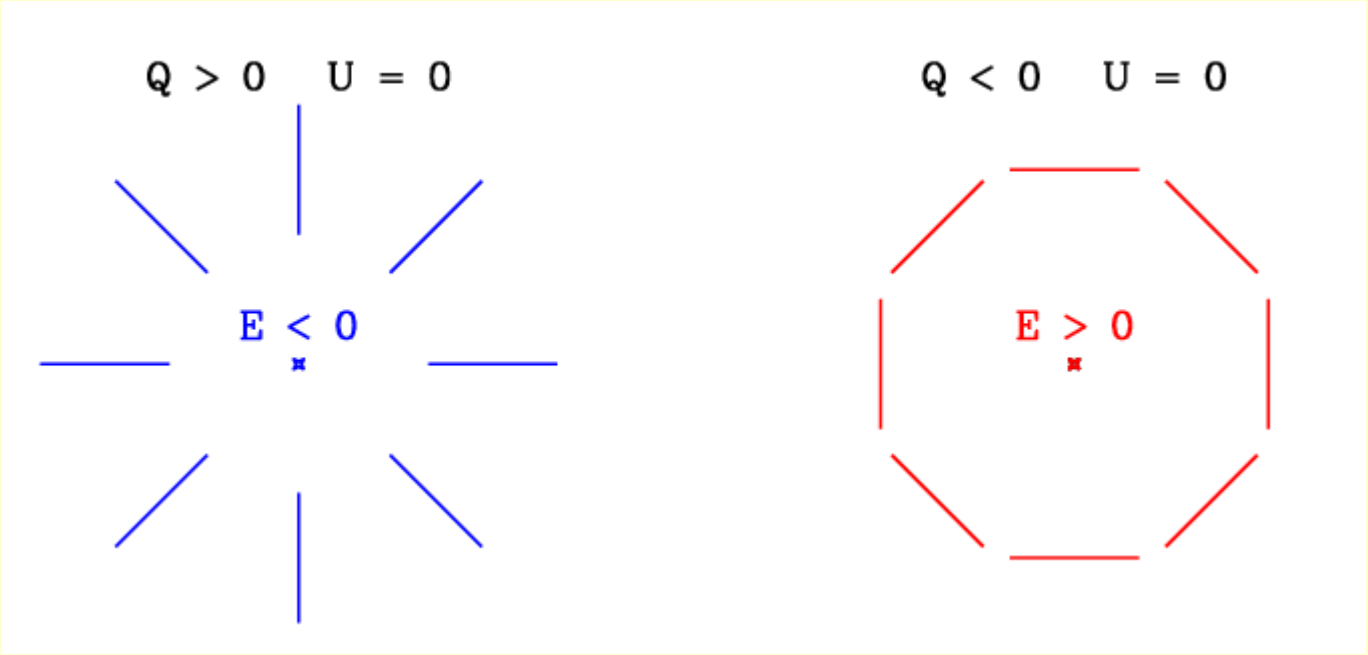

In the case of cold spot (left) polarization pattern is different. The above patterns are so called mode E. Scalar perturbations can only produce E-mode polarization, which is correlated with the temperature fluctuations. (Q, U -Stokes parameters).

Single vortex

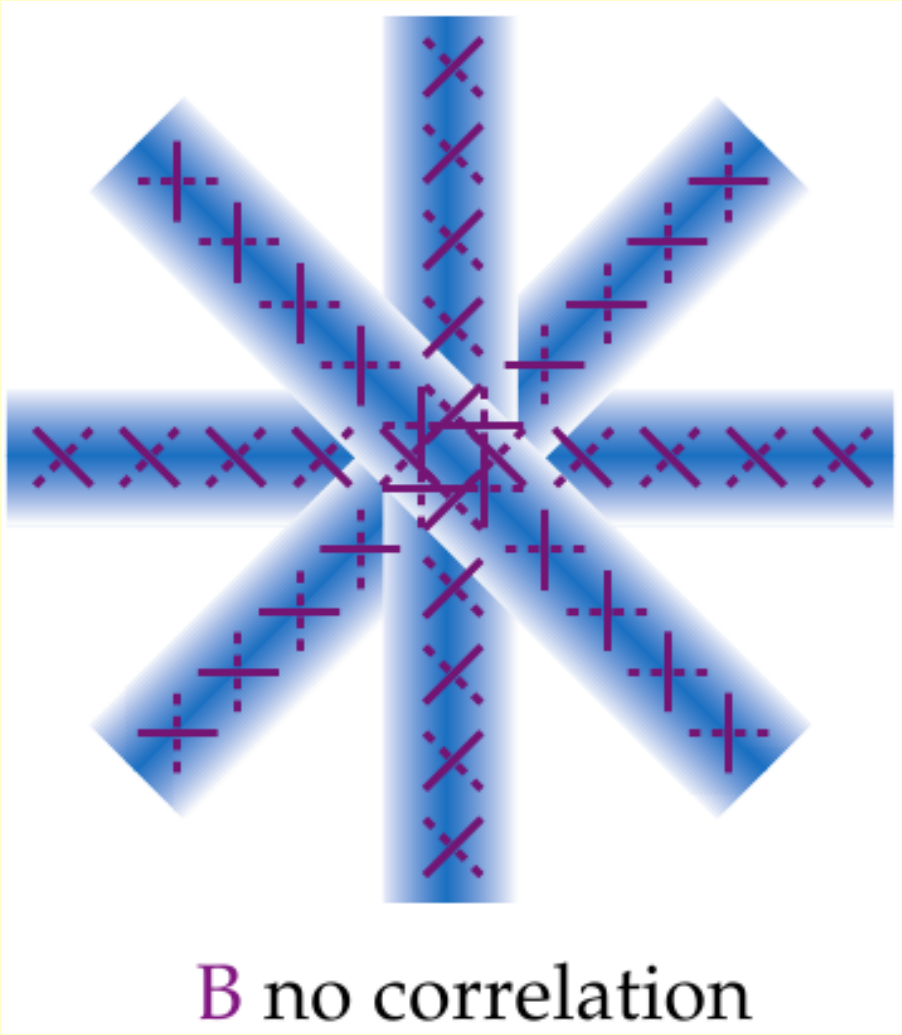

A vortex constructed from 4 crossing crests of vector waves gives a characteristic pattern of polarization around it which is of the B type

B-mode around a vortex

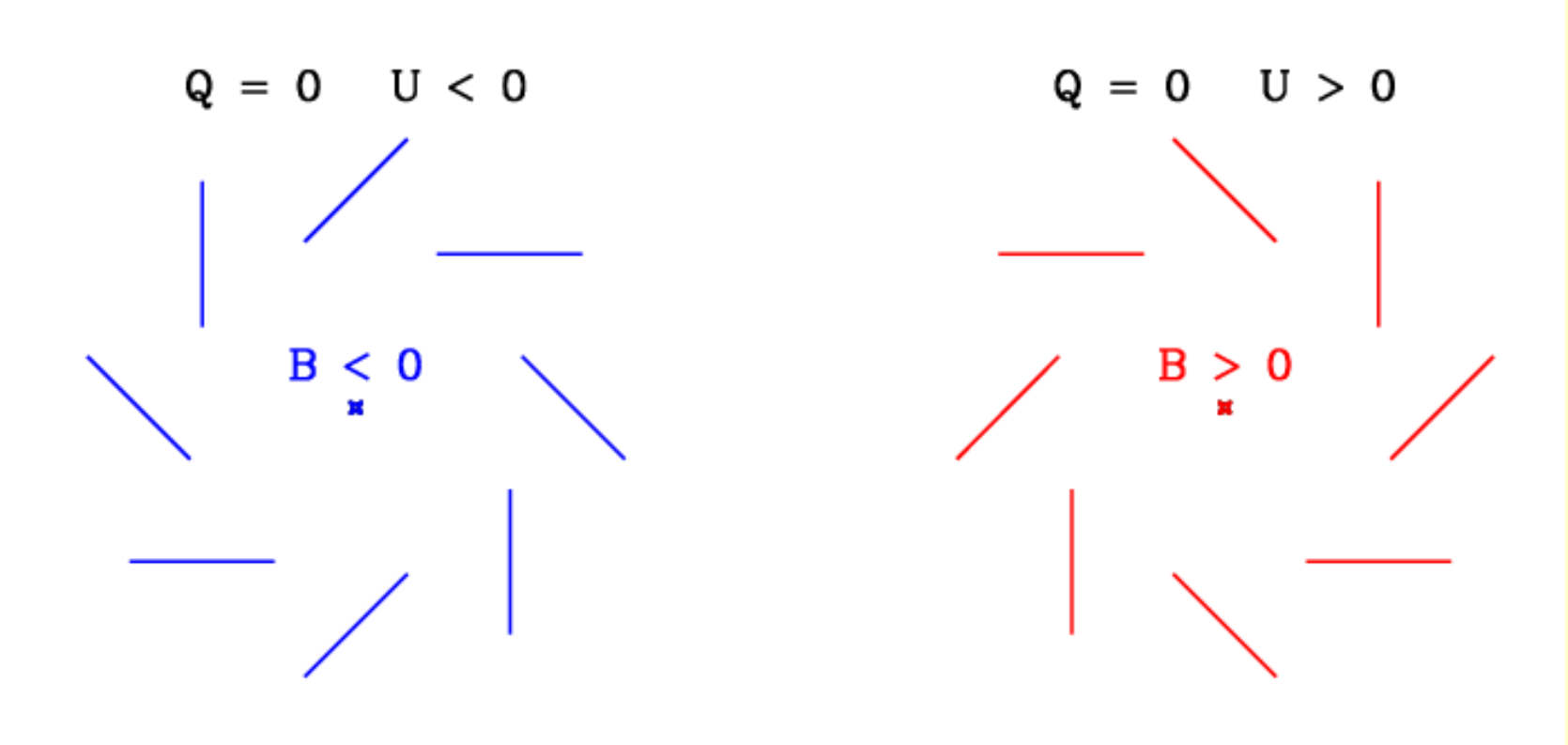

Polarization directions are at 45 deg to crests of vector waves and make characteristic patterns around a vortex called B-mode

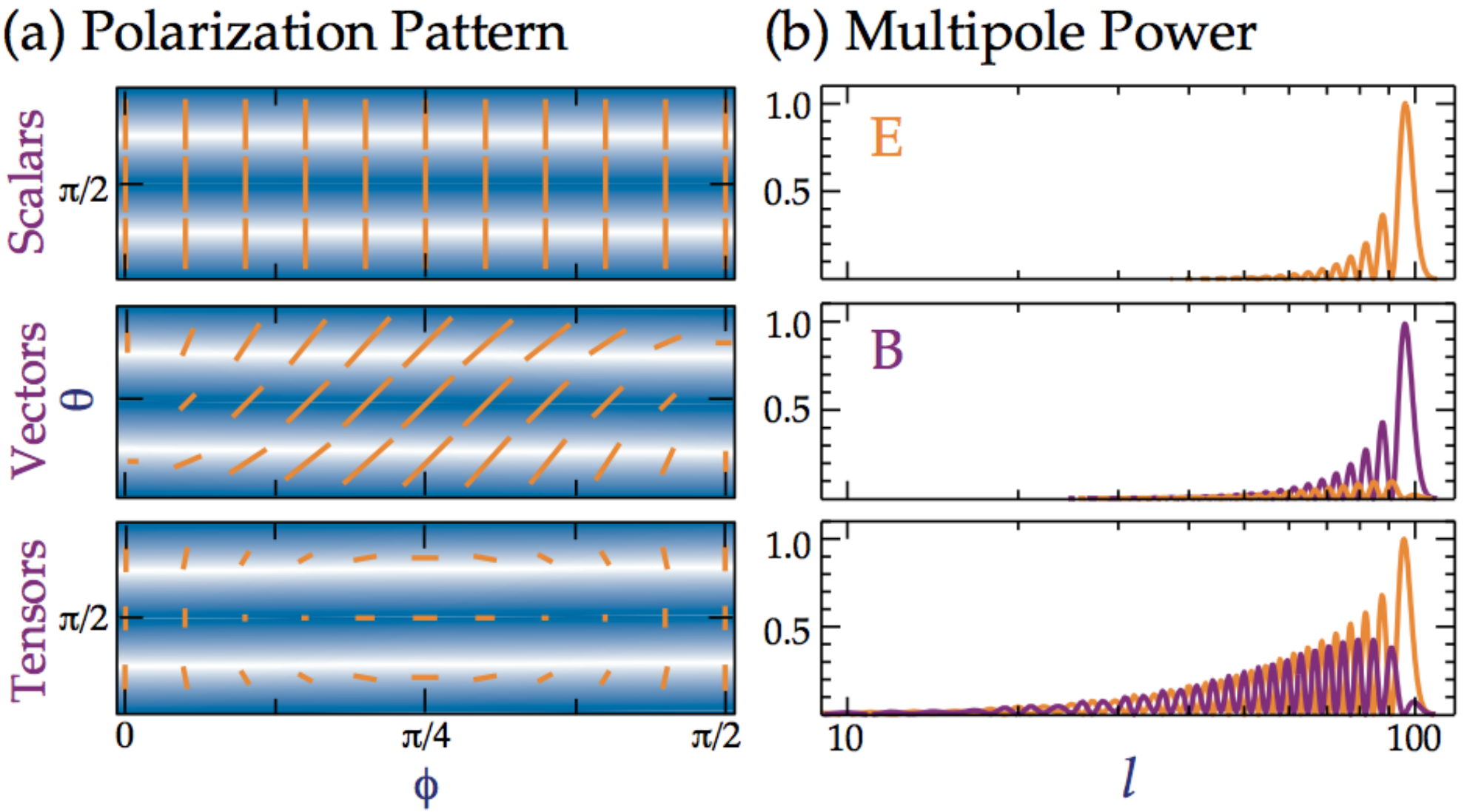

(a) Polarization maps for a single plane wave for different kinds of perturbations; (b) corresponding power spectra for E and B polarization for a wave with kr=100. Density perturbations can only produce E-mode.

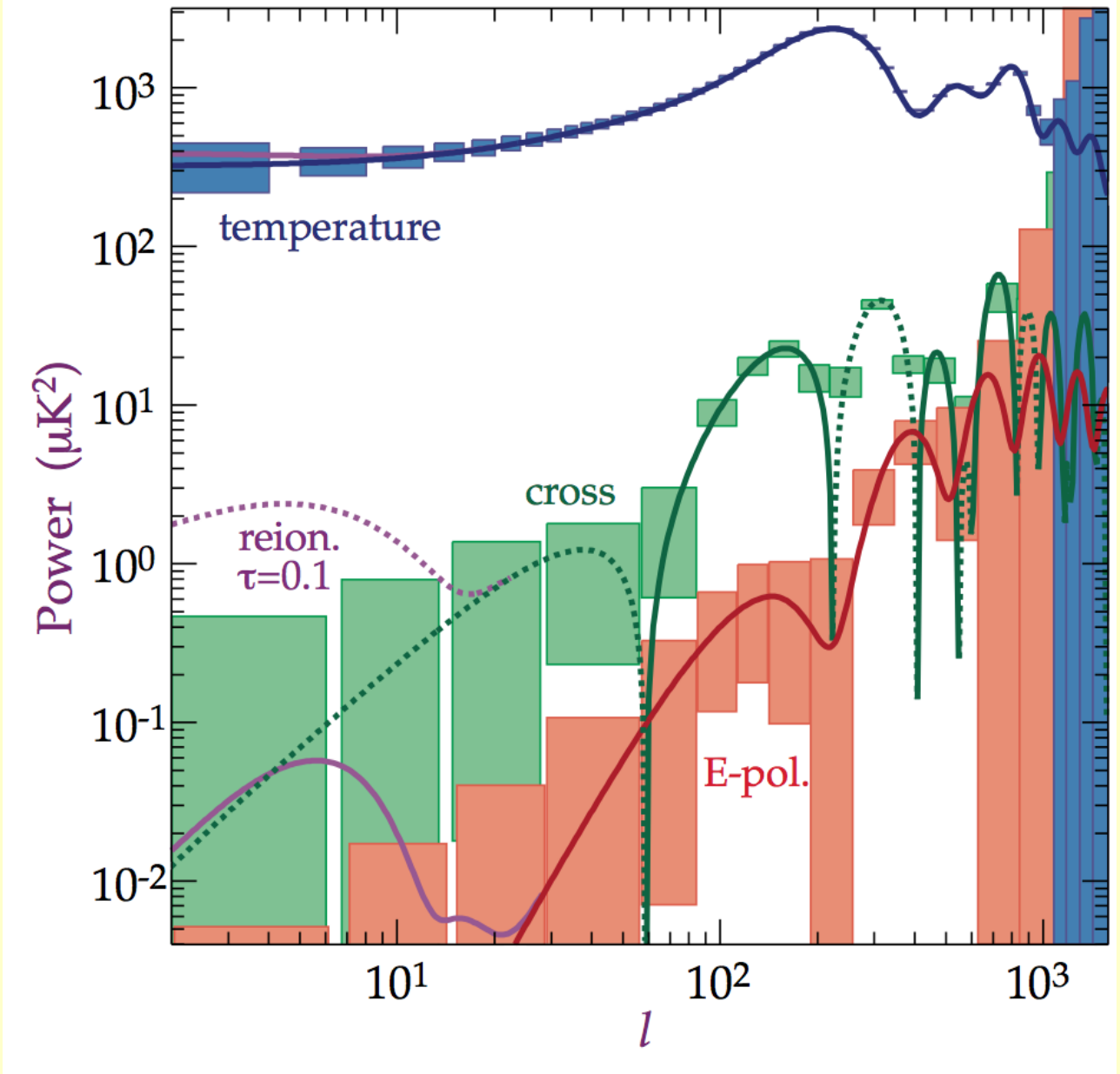

(Expectations 1997) Temperature anisotropy power spectrum (blue), power spectrum for E-mode (red), their correlation (green). Taking into account secondary fluctuations related to scattering after re-ionization (violet).

The first measurement: DASI

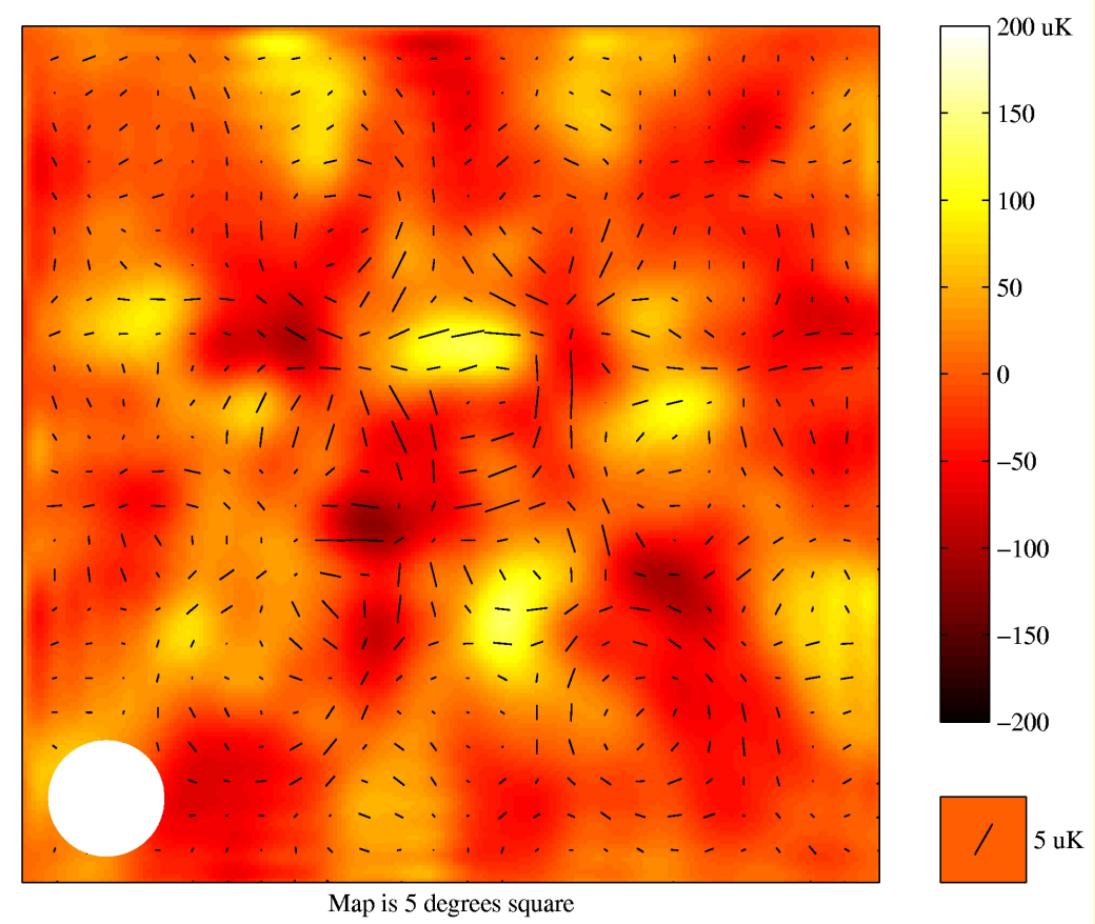

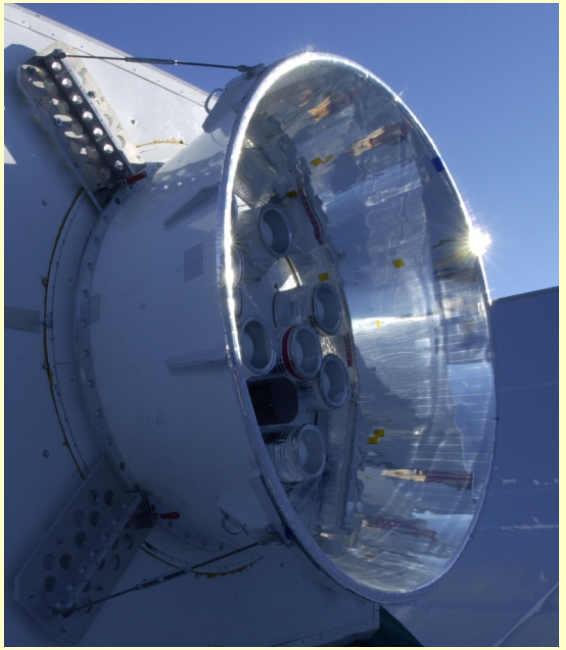

DASI (Biegun Płd.)

An image of the intensity and polarization of the cosmic microwave background radiation made with the Degree Angular Scale Interferometer (DASI) telescope. The small temperature variations of the cosmic microwave background are shown in false color, with yellow hot and red cold.

[Kovac i in. (2002) Nature, 420, 772]

The first measurement: DASI

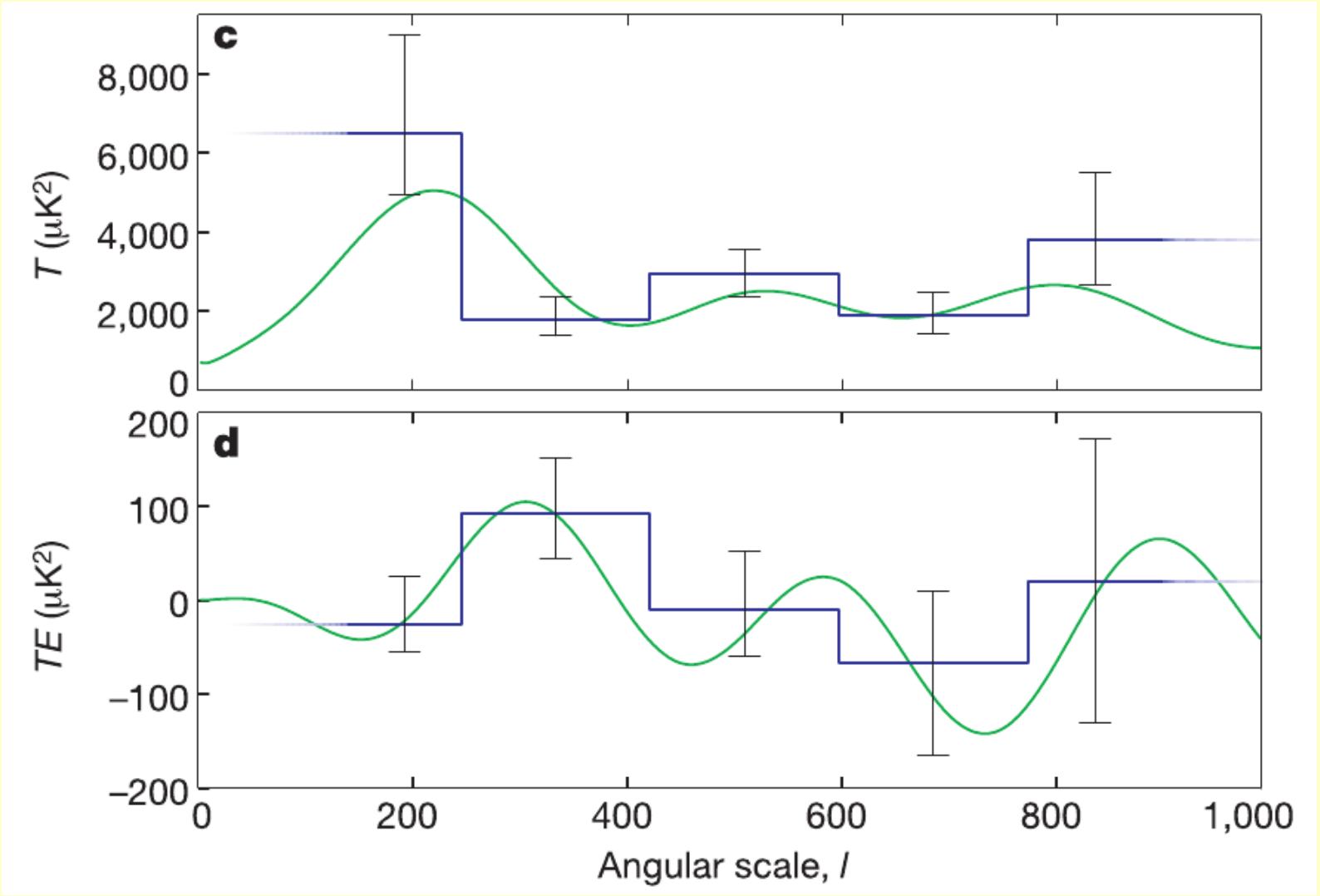

Anisotrotropy spectrum of temperature fluctuations and its correlation with E-component of polarization

[Kovac i in. (2002) Nature, 420, 772]

WMAP 3y

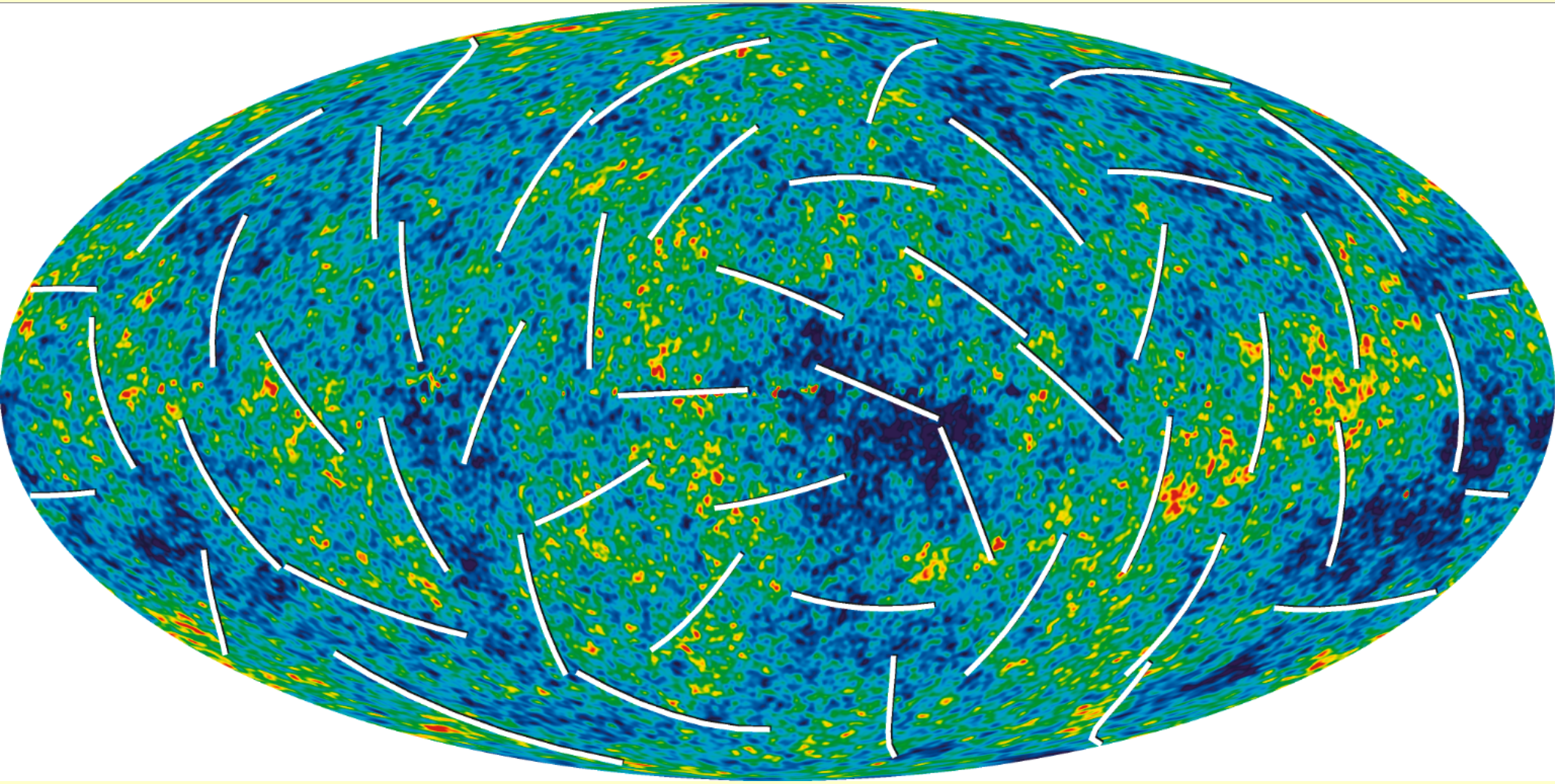

CMB temperature and polarization after 3y WMAP observations.

WMAP 7y

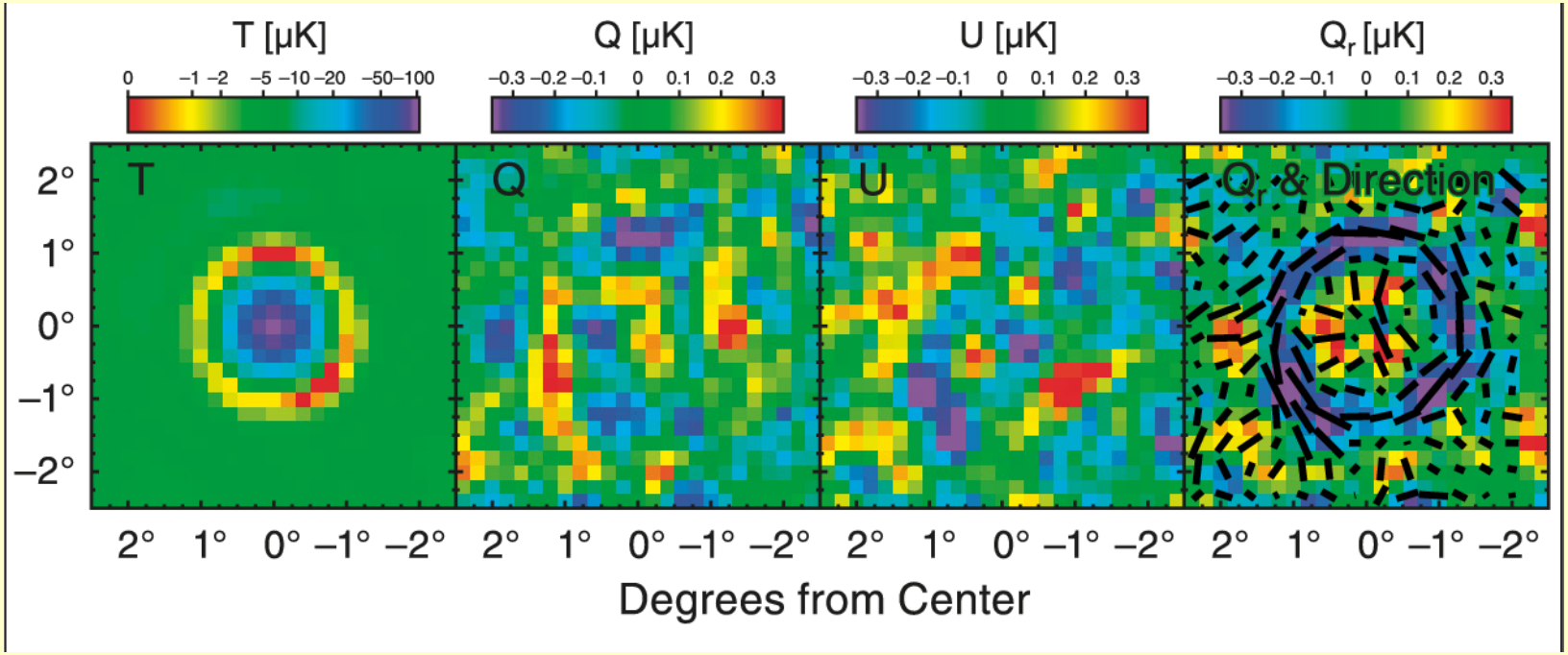

Polarization around a cold (up) and a hot (below) spot. (Stacking of many spots)

[Komatsu et al.. (2011) ApJS, 192, 18]

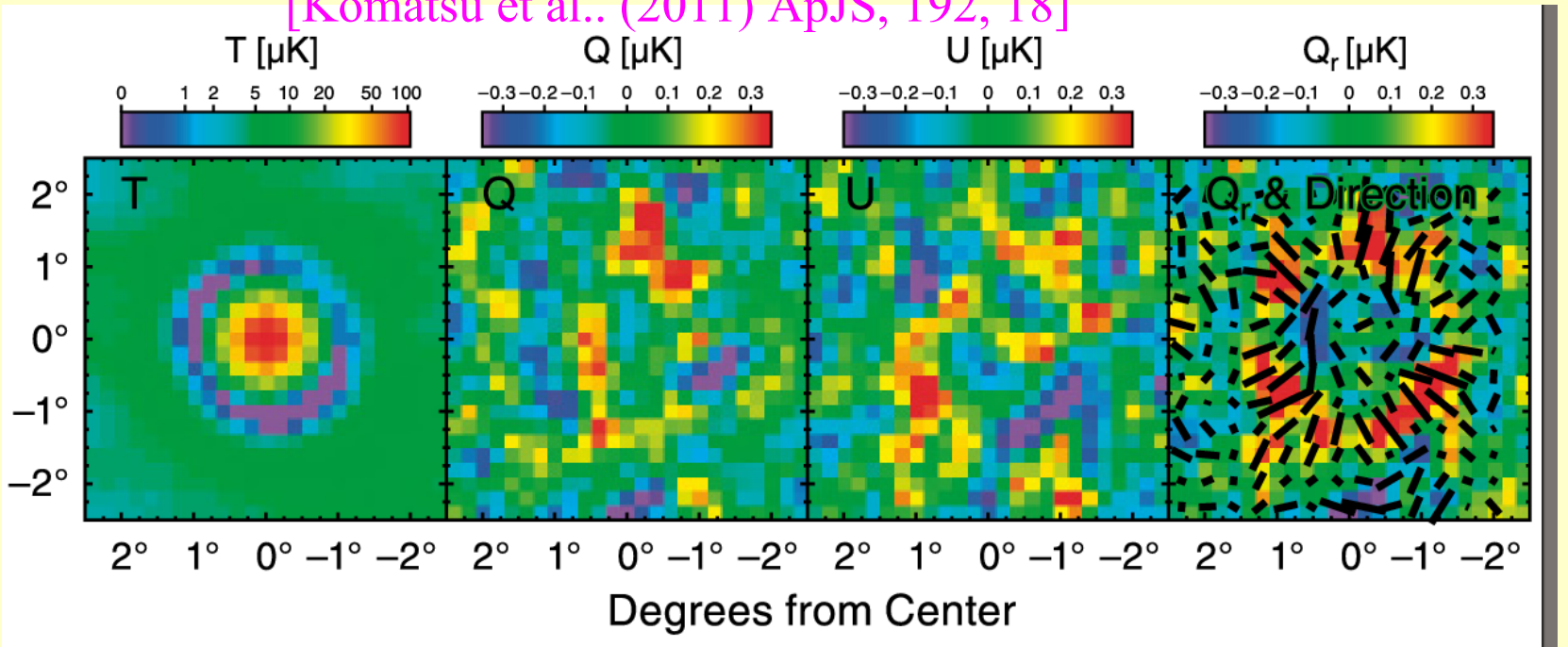

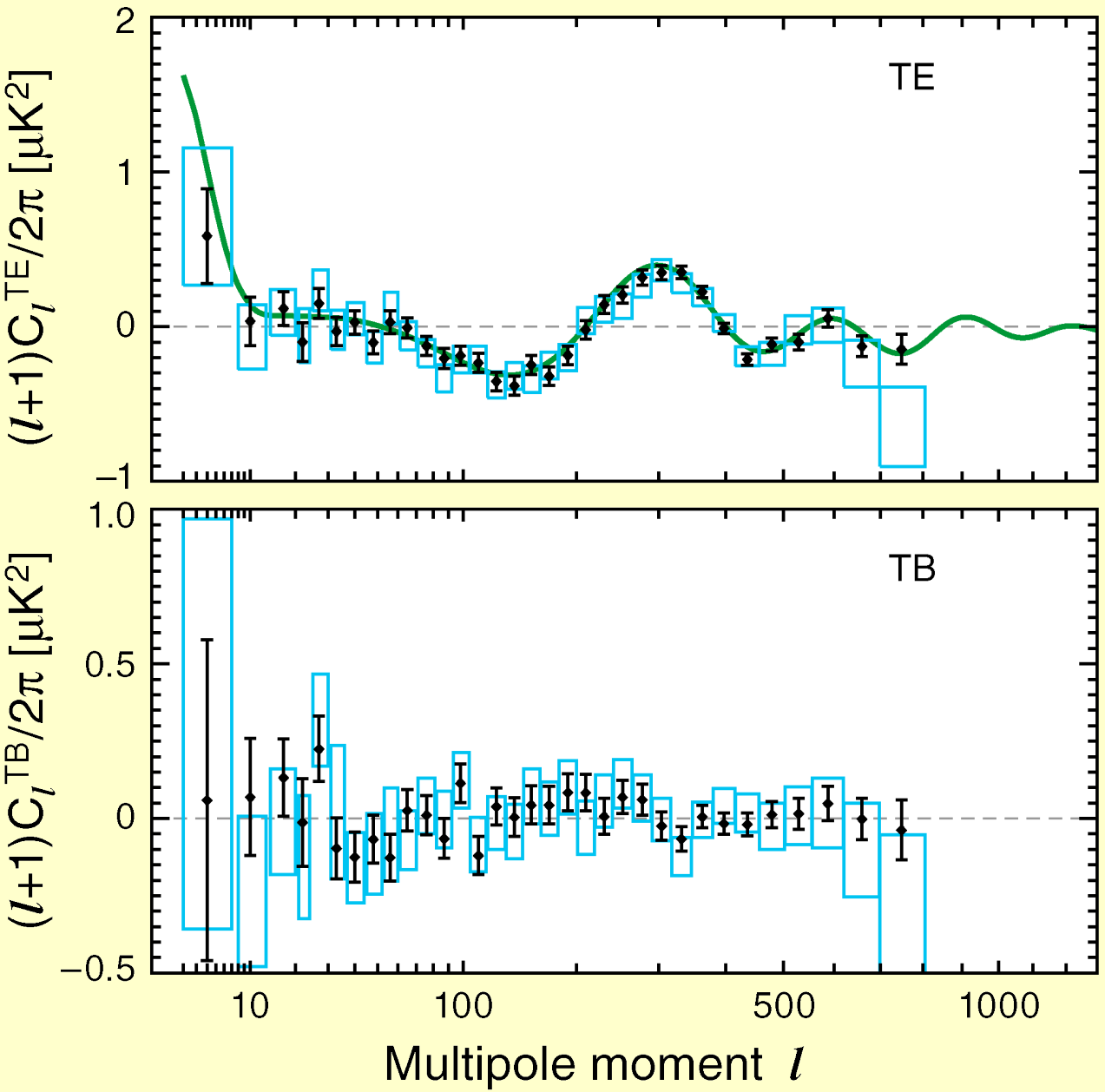

[WMAP Science Team]

Correlations between the temperature fluctuations and polarization patterns E (top) B (bottom) [7y WMAP]

It is (l+1)C_l, not the usual l(l+1)C_l !

Planck

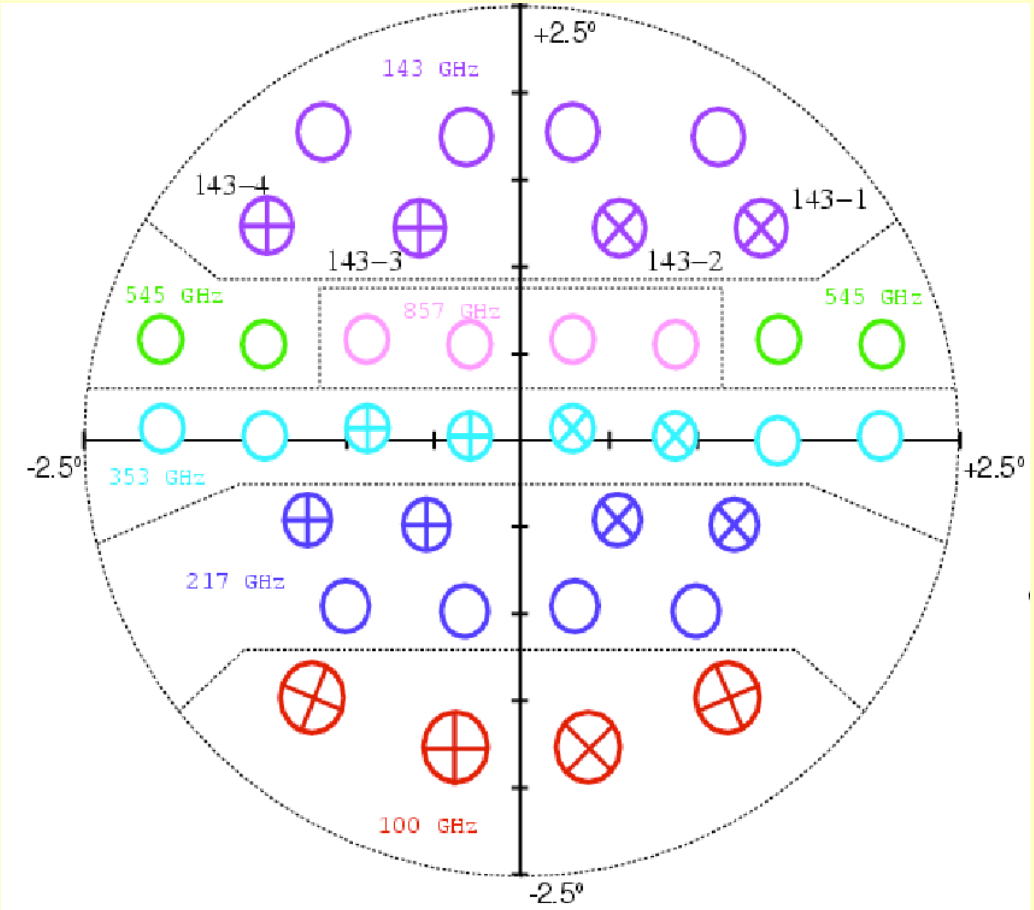

Planck Focal Plane Unit with polarization sensitive bolometers

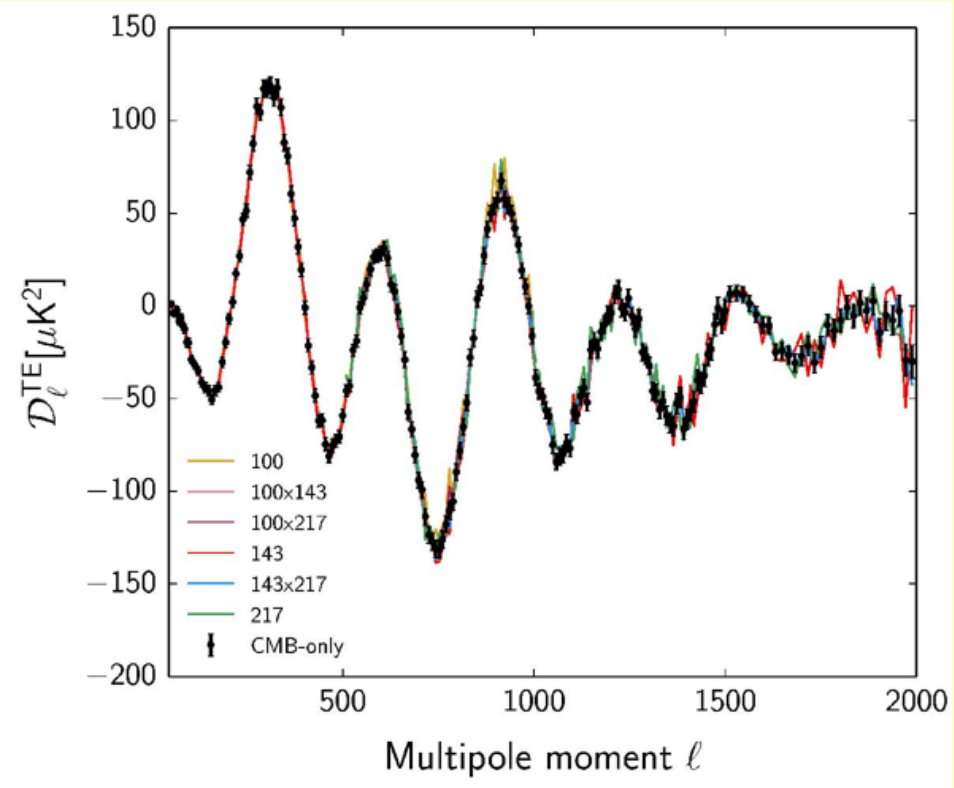

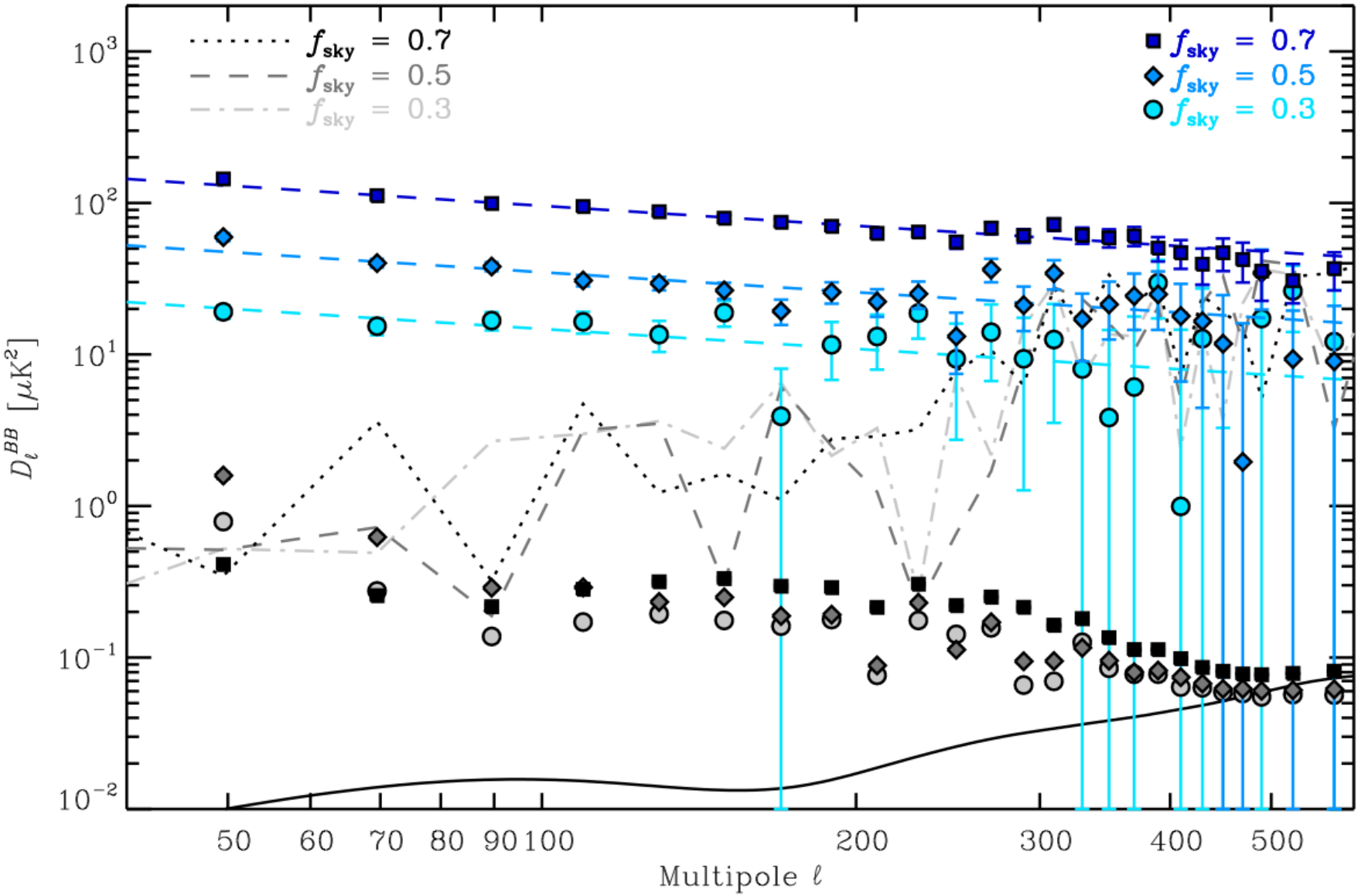

Power spectrum for B polarization. (Mostly due to the dust)
Expected tensor perturbation effect: black line.

Planck XXX (2016)

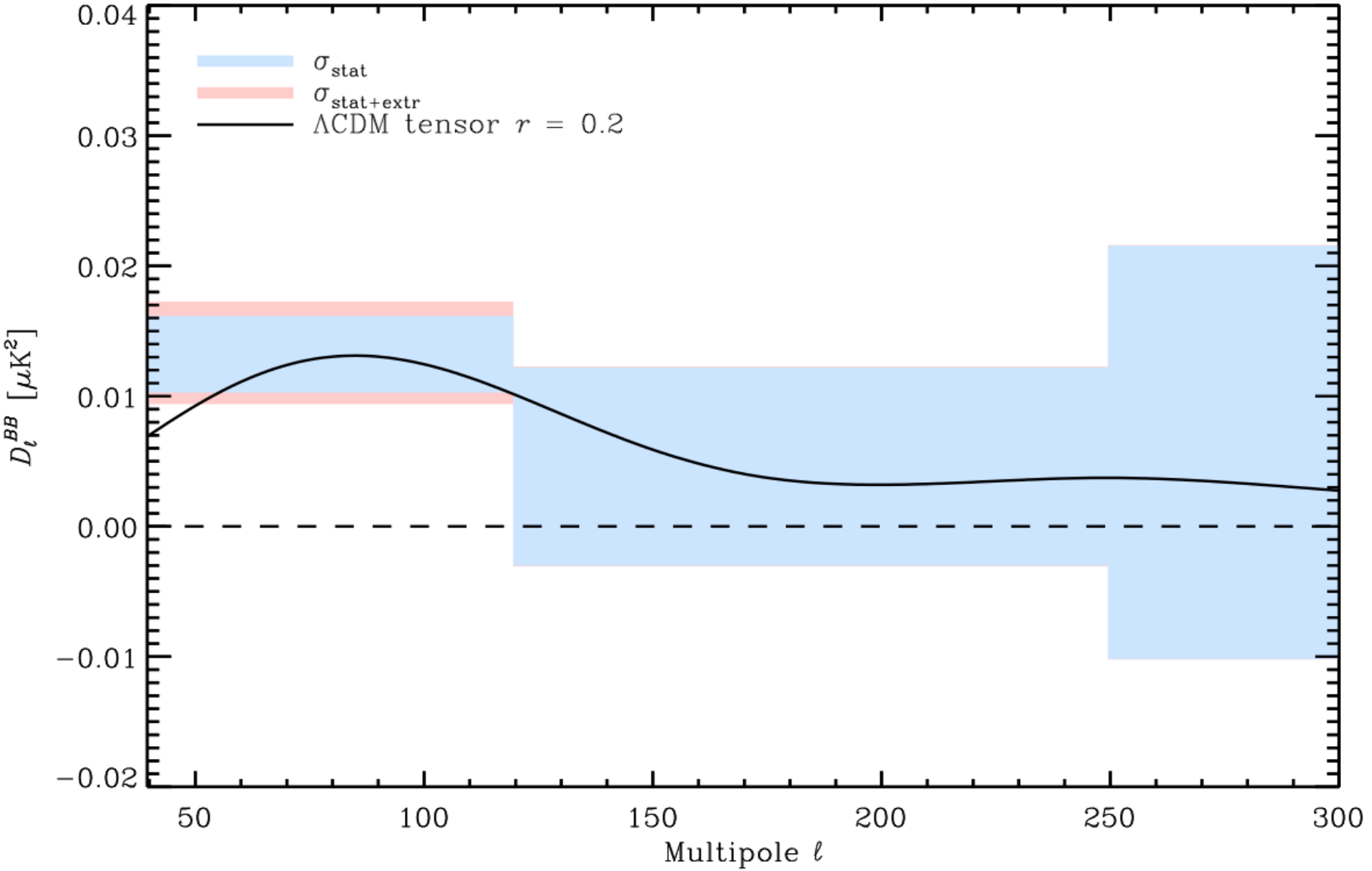

Fig. 9. *Planck* 353 GHz $\mathcal{D}_\ell^{BB}$ angular power spectrum computed on $M_{\rm B2}$ defined in Sect. 6.1 and extrapolated to 150 GHz (box centres). The shaded boxes represent the $\pm 1\sigma$ uncertainties: blue for the statistical uncertainties from noise; and red adding in quadrature the uncertainty from the extrapolation to 150 GHz. The *Planck* 2013 best-fit ΛCDM $\mathcal{D}_\ell^{BB}$ CMB model based on temperature anisotropies, with a tensor amplitude fixed at $r = 0.2$, is overplotted as a black line.

B-mode in the field of BICEP 2, according to Planck. Dust dominating.

Planck XXX (2016)

CMB fast: foundations

After the recombination photons become a collisionless gas except rare scattering on free electrons. Phase space distribution of photons may be described by the *f* function, which obeys the Boltzman equation:

$$dN = f(x, p)dx^1dx^2dx^3dp_1dp_2dp_3$$

$$\frac{\partial f}{\partial t} + \frac{\partial f}{\partial x^a}\frac{dx^a}{dt} + \frac{\partial f}{\partial \gamma_a}\frac{d\gamma_a}{dt} + \frac{\partial f}{\partial p_0}\frac{dp_0}{dt} = \sigma n_e \frac{p'_0}{p_0}(f_+ - f)$$

where "*f*+" describes the distribution of scattered photons. After integration in momentum space one gets the equation for the photon energy density fluctuations:

$$\int f p_0^3 dp_0 \equiv \mathcal{E}(t)[1 + \delta(\theta, \phi)]/4\pi$$

$$\frac{\partial \delta}{\partial t} + \frac{\gamma_a}{a}\frac{\partial \delta}{\partial x^a} - 2\gamma_a\gamma_\beta\frac{\partial h_{a\beta}}{\partial t} = \sigma n_e(\delta_r + 4\gamma_a v^a - \delta)$$

1996ApJ...469..437

[Peebles & Yu 1970, ApJ, 162, 815]

CMB fast

Energy density fluctuations can be replaced by temperature fluctuations, which can be decomposed into plane waves.
A single component can then be expressed as multipole series:

$$\Delta_T(\vec{k},\vec{n}) = \sum_l (2l+1)(-i)^l \Delta_{Tl} P_l(\mu)$$

Where *l* is the multipole number, **k** is the wave-vector and **n** is the propagation direction. *mu*=**k***n.

1996ApJ...469..437

[Seljak & Zaldarriaga (1996) ApJL, 469, L437]

CMB fast

As a consequence of Boltzman equation one gets the following set of equations describing temperature fluctuations and polarization for scalar prturbations:

$$\dot{\Delta}_T^{(S)} + ik\mu\Delta_T^{(S)} = \dot{\phi} - ik\mu\psi + \dot{\kappa}\{-\Delta_T^{(S)} + \Delta_{T0}^{(S)} + i\mu v_b + \frac{1}{2}P_2(\mu)\Pi\}$$

$$\dot{\Delta}_P^{(S)} + ik\mu\Delta_P^{(S)} = \dot{\kappa}\{-\Delta_P^{(S)} + \frac{1}{2}[1 - P_2(\mu)]\Pi\}$$

$$\Pi = \Delta_{T2}^{(S)} + \Delta_{P2}^{(S)} + \Delta_{P0}^{(S)}.$$

Where (S) stands for scalar mode T -temperature fluctuations and P – polarization. Scattering terms are in "{}" and the coefficient in front is the scattering rate.

1996ApJ...469..437

[Seljak & Zaldarriaga (1996) ApJL, 469, L437]

CMB fast

$$\dot{\Delta}^{(S)}_{T0} = -k\Delta^{(S)}_{T1} + \dot{\phi}\,,$$

$$\dot{\Delta}^{(S)}_{T1} = \frac{k}{3}\left[\Delta^{(S)}_{T0} - 2\Delta^{(S)}_{T2} + \psi\right] + \dot{\kappa}\left(\frac{v_b}{3} - \Delta^{(S)}_{T1}\right),$$

$$\dot{\Delta}^{(S)}_{T2} = \frac{k}{5}\left[2\Delta^{(S)}_{T1} - 3\Delta^{(S)}_{T3}\right] + \dot{\kappa}\left[\frac{\Pi}{10} - \Delta^{(S)}_{T2}\right],$$

$$\dot{\Delta}^{(S)}_{Tl} = \frac{k}{2l+1}\left[l\Delta^{(S)}_{T(l-1)} - (l+1)\Delta^{(S)}_{T(l+1)}\right] - \dot{\kappa}\Delta^{(S)}_{Tl}\,, l > 2$$

$$\dot{\Delta}^{(S)}_{Pl} = \frac{k}{2l+1}\left[l\Delta^{(S)}_{P(l-1)} - (l+1)\Delta^{(S)}_{P(l+1)}\right] + \dot{\kappa}\left[-\Delta^{(S)}_{Pl} + \frac{1}{2}\Pi\left(\delta_{l0} + \frac{\delta_{l2}}{5}\right)\right]$$

In multipole decomposition one gets the above infinite set of equations. For l>2 the equation for l multipole contains only l-1, l, and l+1 multipoles in RHS

To get a spectrum up to l=1000 one should solve a set of few thousands of equations. One should also decide on the number of multipoles taken into account from their infinite number. This makes the set incomplete.

1996ApJ...469..437

[Seljak & Zaldarriaga (1996) ApJL, 469, L437]

CMB fast

Formally one can express the observed T and P as integrals along photon trajectories:

$$\Delta_T^{(S)} = \int_0^{\tau_0} d\tau e^{ik\mu(\tau-\tau_0)} e^{-\kappa} \{\dot{\kappa} e^{-\kappa} [\Delta_{T0} + i\mu v_b + \frac{1}{2} P_2(\mu)\Pi] + \dot{\phi} - ik\mu\psi\}$$

$$\Delta_P^{(S)} = -\frac{1}{2} \int_0^{\tau_0} d\tau e^{ik\mu(\tau-\tau_0)} e^{-\kappa} \dot{\kappa} [1 - P_2(\mu)]\Pi.$$

Under the integrals only low multipoles are present. They should be computed for each point along the trajectory using the former set, but containing much lower number of equations.
Integrating by parts one can replace *mu*-dependence by *tau*-derivatives.

1996ApJ...469..437

[Seljak & Zaldarriaga (1996) ApJL, 469, L437]

CMB fast

Finally:

$$\Delta_{T,P}^{(S)} = \int_0^{\tau_0} d\tau e^{ik\mu(\tau-\tau_0)} S_{T,P}^{(S)}(k,\tau)$$

$$S_T^{(S)}(k,\tau) = g\left(\Delta_{T0} + \psi - \frac{\dot{v}_b}{k} - \frac{\Pi}{4} - \frac{3\ddot{\Pi}}{4k^2}\right)$$

$$+ e^{-\kappa}(\dot{\phi}+\dot{\psi}) - \dot{g}\left(\frac{v_b}{k} + \frac{3\dot{\Pi}}{4k^2}\right) - \frac{3\ddot{g}\Pi}{4k^2}$$

$$S_P^{(S)}(k,\tau) = -\frac{3}{4k^2}\left(g\{k^2\Pi + \ddot{\Pi}\} + 2\dot{g}\dot{\Pi} + \ddot{g}\Pi\right).$$

Only low multipoles. S&Z show that it is enough to use really low number of them!

1996ApJ...469..437

[Seljak & Zaldarriaga (1996) ApJL, 469, L437]

CMB fast

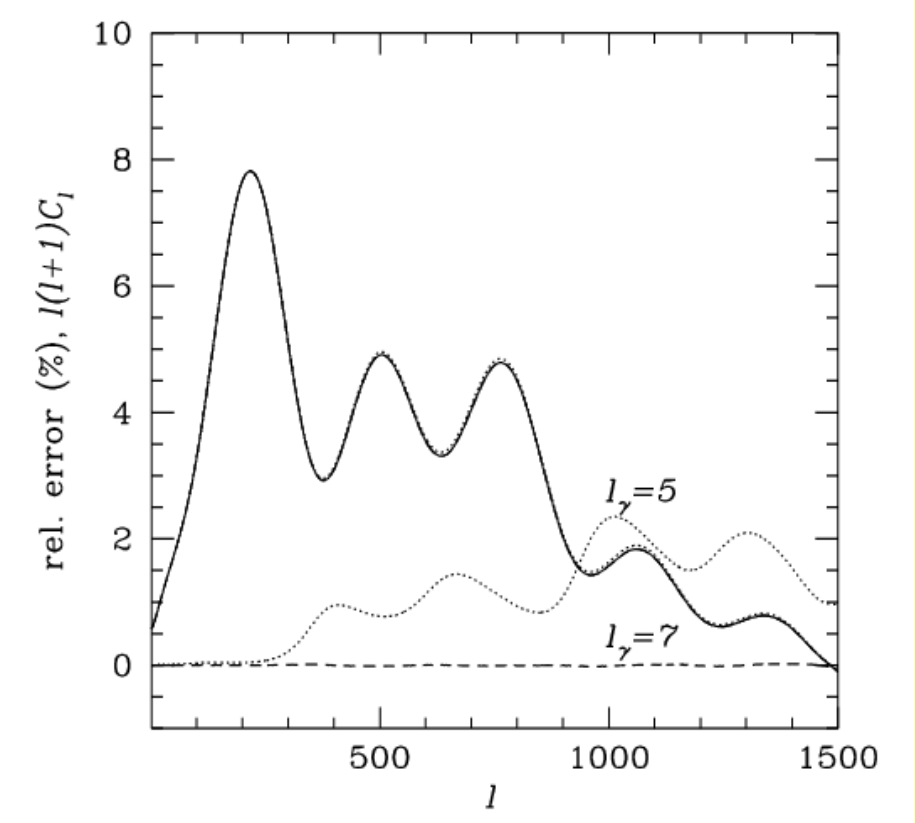

The seven lowest multipoles is enough to get very (?) precise CMB anisotropy power spectrum ...

CMB fast has been employed to fit cosmological models to CMB data for decades.

It is still valid but less popular...

1996ApJ...469L.437.

[Seljak & Zaldarriaga (1996) ApJL, 469, L437]

Secondary anisotropies of the CMB

Nabila Aghanim[1], Subhabrata Majumdar[2] and Joseph Silk[3]

(2008) Rept. Prog. Phys. 70:066102

(i) The integrated Sachs-Wolfe (ISW) effect is due to CMB photons traversing a time-varying linear gravitational potential. The relevant scale is the curvature scale freeze-out in concordance cosmology: the horizon at $1 + z \sim (\Omega_\Lambda/\Omega_\mathrm{m})^{1/3}$. This corresponds to an angular scale of about 10°.

(ii) The Rees-Sciama (RS) effect is due to CMB photons traversing a non-linear gravitational potential, usually associated with gravitational collapse. The relevant scales are those of galaxy clusters and superclusters, corresponding to angular scales of 5-10 arc minutes.

(iii) Gravitational lensing of the CMB by intervening large-scale structure does not change the total power in fluctuations, but power is redistributed preferentially towards smaller scales. The effects are significant only below a few arc minutes. Its effects may be significant on large scales when the observable of interest is the B-mode power spectrum.

Secondary anisotropy: gravitation

Sachs-Wolfe (SW) and integrated Sachs-Wolfe (ISW):

$$\frac{\Delta T(\mathbf{n})}{T} = (\phi_{\rm rec} - \phi_0) + \int_{\eta_{\rm rec}}^{\eta_0} 2\dot{\phi} d\eta,$$

The first term shows the influence of the gravitational potential difference between the observer and the emission place on LSS. The second: influence of the inhomogeneities along propagation path.
Investigating the influence of a single density perturbation we follow the Rees-Sciama scenario: photons enter a lower amplitude perturbation and leave a stronger one (due to ongoing instability). That implies loosing of energy by all photons going through the increased density region, which might be observed as correlations between the positions of CMB cold spots and the positions of large scale structure on the sky.

Secondary anisotropy: gravitation

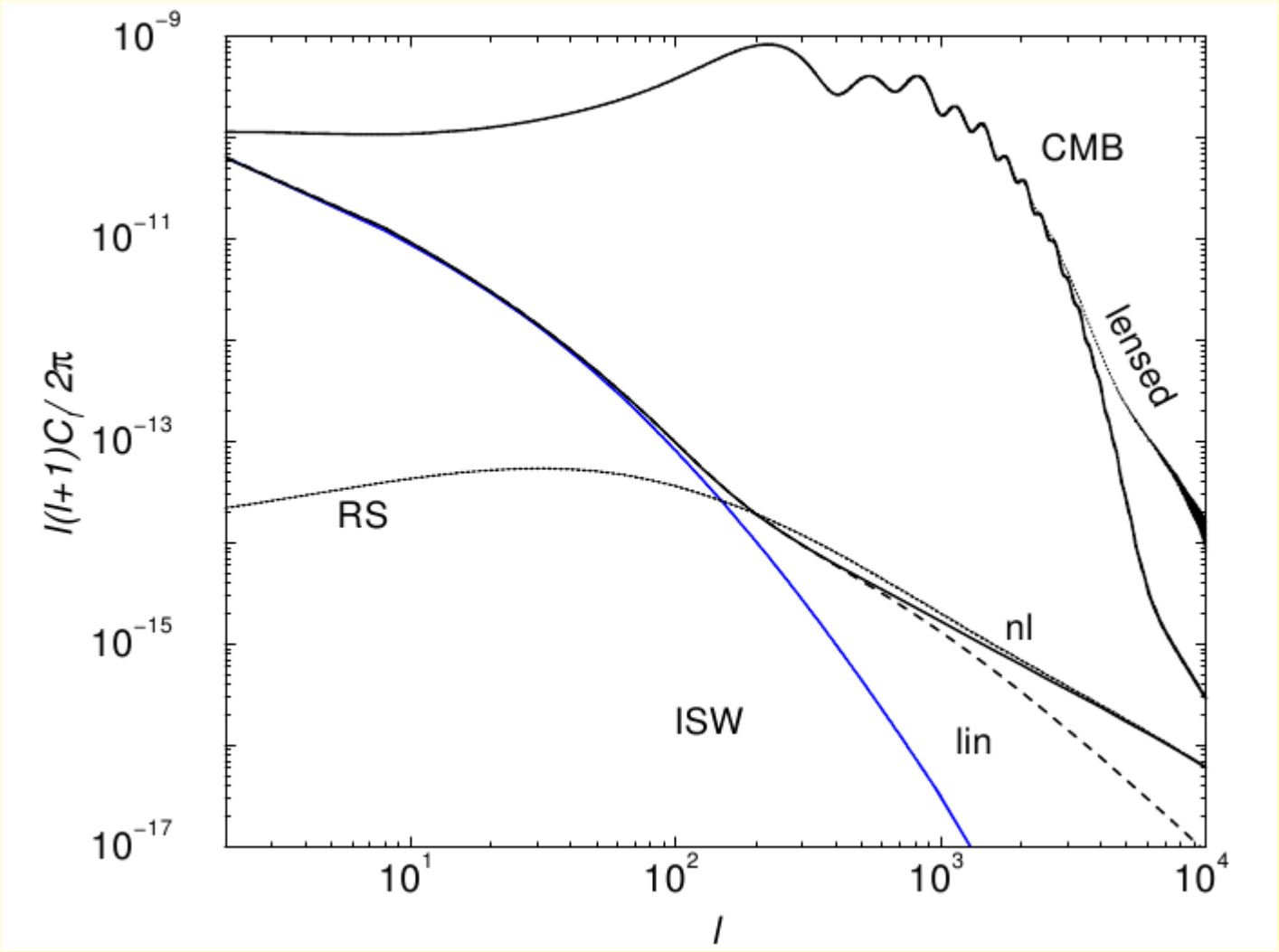

The influence of the Sachs-Wolfe effect and its nonlinear analog (RS) on the CMB anisotropy spectrum

[Cooray (2002) PhysRevD 65, 083518]

Secondary anisotropy: gravitational lensing

The deflection of rays does not change the energy of propagating photons but changes their observed positions on the sky:

$$T_{\rm obs}(\theta) = T(\theta + \xi(\theta))$$

Expanding:

$$T_{\rm obs}(\theta) \sim T(\theta) + \xi^i(\theta) \cdot T_{,i} + \frac{1}{2}\xi^i(\theta)\xi^j(\theta) \cdot T_{,ij}$$

where:

$$\xi_i(\theta) = \frac{-3}{2}\Omega_0 \int \frac{dz'}{H(z')}\frac{1}{a}\frac{D_0(z')D_0(z,z')}{D_0(z)}\varphi^{(1)}_{,i}(\theta, z)$$

defines the shift in emission place relative to an “undeflected ray”.

Stokes parameters

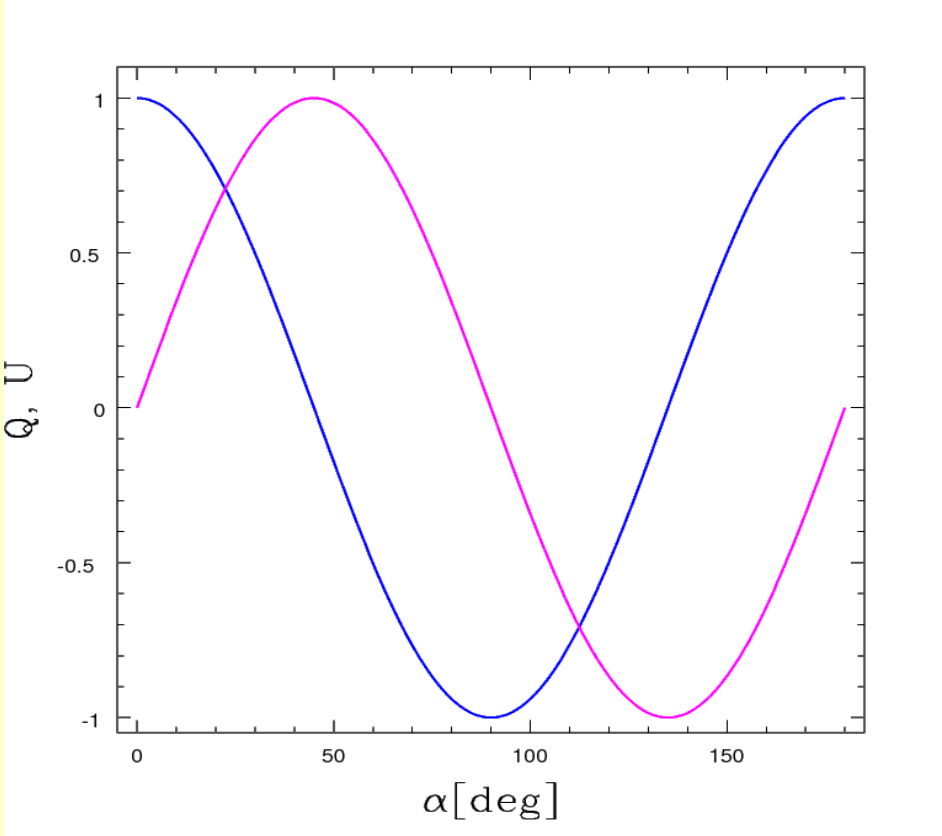

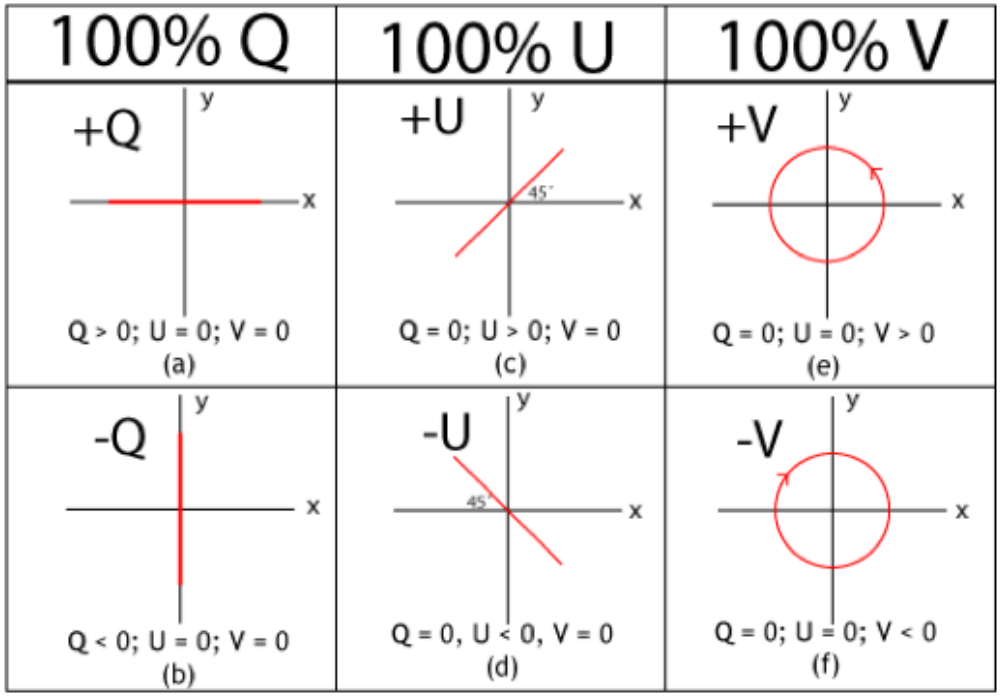

Definitions

The Stokes parameters are defined by

$$
\begin{aligned}
I &\equiv |E_x|^2 + |E_y|^2, \\
I &= |E_a|^2 + |E_b|^2, \\
I &= |E_l|^2 + |E_r|^2, \\
Q &\equiv |E_x|^2 - |E_y|^2, \\
U &\equiv |E_a|^2 - |E_b|^2, \\
V &\equiv |E_l|^2 - |E_r|^2,
\end{aligned}
$$

Stokes parameters

We neglect circular polarization as absent in CMB. For two modes of linear polarization one has:

$$
\begin{aligned}
E_a &= \sqrt{\frac{1}{2}}(+E_x + E_y) \qquad E_b = \sqrt{\frac{1}{2}}(-E_x + E_y) \\
Q &= E_x^2 - E_y^2 \qquad U = E_a^2 - E_b^2 = 2E_xE_y \qquad \Rightarrow \\
E_x^2 &= \frac{1}{2}(\sqrt{Q^2+U^2} + Q) \qquad E_y^2 = \frac{1}{2}(\sqrt{Q^2+U^2} - Q) \\
\tan\alpha &= \sqrt{\frac{\sqrt{Q^2+U^2} - Q}{\sqrt{Q^2+U^2} + Q}}
\end{aligned}
$$

where α is the direction of polarization relative to x axis. (If $U = 0$ and $Q > 0$ we get $\alpha = 0$ – polarization along x axis, if $U = 0$ and $Q < 0$ we get $\alpha = \pi/2$ – polarization along y axis, as expected. For $Q = 0$ one gets $|\tan\alpha| = 1$ corresponding to $\alpha = \pi/4$ ($U > 0$) or $\alpha = 3\pi/4$ ($U < 0$) – as expected. If $Q > 0$ and $U > 0$ one has $0 \leq \alpha \leq \pi/4$ and similarly for othe sign combinations.)

Lensing: polarization

Polarization maps are also deformed. For polarization defined as P=Q+/-iU one has (as for the temperature):

$$P_{\rm obs}(\theta) = P(\theta_{\rm obs}) = P(\theta + \xi)$$

$$P_{\rm obs}(\theta) \sim P(\theta) + \xi^i(\theta) \cdot P_{,i} + \frac{1}{2}\xi^i(\theta)\xi^j(\theta) \cdot P_{,ij}$$

Hard

$$\Delta E_{\rm obs} = (1-2\kappa)\Delta E + \xi \cdot \nabla(\Delta E) - 2\delta^{ij}(\gamma_i \Delta P_j + \nabla\gamma_{\mathbf{i}} \cdot \nabla P_j)$$
$$\Delta B_{\rm obs} = (1-2\kappa)\Delta B + \xi \cdot \nabla(\Delta B) - 2\epsilon^{ij}(\gamma_i \Delta P_j + \nabla\gamma_{\mathbf{i}} \cdot \nabla P_j)$$

So the E and B modes are coupled. Even if B is absent on the "primary sky" it $\Delta B = -2\epsilon^{ij}(\gamma_i \Delta P_j + \nabla\gamma_i \cdot \nabla P_j)$ in the case of scalar perturbation.

Where *gamma* stands for shear, *kappa* for convergence, and *epsilon* is the anti-symmetric tensor.

Lensing: polarization

Using polarization tensors instead:

$$\mathcal{P}_{ab}(x,y) = \left\| \begin{array}{cc} Q & -U \\ -U & -Q \end{array} \right\| \qquad \mathcal{P}_{a'b'}(x',y') = \left\| \begin{array}{cc} Q' & -U' \\ -U' & -Q' \end{array} \right\|$$

On the small region near a SIS lens at the origin of Cartesian coordinate system the lens equation [(x',y') → (x,y) transformation] reads:

$$\begin{aligned} r' &= \sqrt{x'^2 + y'^2} \qquad r = r' - \Delta r \\ x &= r * \frac{x'}{r'} \\ y &= r * \frac{y'}{r'} \end{aligned}$$

Lensing: polarization

The partial derivatives are:

$$\frac{\partial x}{\partial x'} = 1 - \frac{\Delta r}{r'} + \frac{\Delta r * x\prime^2}{r'^3} \equiv a$$
$$\frac{\partial x}{\partial y'} = \frac{\partial y}{\partial x'} = \frac{\Delta r * x\prime * y'}{r'^3} \equiv c$$
$$\frac{\partial y}{\partial y'} = 1 - \frac{\Delta r}{r'} + \frac{\Delta r * y\prime^2}{r'^3} \equiv b$$

Making the transformatio

$$\mathcal{P}_{a'b'} = \frac{\partial x^a}{\partial x^{a'}} \frac{\partial x^b}{\partial x^{b'}} \mathcal{P}_{ab}$$

And assuming

$$Q' = (a^2 - c^2) * Q \qquad U' = (a - b) * c * Q$$

$$U' \propto (\Delta r/r)^2 * Q$$

So lensing induces B-mode (U') even if it was originally absent.
The term is of low order: at least in the case of weak lensing.

Lensing: polarization

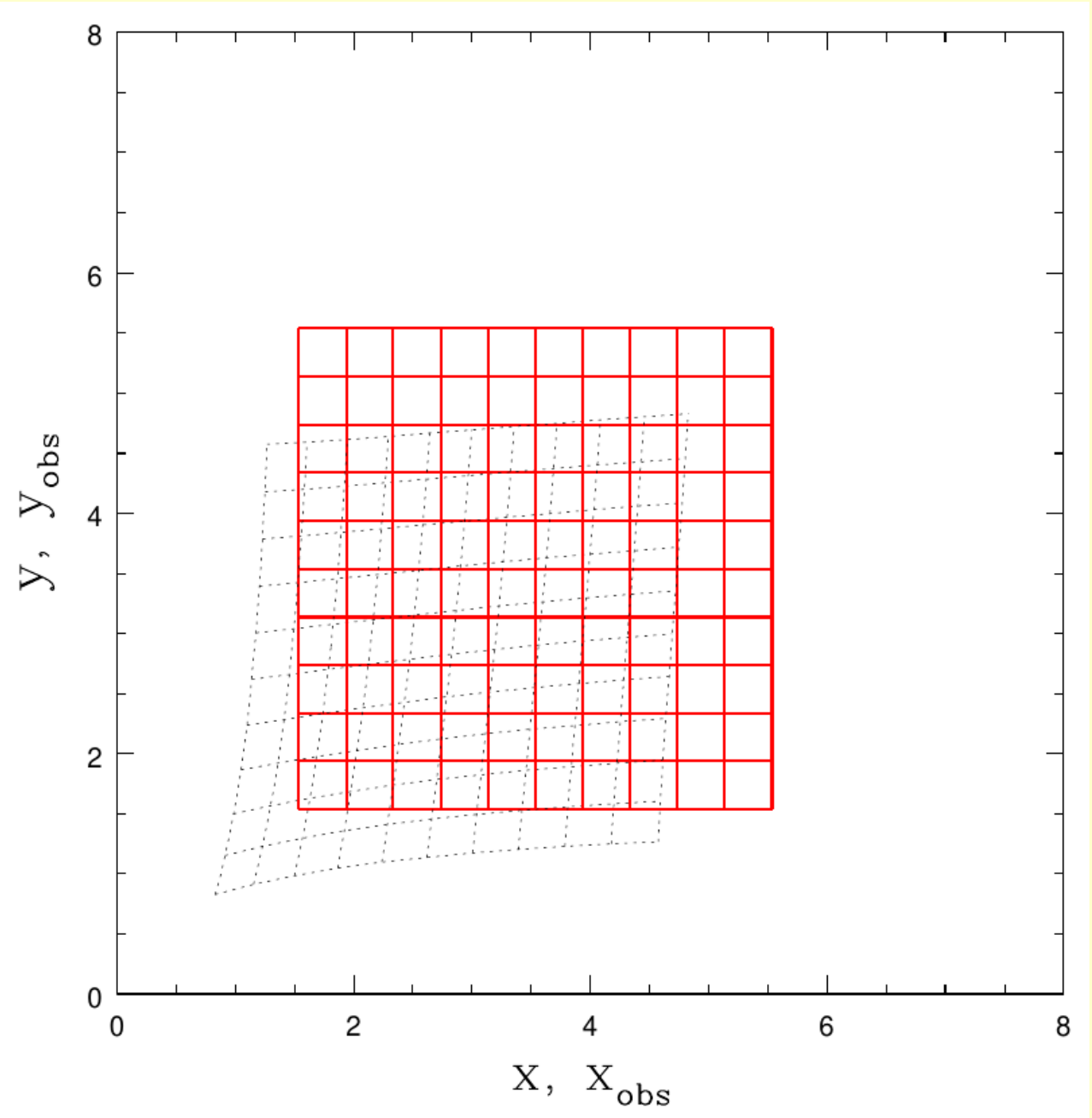

Red: rectangular grid on the sky. Black dotted: corresponding unlensed positions

Lensing: polarization

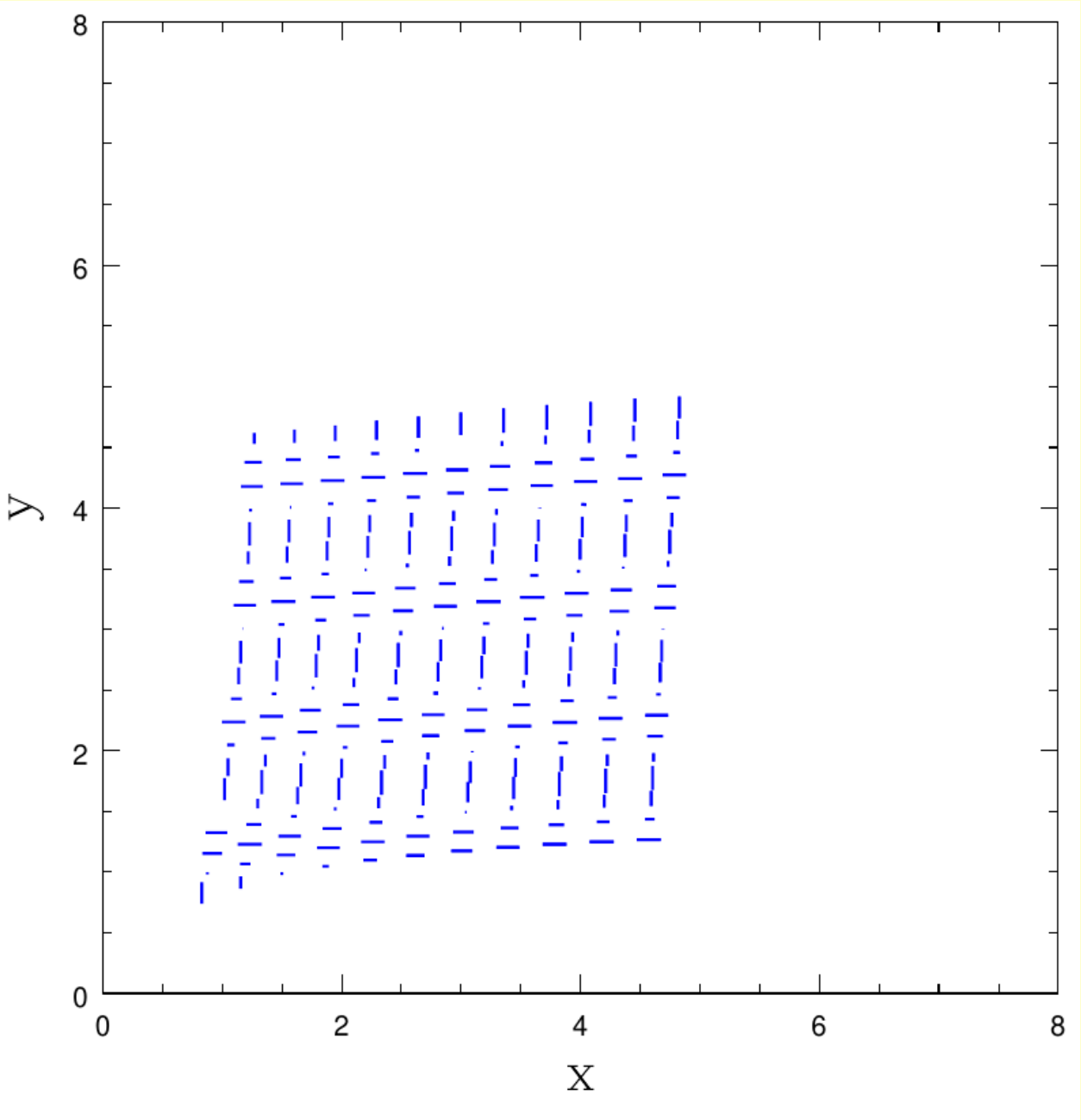

Polarization (pure E-mode)
at original positions

Lensing: polarization

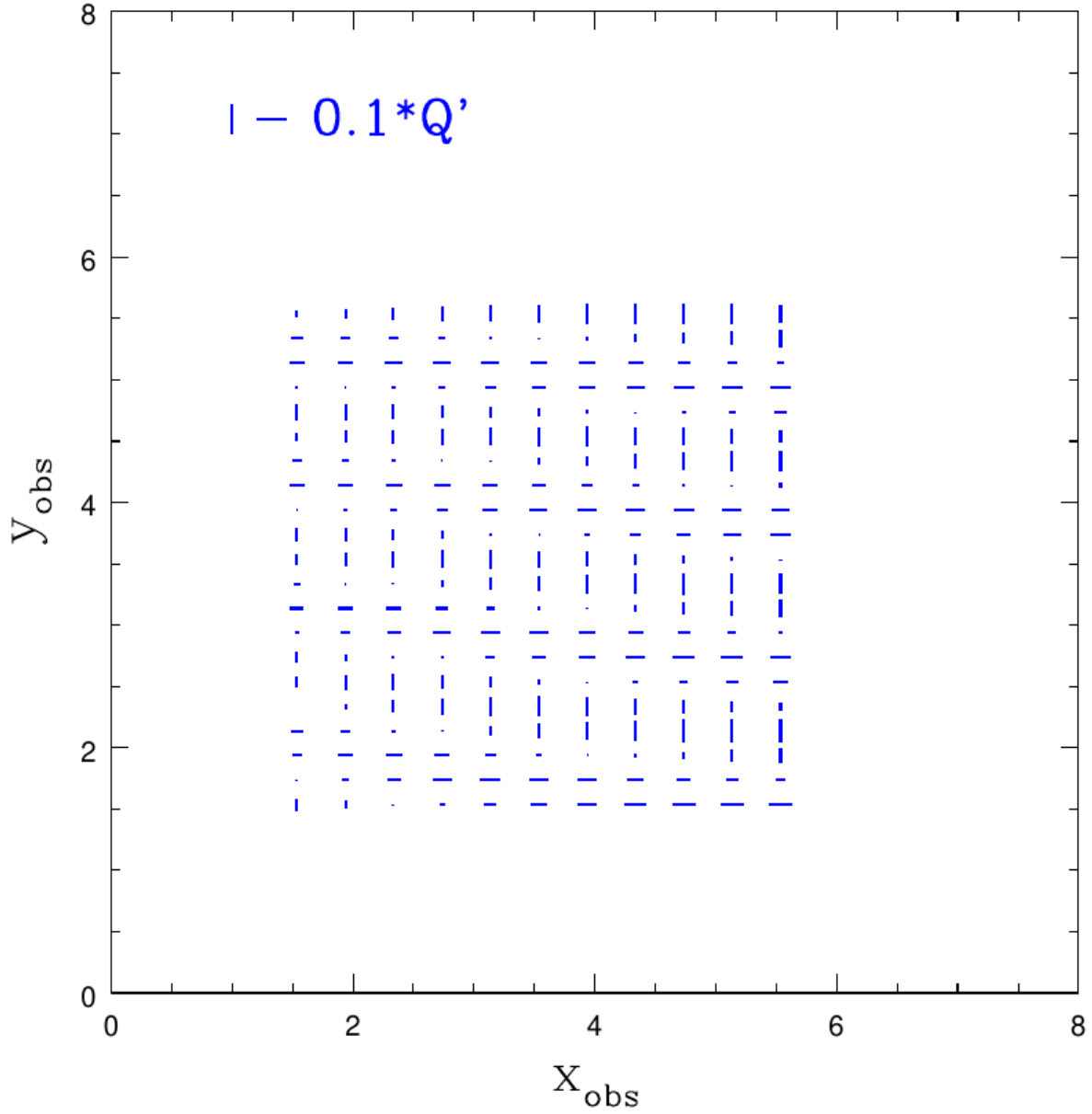

Polarization (pure E-mode) at corresponding positions on the sky

Lensing: polarization

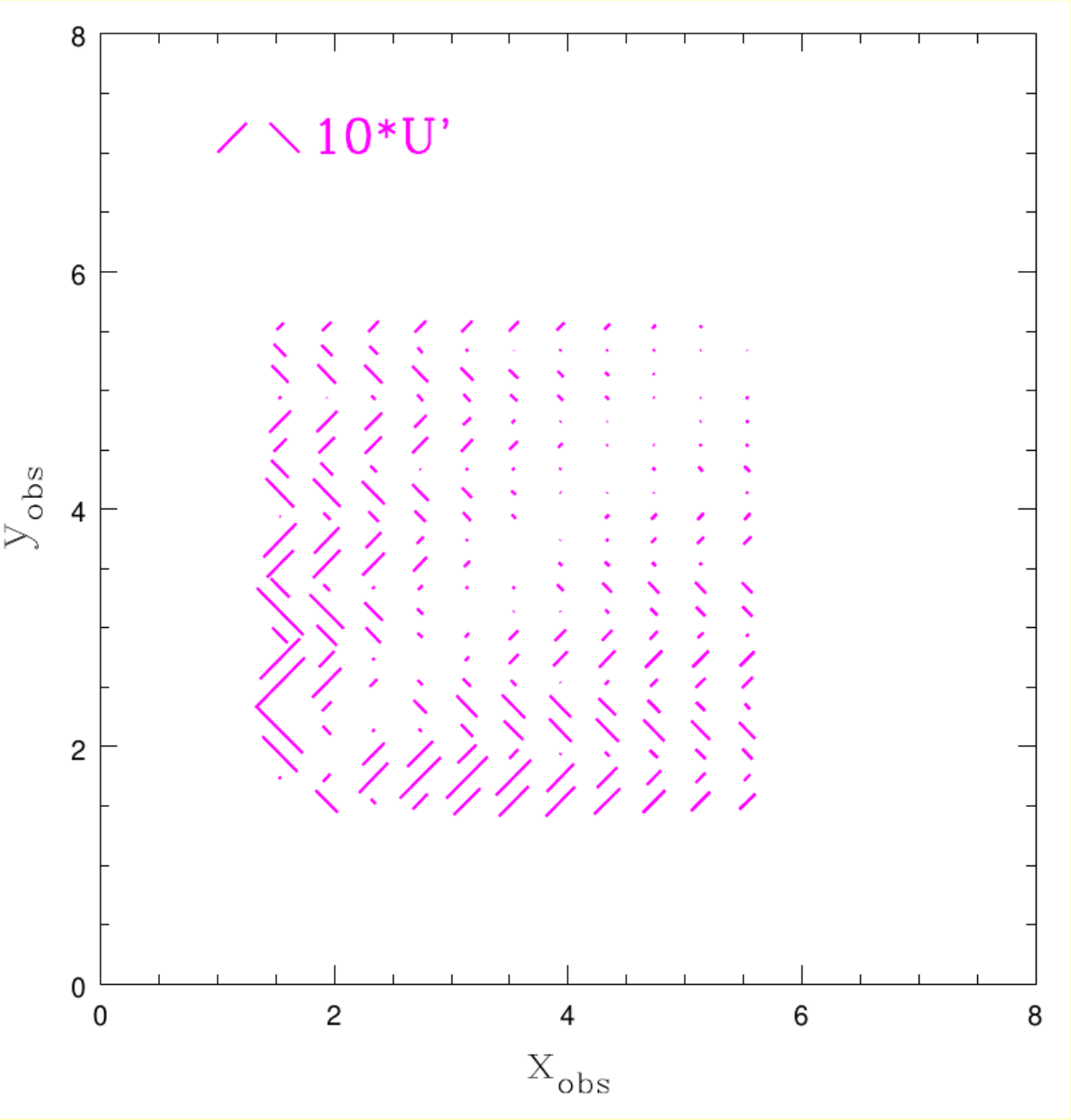

Polarization (pure B-mode) at corresponding positions on the sky

Lensing: polarization

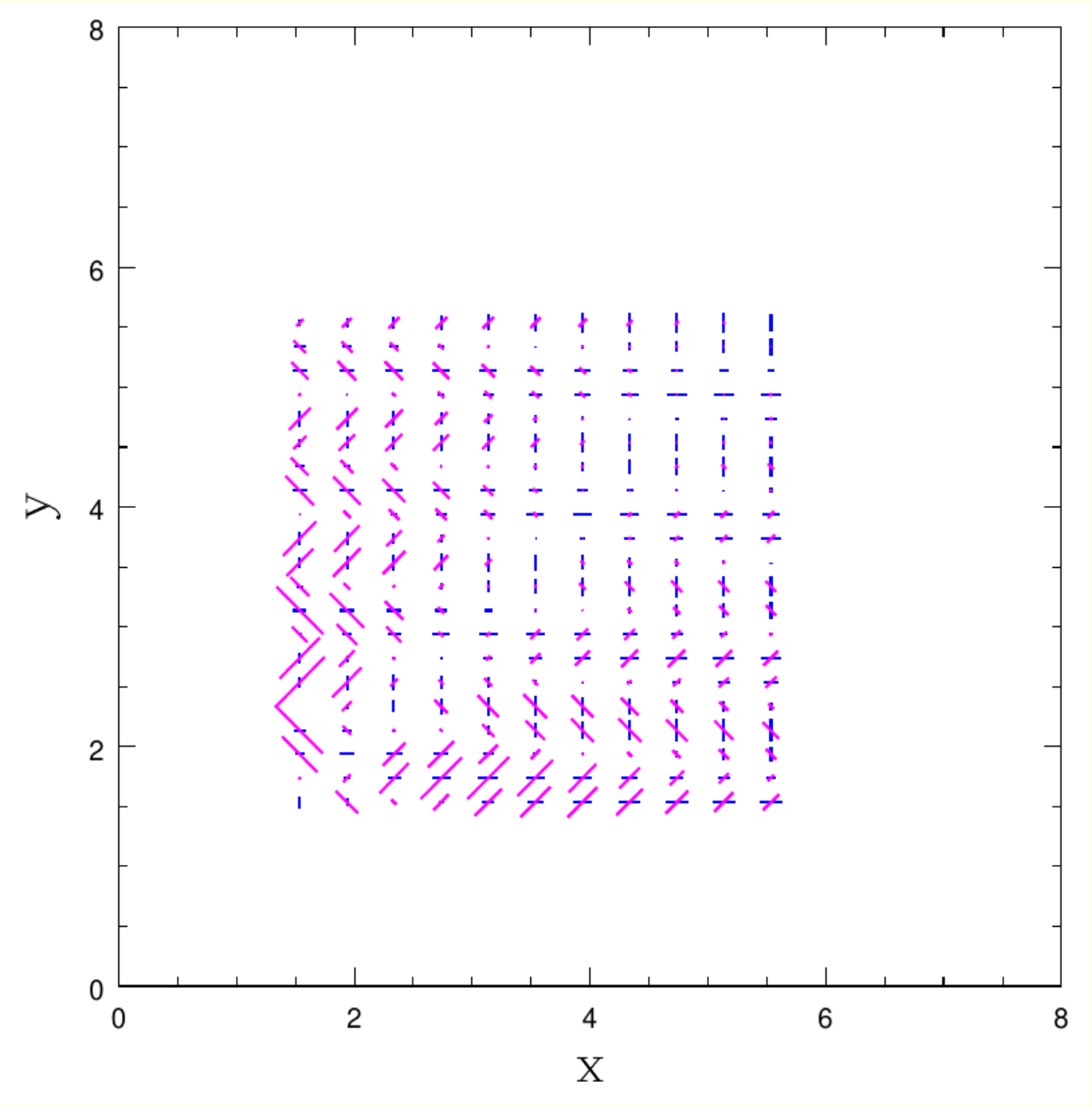

E and B-modes overplotted on the sky

Lensing: influence on the anisotropy spectrum

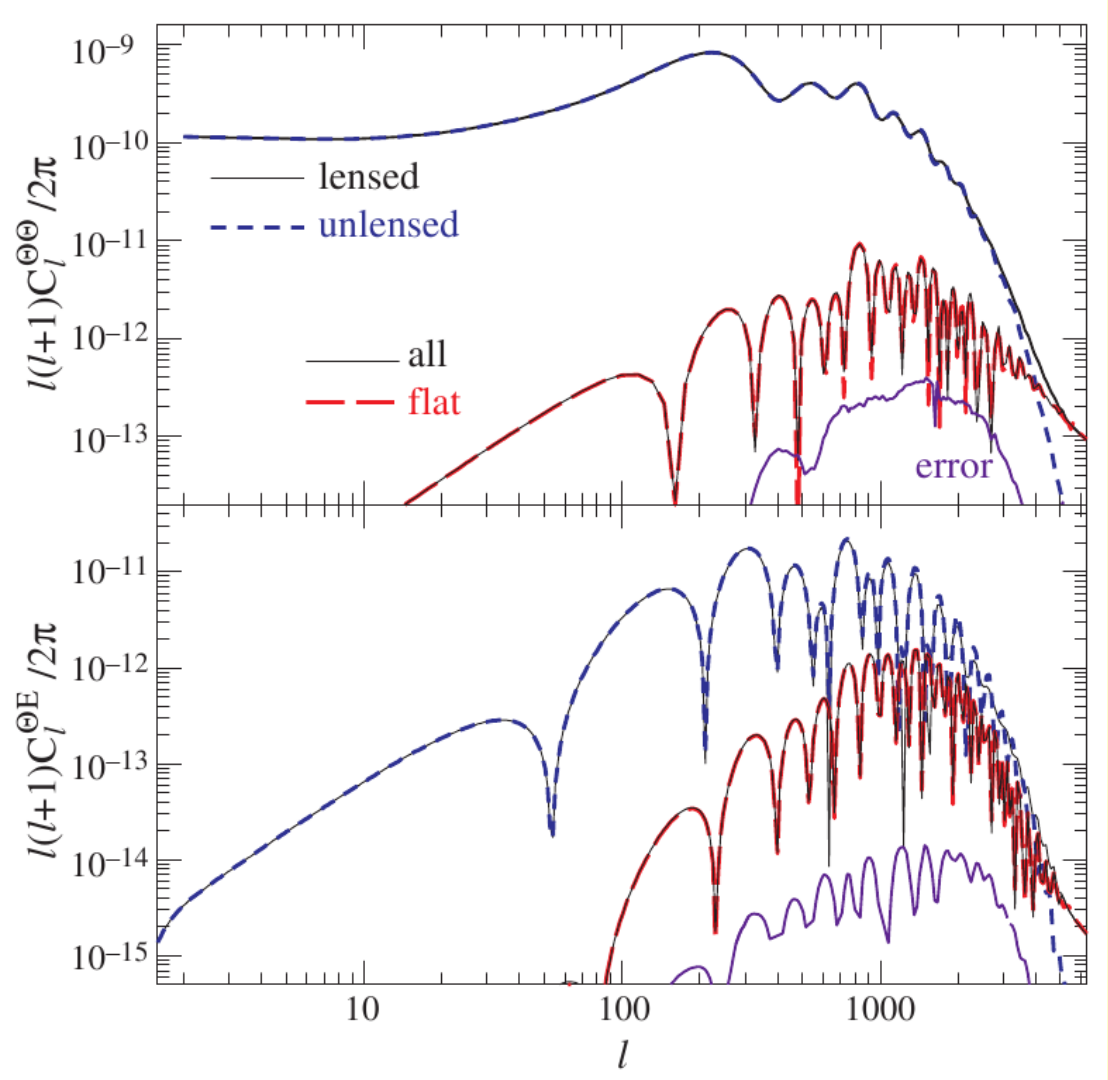

Temperature anisotropy spectrum (top) and its correlations with E mode (bottom). Lensing becomes dominating at l>3000.

[Hu (2000) Phys.Rev.D, 62, 043007]

Lensing: a simulation

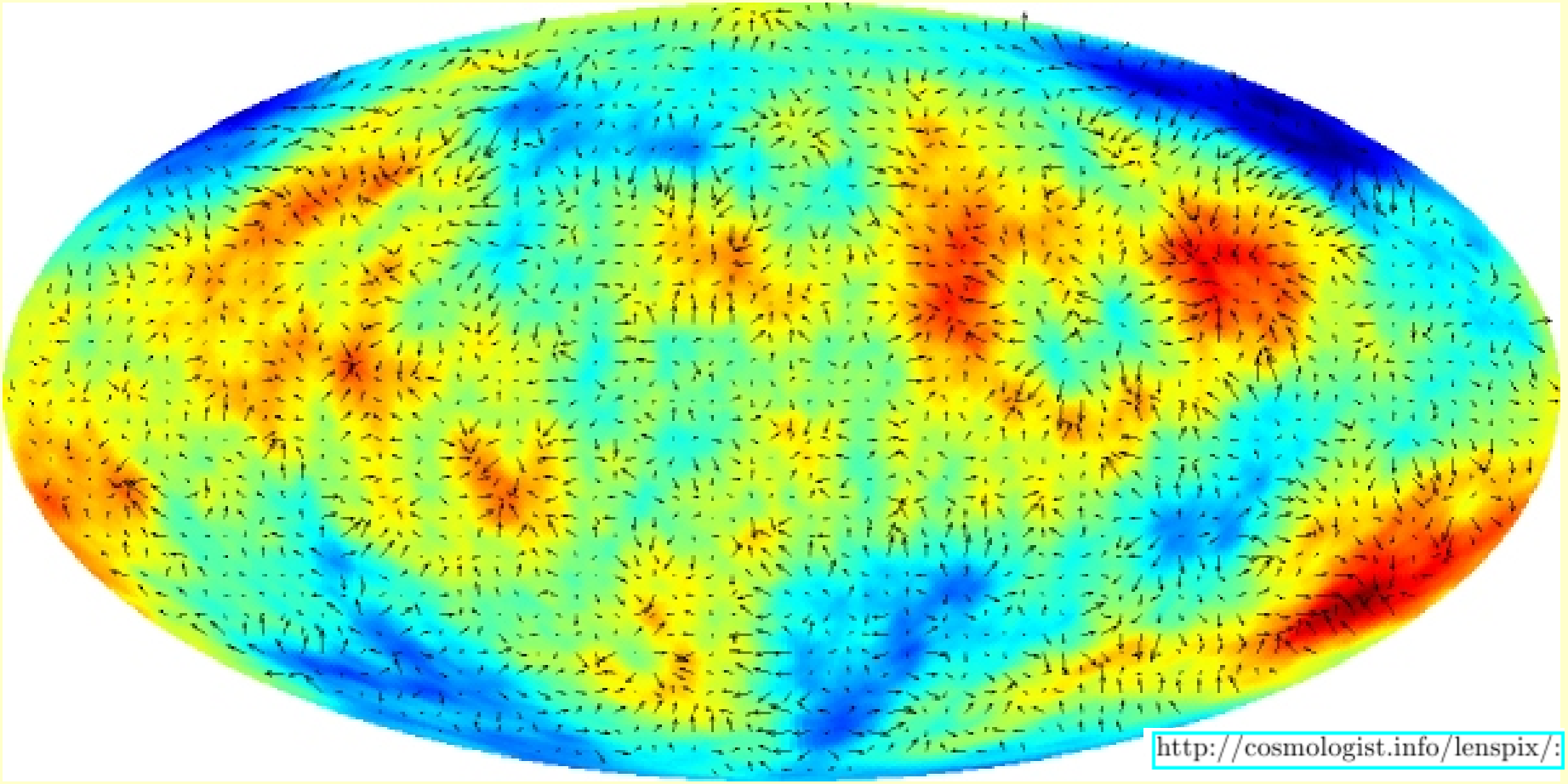

A synthetic map of the temperature and polarization on the sky with lensing taken into account.

A MEASUREMENT OF THE COSMIC MICROWAVE BACKGROUND LENSING POTENTIAL AND POWER SPECTRUM FROM 500 DEG^2 OF SPTPOL TEMPERATURE AND POLARIZATION DATA

W. L. K. Wu[1,†], L. M. Mocanu[1,2,3,‡], P. A. R. Ade[4], A. J. Anderson[5], J. E. Austermann[6], J. S. Avva[7], J. A. Beall[6],

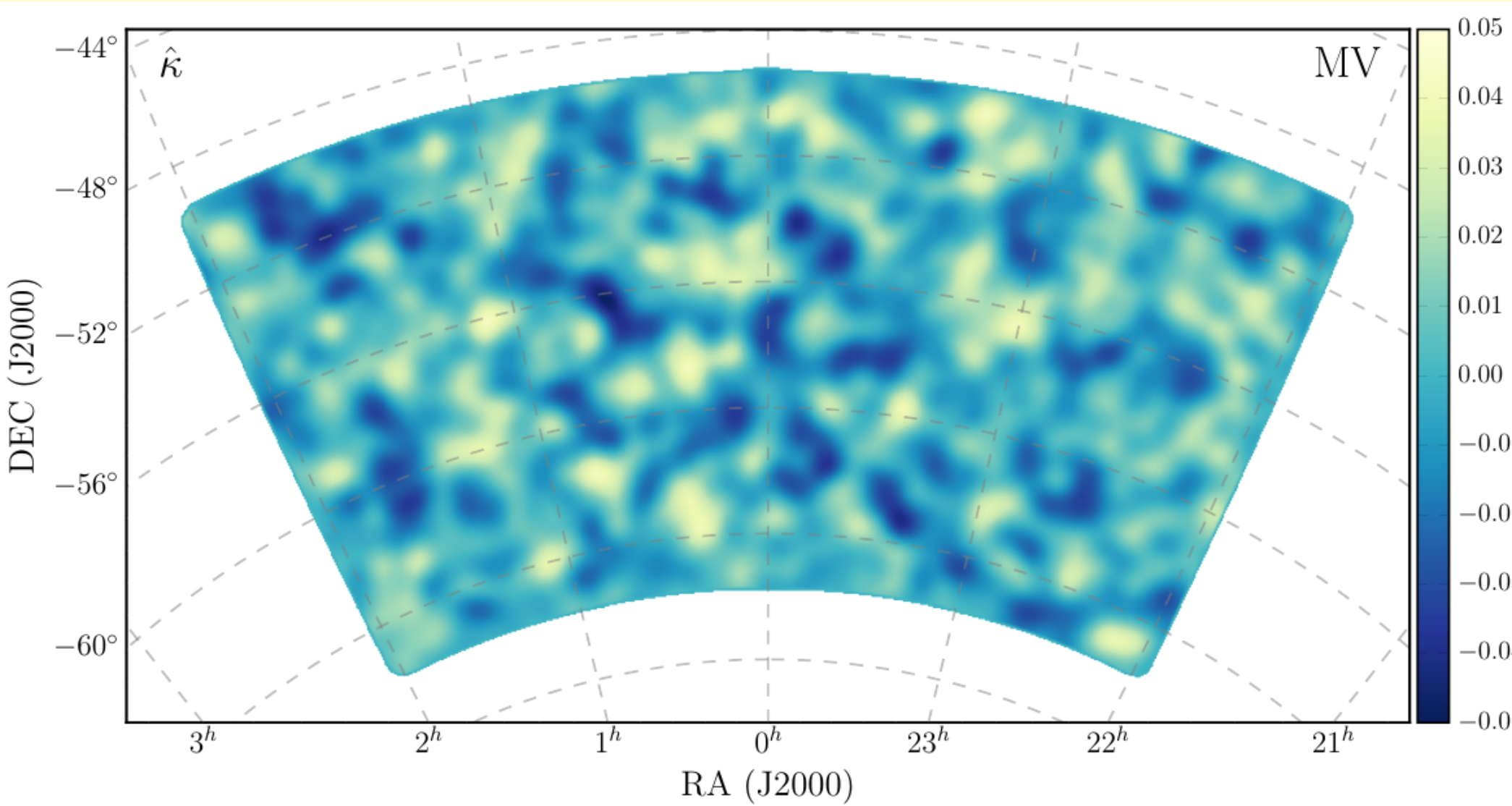

Convergence (*kappa*) map

[arXiv:1905.05777]

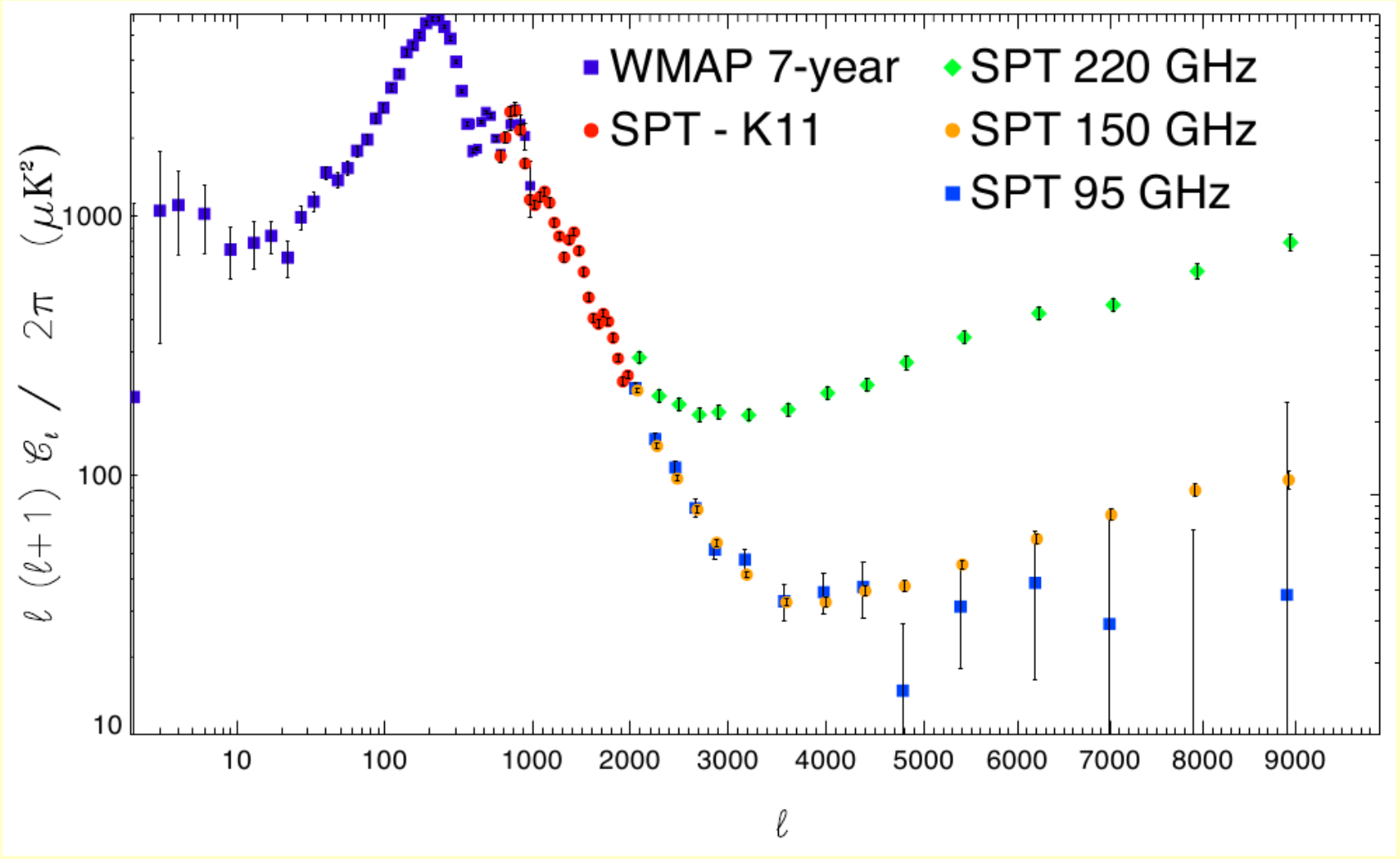

South Pole Telescope [Reichardt i in. (2011) arXiv:1111.0932] Anisotropy spectrum for high (l>3000). Strong synchrotron and infrared backgrounds imply dependence of the results on frequency used.

Secondary anizotropy

(iv) The Sunyaev-Zel'dovich (SZ) effect from hot gas in clusters is due to the first order correction for energy transfer in Thomson scattering. It is on the scale of galaxy clusters and superclusters, although it may be produced on very small scales by the first stars in the universe. There is a spectral distortion, energy being transferred from photons in the Rayleigh-Jeans tail of the cosmic blackbody radiation to the Wien tail.

(v) The kinetic Sunyaev-Zel'dovich effect is the Doppler effect due to the motion of hot gas in clusters that scatters the CMB. It causes no spectral distortion.

(vi) The Ostriker-Vishniac (OV linear) effect is also due to Doppler boosting. It is the linear version of the kinetic Sunyaev-Zel'dovich effect. It is proportional to the product of Δn_e and Δv,. This is effective on the scale of order 1 arc minute.

Secondary anisotrophy

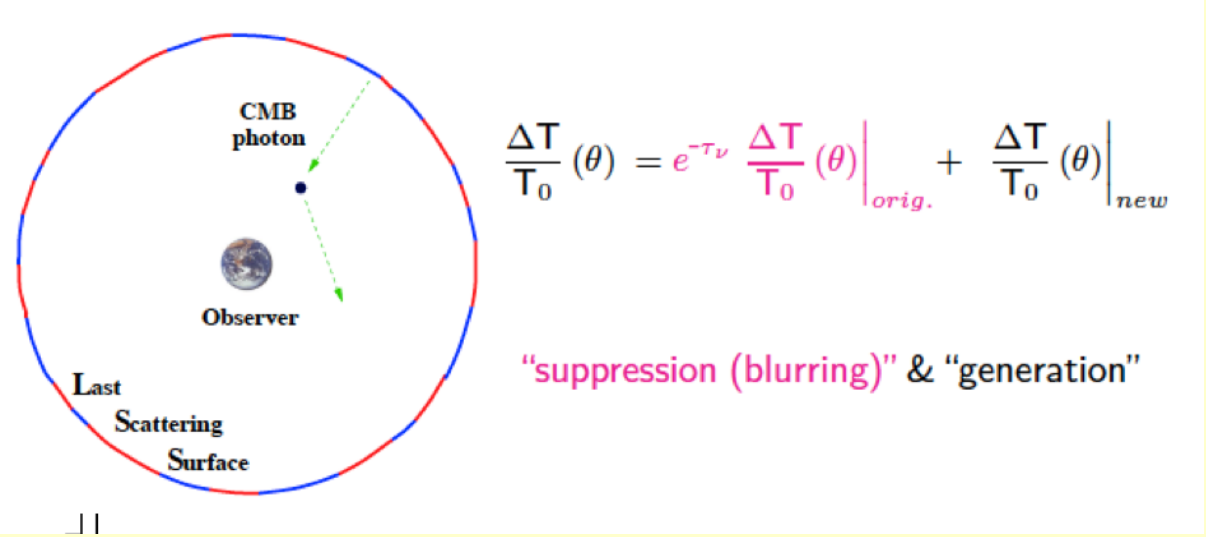

$$\frac{\Delta T}{T_0}(\theta) = e^{-\tau_\nu} \frac{\Delta T}{T_0}(\theta)\Big|_{orig.} + \frac{\Delta T}{T_0}(\theta)\Big|_{new}$$

"suppression (blurring)" & "generation"

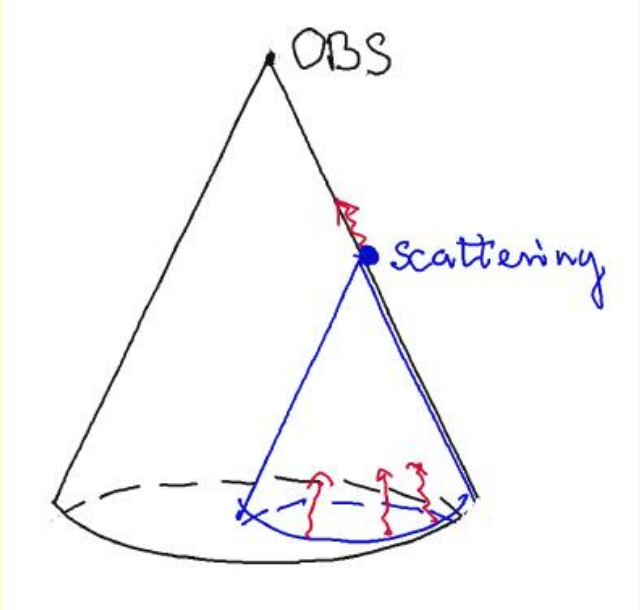

Electron scattering removes from the observed ray bundle a fraction of "primary" photons. Simultaneously "supplies" to the bundle "secondary" photons which were moving elsewhere. Scattering region "sees" photons from "its own" sphere of last scattering (which is placed inside our past cone, on the recombination hypersurface). The probability of scattering depends on polarization and direction, so the scaterred component is partially polarized.

Secondary anizotropy

$$\frac{d\sigma}{d\Omega} = r_e^2 \ \vec{n} \cdot \vec{n}'$$

$$\frac{d\sigma_\perp}{d\Omega} = \frac{1}{2} r_e^2$$

$$\frac{d\sigma_\parallel}{d\Omega} = \frac{1}{2} r_e^2 \ \cos^2 \chi$$

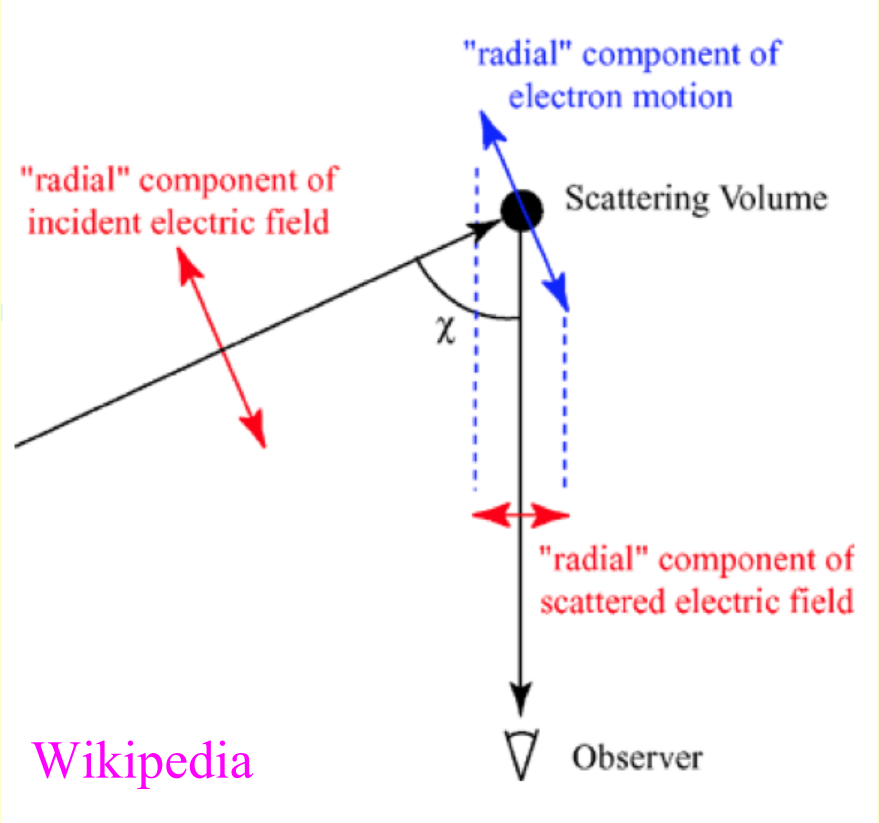

Vectors n, n' give the polarization direction before and after the scattering. For the polarization parallel to the scattering plane (defined by the paths of photon before and after) there is a dependence of the scattering probability on the scattering angle *chi*. For the perpendicular polarization there is no such dependence. (r_e is the classic electron radius, integration over the sphere would give the Thomson cross-section (8*pi/3)*r_e^2)

Sunyajev - Zeldovich (S-Z) effect

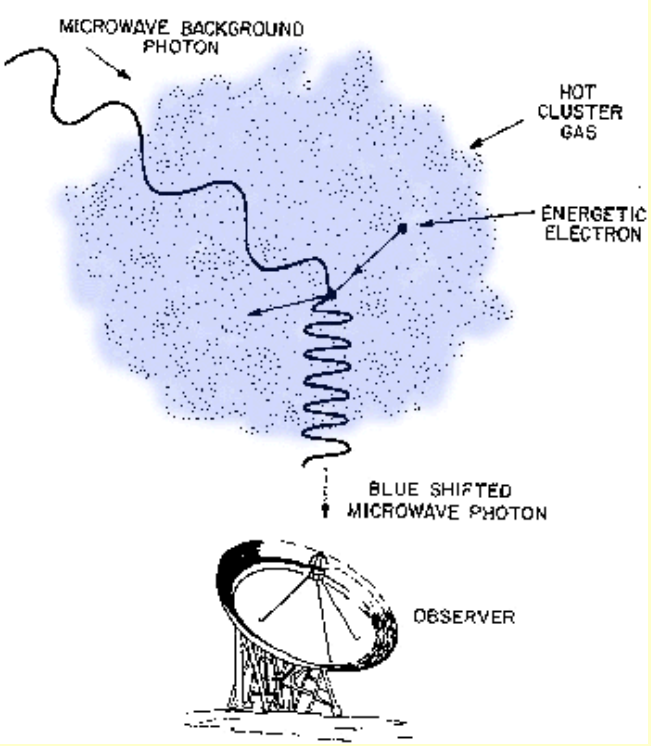

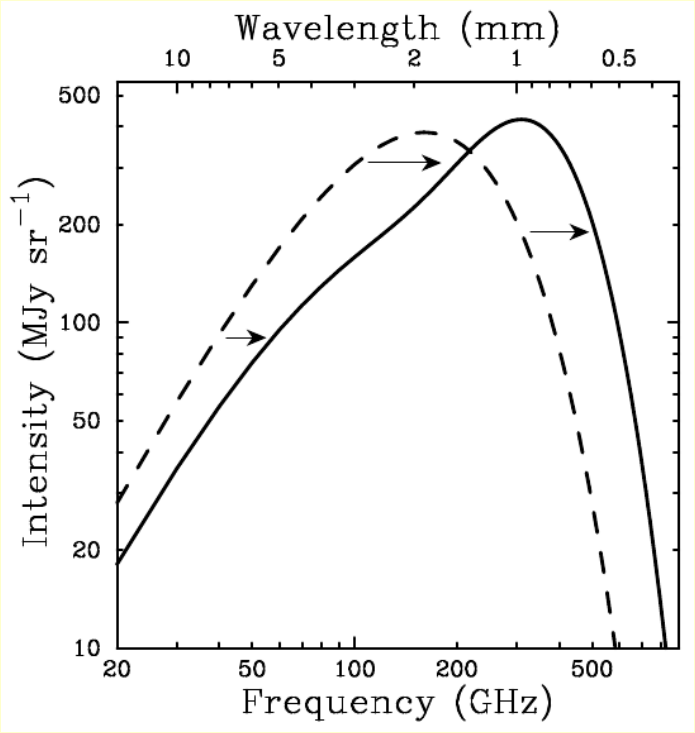

[Adapted from L. Van Speybroeck]

[Carlstrom i in. (2002) ARAA, 40, 643]

S-Z effect qualitatively: electrons in a ionized gas with kT~1 keV scatter photons to higher enrgy. The number of photons is conserved, the number of low energy photons (<218 GHz as measured today) is decreased and the number of high energy photons is increased. The energy spectrum of radiation is changed (picture on the right: exaggeration). For low frequencies the spectrum resembles the Rayleigh-Jeans spectrum of lower temperature.

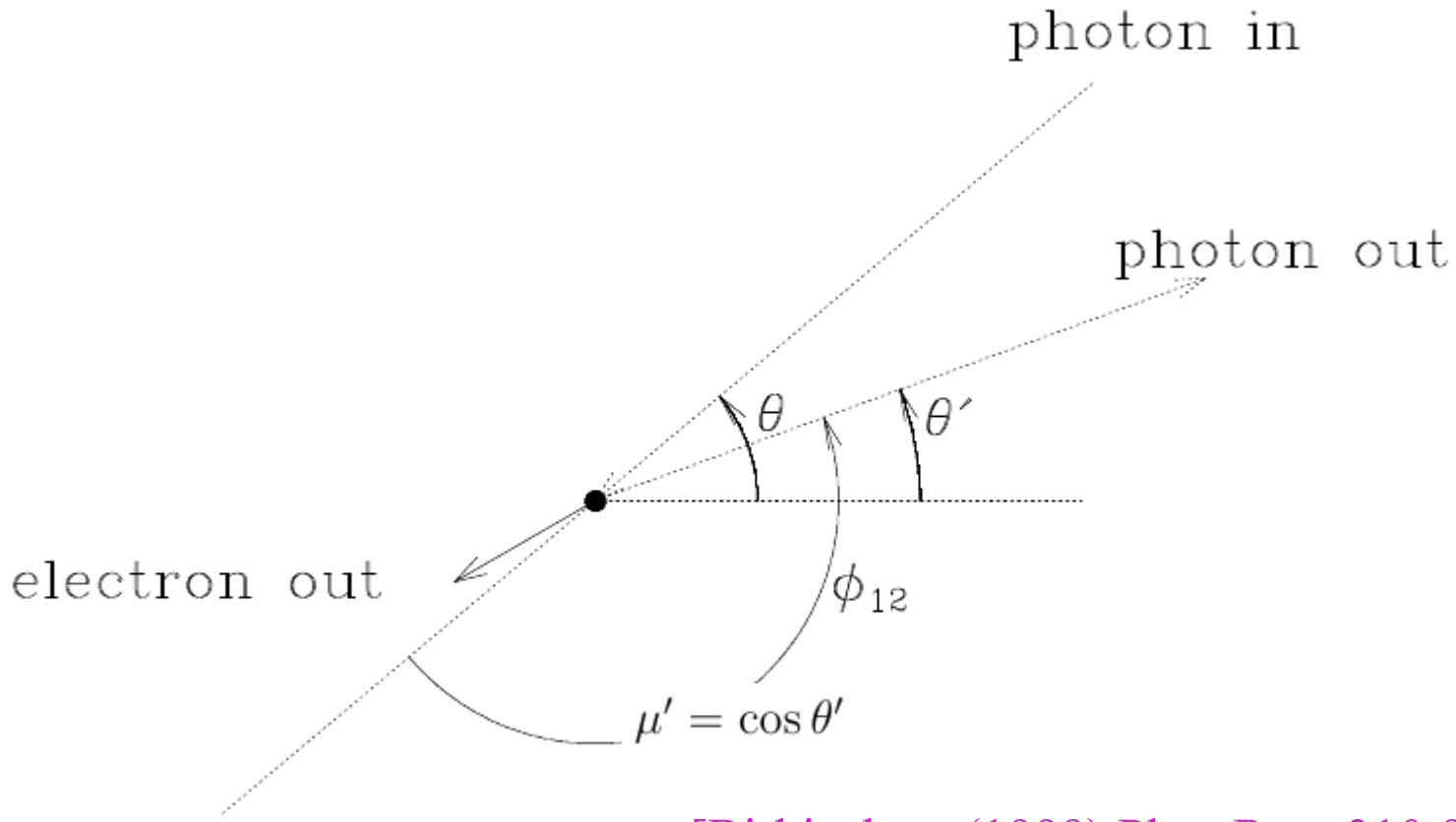

[Birkinshaw (1999) Phys.Rept.310:97-195]

Fig. 3.— The scattering geometry, in the frame of rest of the electron before the interaction.

$$\nu'' = \nu\,(1+\beta\mu')\,(1-\beta\mu)^{-1}$$

$v_e = \beta c$, and $\mu = \cos\theta$

$\mu' = \cos\theta'$

Single photon scattering. Electron moves to the right.

Thermal S-Z effect

- Electrons have a thermal energy distribution
- Scattering by electrons moving toward the observer are better visible: scattered photons have energies (1+kT_e/mc^2) times higher on average
- Scattering probability (<<1) is equal to the optical thickness:

$$\tau_{\rm e} \;=\; \int n_{\rm e}(\mathbf{r})\,\sigma_{\rm T}\,dl$$

- The characteristic parameter (measuring probability times relative energy change) is:

$$y \;=\; \int n_{\rm e}(\mathbf{r})\,\sigma_{\rm T}\,\frac{k_{\rm B}T_{\rm e}(\mathbf{r})}{m_{\rm e}c^2}\,dl$$

- For low frequencies the temperature changes by:

$$\Delta T_{\rm RJ} \;=\; -2\,y\,T_{\rm rad}$$

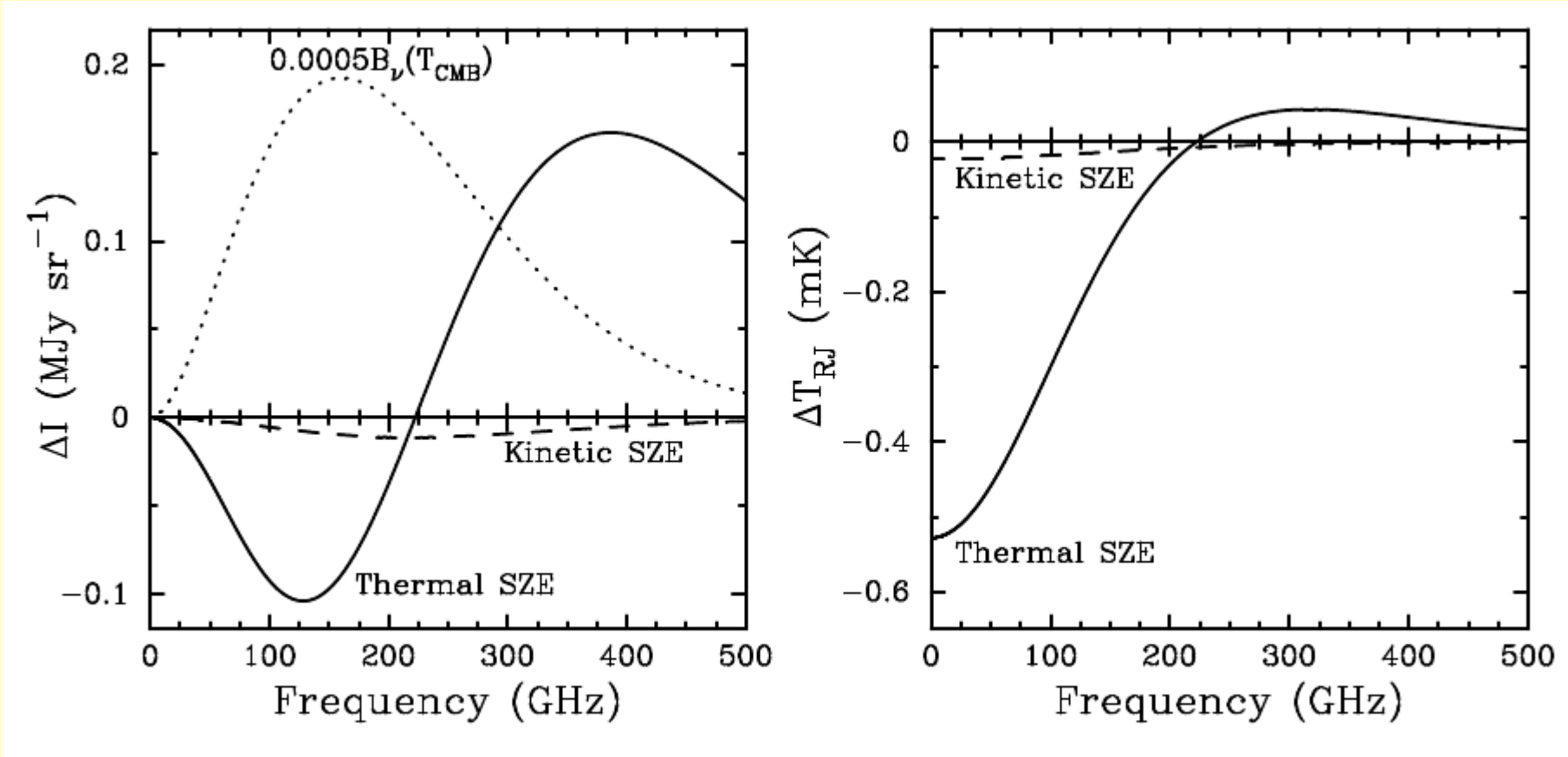

[Carlstrom i in. (2002) ARAA, 40, 643]

Change in intensity (on the left) and the RJ temperature (on the right) resulting from the S-Z effect.

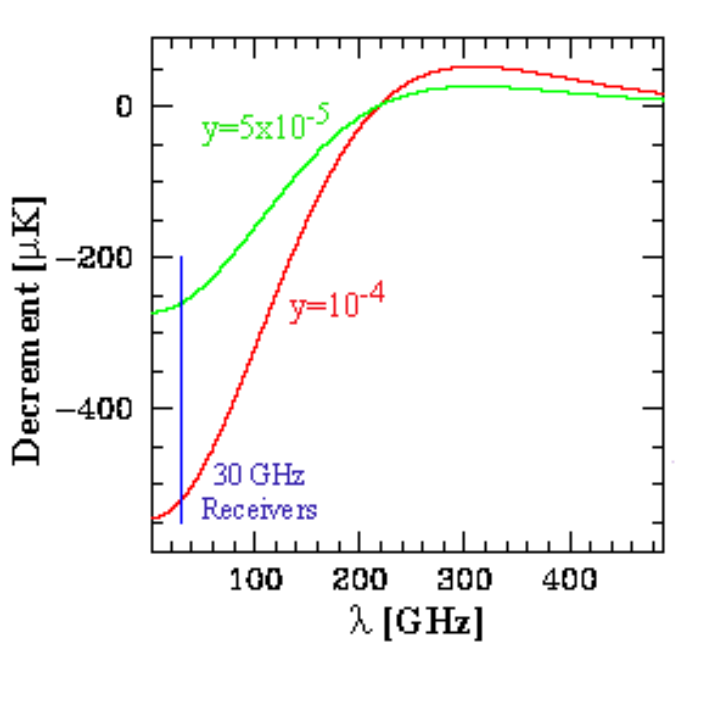

Change of the spectra (and RJ temperature) for two typical values of *y* parameter.

[http://astro.uchicago.edu/sza/primer.html]

The Atacama Cosmology Telescope: Component-separated maps of CMB temperature and the thermal Sunyaev-Zel'dovich effect

Mathew S. Madhavacheril,[1, 2, *] J. Colin Hill,[3, 4, 5] Sigurd Næss,[4] Graeme E. Addison,[6] Simone Aiola,[4]

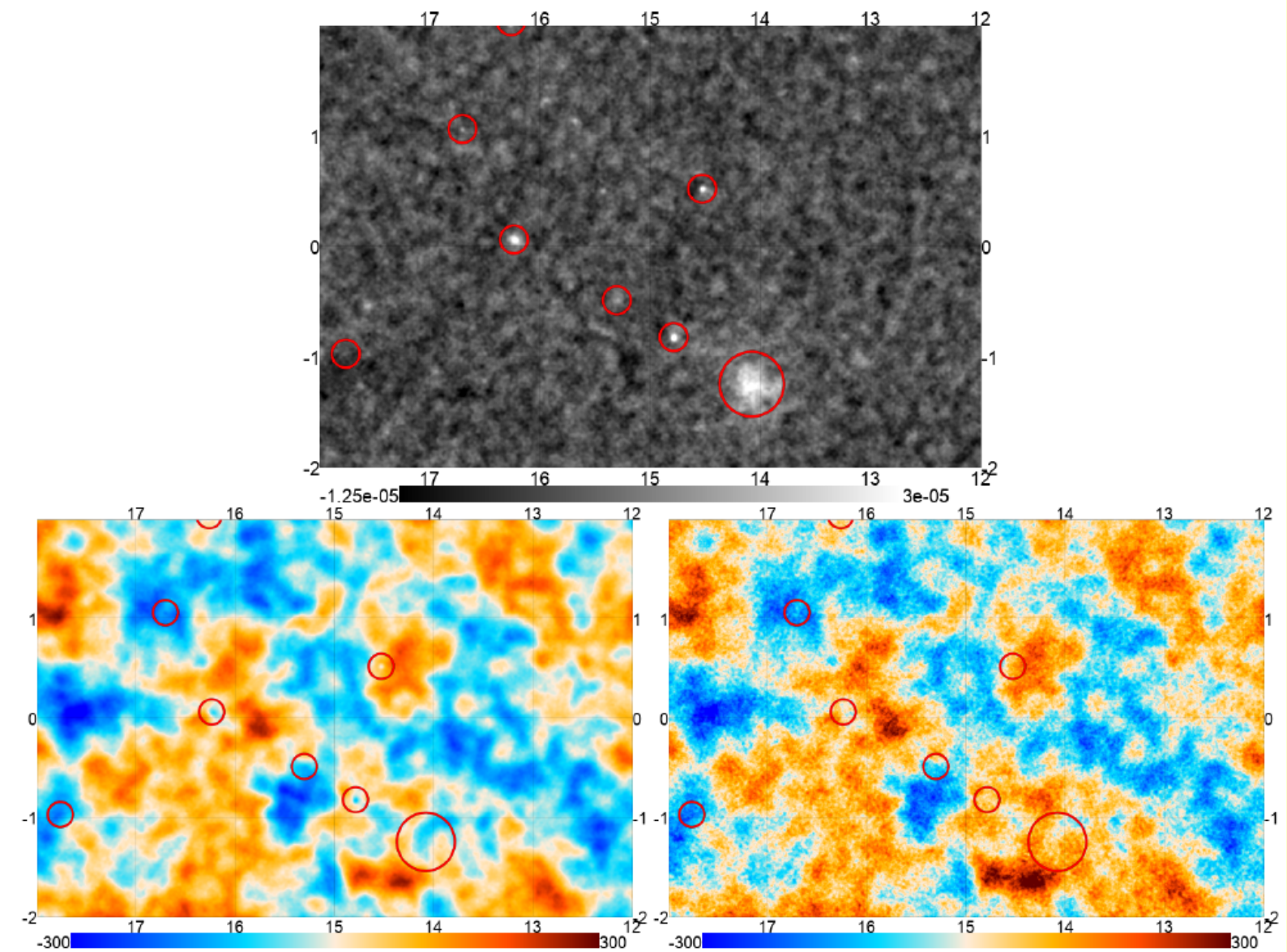

Top: *y*-parameter map. Left: temperature map: clusters correspond to cold spots. Right: S-Z effect removed at the cost of increased noise. [arXiv:1911.05717]

Kinematic S-Z effect

The peculiar velocities of galaxy clusters are typically ~few hundred km/s << c. CMB radiation from their directions contains a small part of scaterred component which is shifted due to the Doppler effect. That gives:

$$\frac{\Delta T_{SZE}}{T_{CMB}} = -\tau_e \left(\frac{v_{pec}}{c} \right)$$

The observed spectrum is a weighted sum of the primary radiation and a tiny scattered part. At 218 GHz the thermal S-Z effect is absent. At this frequency one can distinguish the kinematic S-Z effect.
(It may be applied to the measurement of the cluster peculiar velocity relative to the CMB frame.)

South Pole Telescope

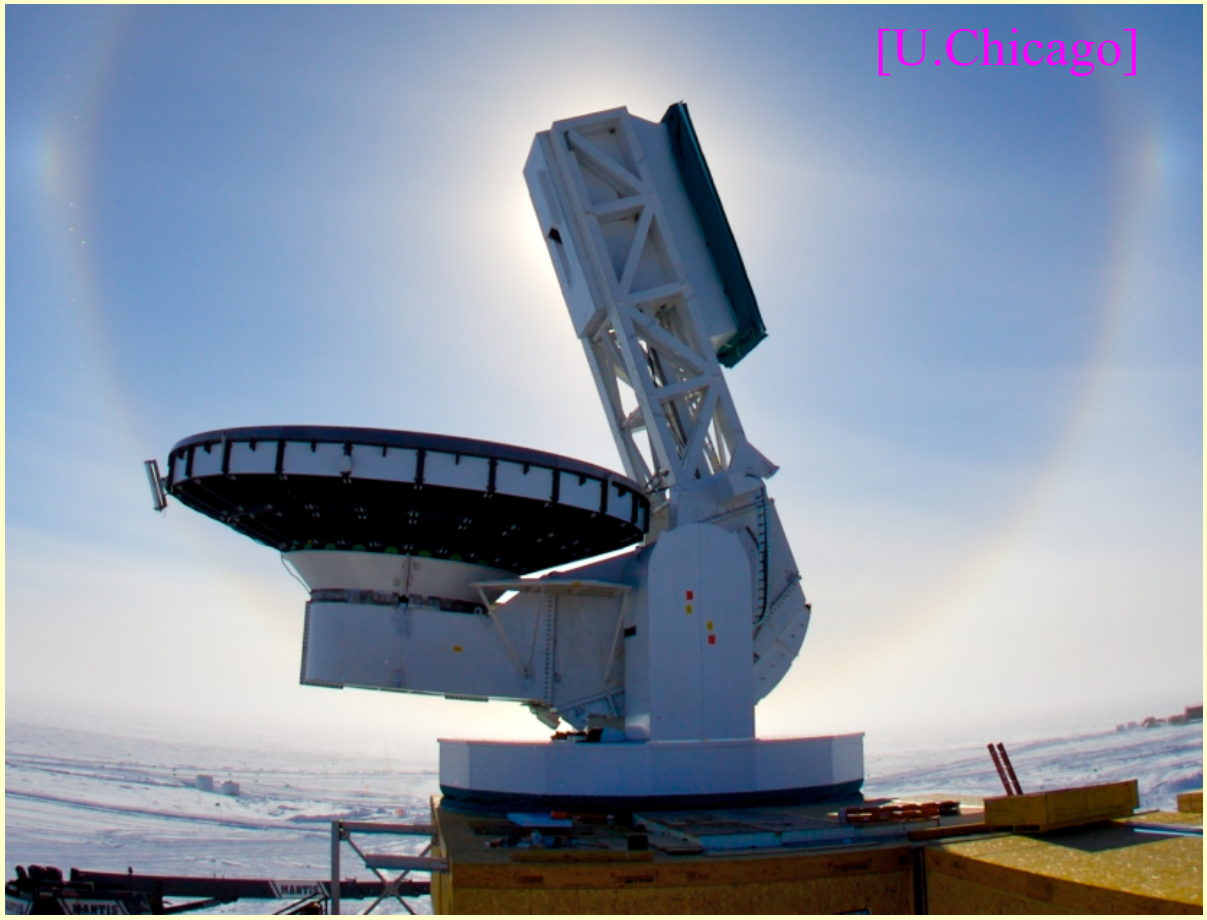

This paper presents a catalog of the 26 most significant SZ cluster detections in the full survey region. The catalog includes 14 clusters which have been previously identified and 12 that are new discoveries. These clusters were identified in fields observed to two differing noise depths: 1500 deg^2 at the final SPT survey depth of 18 μK-arcmin at 150 GHz, and 1000 deg^2 at a depth of 54 μK-arcmin. Clusters were selected on the basis of their SZ signal-to-noise ratio (S/N) in SPT maps, a quantity which has been demonstrated to correlate tightly with cluster mass. The S/N thresholds were chosen to achieve

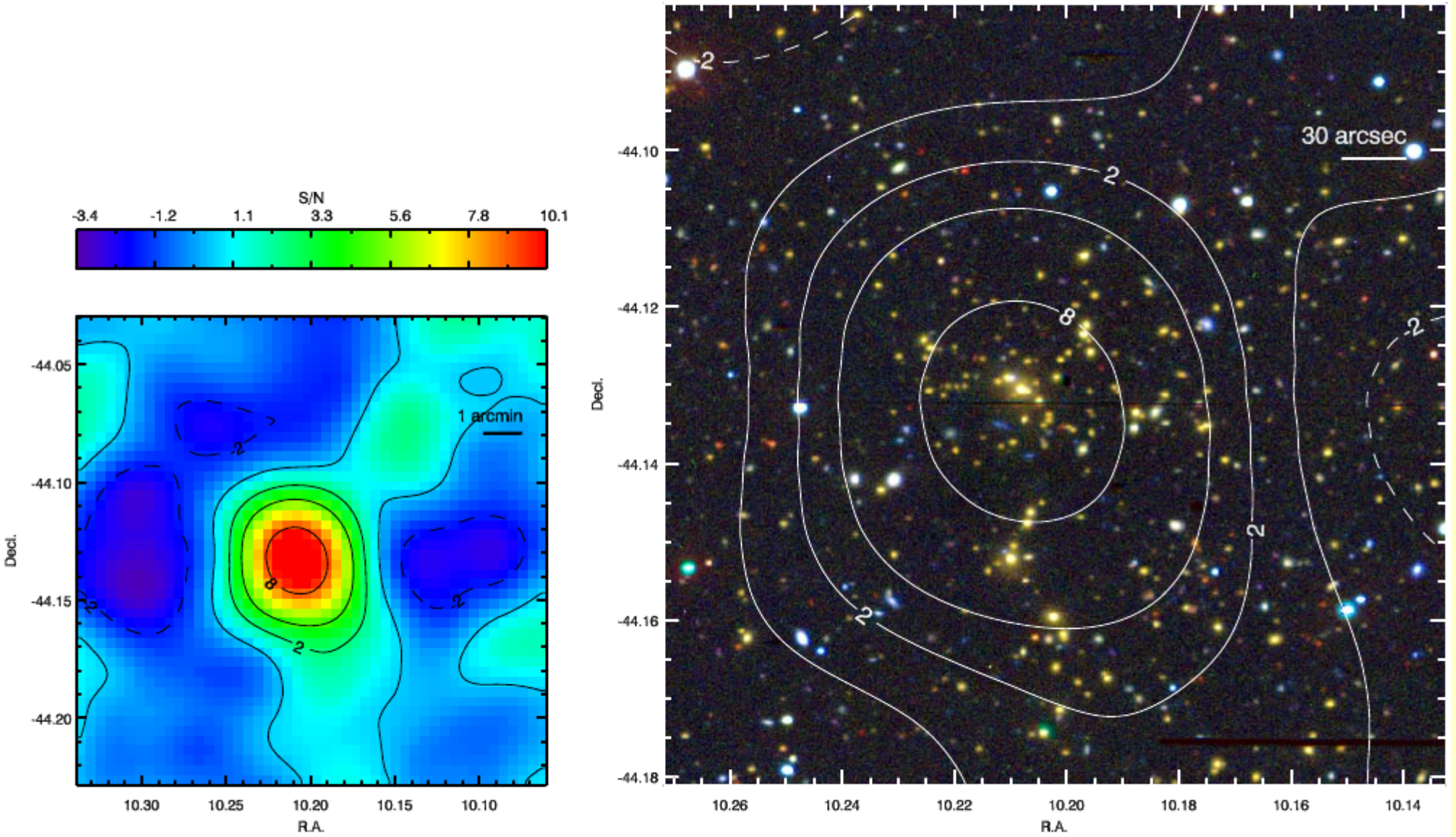

FIG. 6.— SPT-CL J0040-4407 at $z_{\rm rs} = 0.40$. Blanco/MOSAIC-II *irg* images are shown in the optical/infrared panel.

Pomiar temperatury CMB (po lewej) i odpowiadająca mu mapa opt-IR (po prawej).

["An SZ-selected sample of the most massive galaxy clusters in the 2500-square-degree South Pole Telescope survey" Williamson i in. (2011) arXiv:1101.1290]

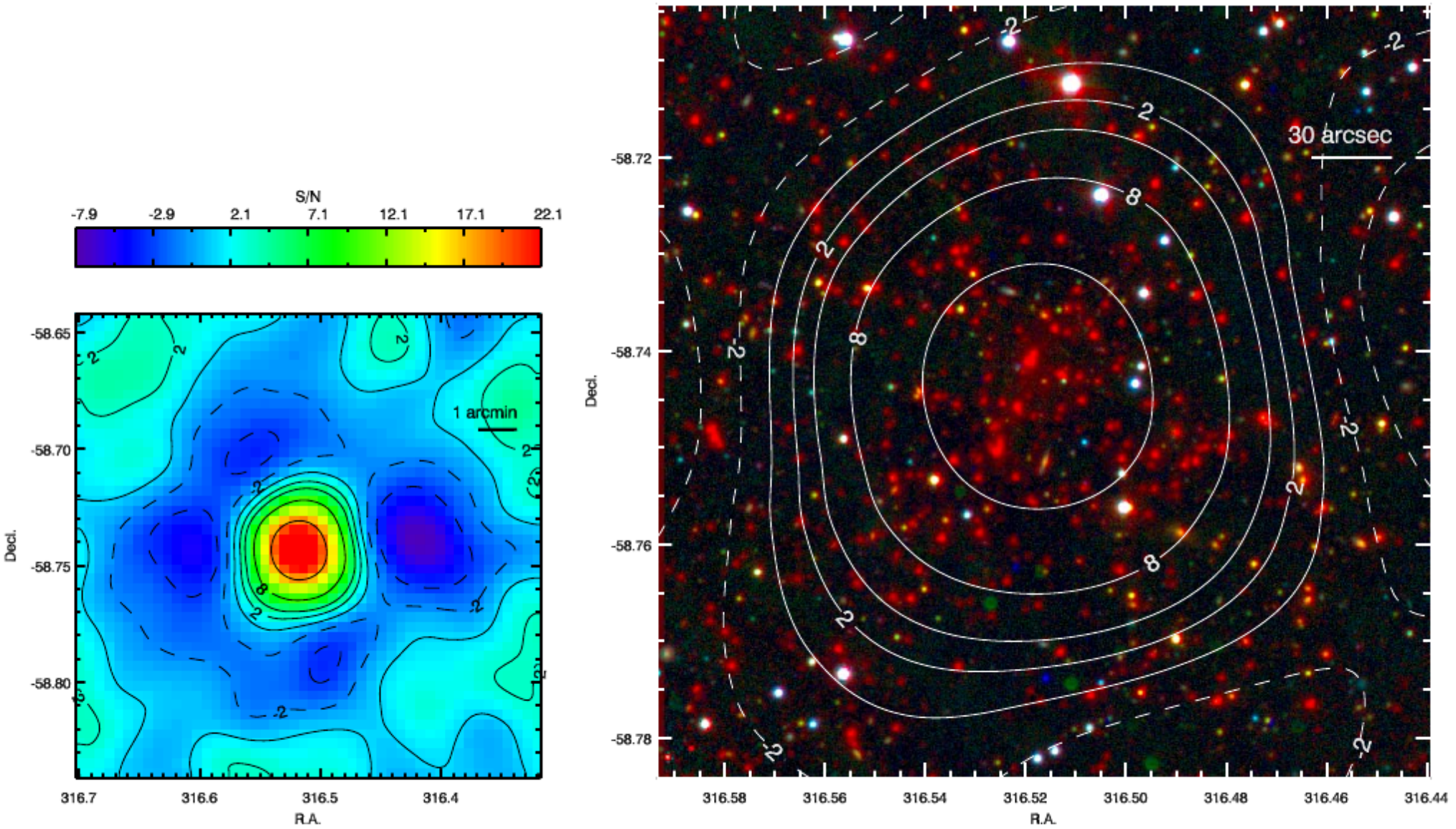

FIG. 26.— SPT-CL J2106-5844 at $z_{\rm spec} = 1.133$. Spitzer/IRAC [3.6] and Magellan/LDSS3 *ig* images are shown in the optical/infrared panel.

Pomiar temperatury CMB (po lewej) i odpowiadająca mu mapa opt-IR (po prawej).

["An SZ-selected sample of the most massive galaxy clusters in the 2500-square-degree South Pole Telescope survey" Williamson i in. (2011) arXiv:1101.1290]

Influence of re-ionization

CMB scatters on ionized gas. If the gas moves along LOS the Doppler effect changes the observed temperature of the scattered radiation:

$$\frac{\Delta T}{T}(\vec{\theta}) = -\int c dt\ \sigma_T\ n_e(\vec{\theta}, t)\ e^{-\tau(\vec{\theta},t)}\ \frac{v_r(\vec{\theta}, t)}{c} \tag{1}$$

$$n_e(\vec{\theta}, t) = n(\vec{\theta}, t) \times \chi_e(\vec{\theta}, t) \tag{2}$$

$$n_e(\vec{\theta}, t) = \langle n_e \rangle (t)(1 + \delta + \delta_\chi) \tag{3}$$

There are two 2$^{\text{nd}}$ order contributions to the integral: the product of velocity and density fluctuations and the product of velocity and ionization degree fluctuations

Influence of plasma inhomogeneity

In a fully ionized plasma both density fluctuations and their peculiar velocities play roles, the effect ~ *delta*^2. In thids order it is also called Ostrikr-Vishniac effect (OV). Taking into account nonlinear, gravitationally bound structures is called kinematic Synyaev-Zeldovich (KSZ) effect and is important for small angular scales

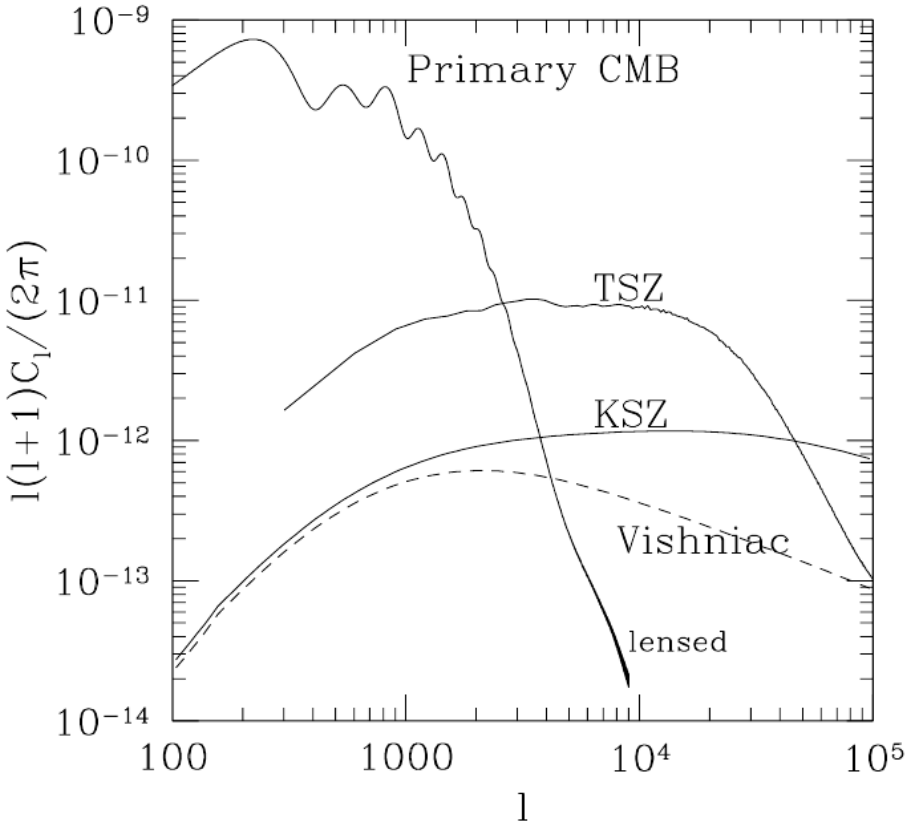

Zhang, Pen & Trac (2004):

Influence of the ionization degree

The problem is not appropriate for analytic estimates: re-ionization is a strongly non-linear process with a feedback. Simulations allow to estimate the CMB anisotropy

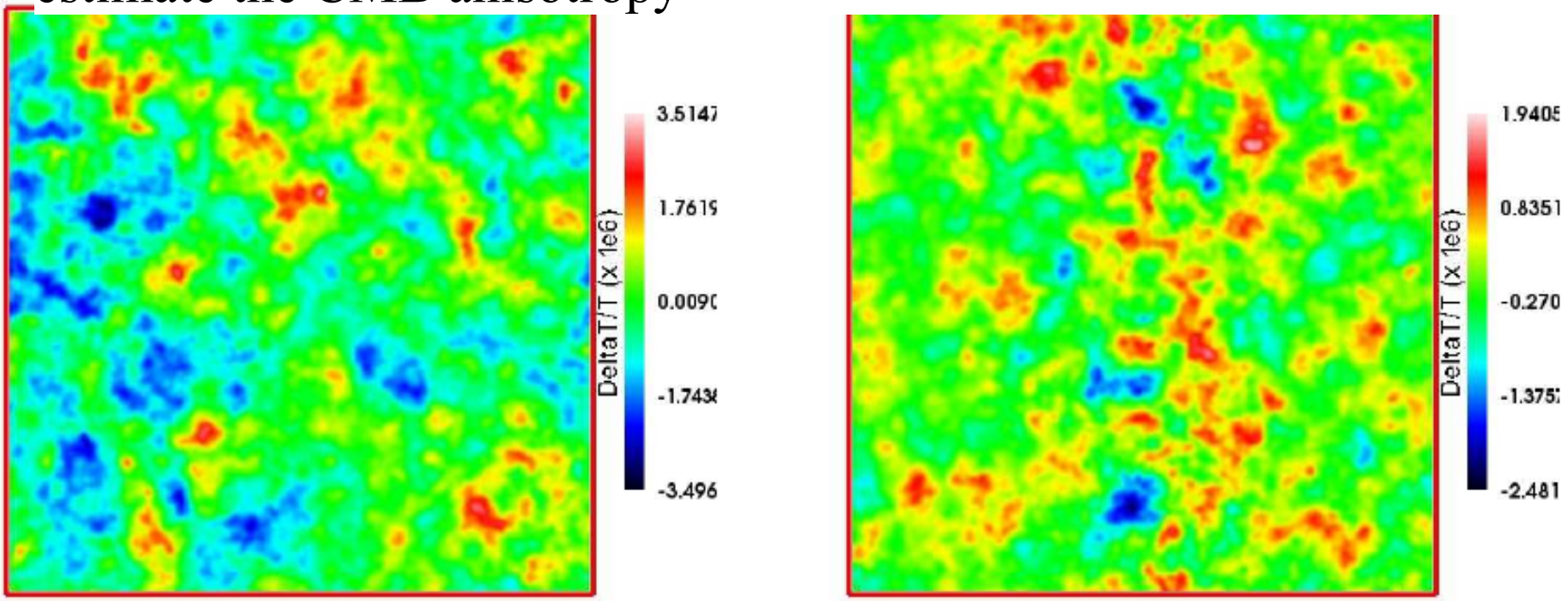

Figure 4. From Iliev et al. (2007b): Doppler effect induced temperature fluctuation maps from numerical simulations including radiative transfer (right panel). The left panel shows the result after correcting for the missing large-scale velocities.

Tertiary anizotropy

(vii) Discrete sources provide an appreciable foreground, especially at lower frequencies for radio sources and high frequencies for infra-red and submillimetre sources.

(viii) Polarisation is primarily a secondary phenomenon. The primary effect from last scattering is induced by out-of-phase velocity perturbations and provides evidence for the acausal nature of the fluctuations. The secondary polarisation is associated with the reionisation of the universe and is on large scales corresponding to the horizon at reionisation. Inhomogeneous reionisation and scattering at the galaxy cluster scale leads to smaller scale polarisation. The reionisation signal is weak, amounting to no more than 10 percent of the primary signal.

(ix) B-mode polarisation can be induced by shear perturbations. One source is gravitational lensing of primary CMB fluctuations. A second is relic gravity waves from inflation. These are pure B-modes, and fall off rapidly on scales smaller than the horizon at recombination, corresponding to about half a degree. Mixing by Faraday rotation in the intracluster medium also contributes to B-mode generation on small angular scales. The B-mode polarisation amplitude only amounts to about a percent of the primary signal, and its discovery will pose the major challenge for future experiments.

Problem: promieniowanie źródeł astronomicznych

(CMB Task Force Report)

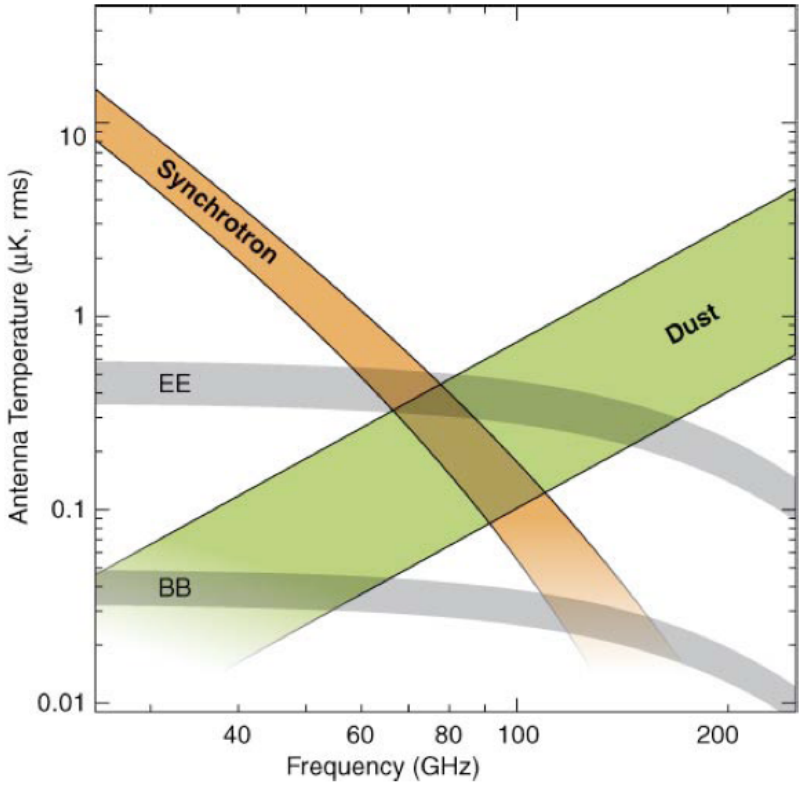

RMS fluctuations in the polarized CMB and foreground signals as function of frequency

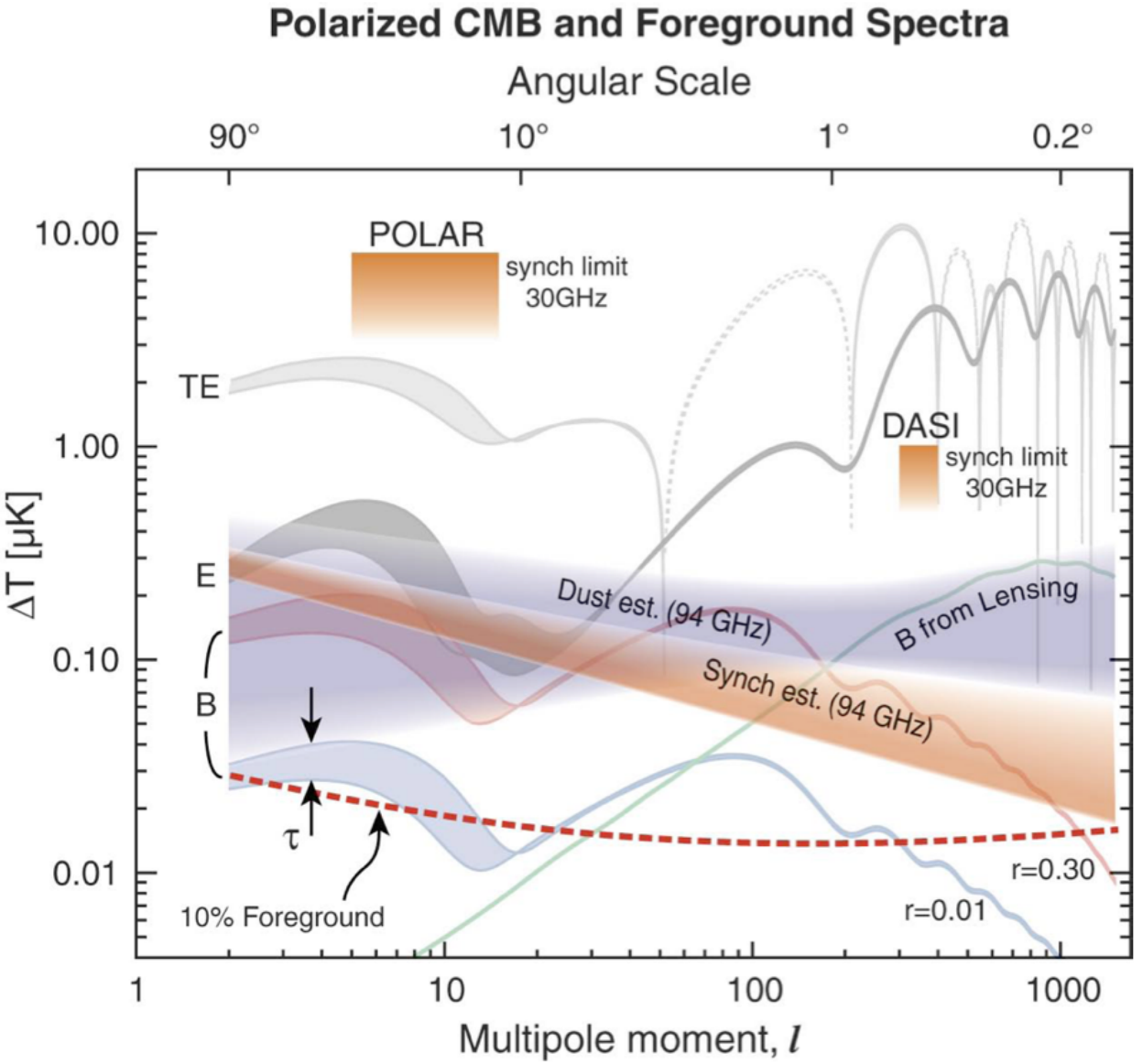

Few pictures

Interferometers

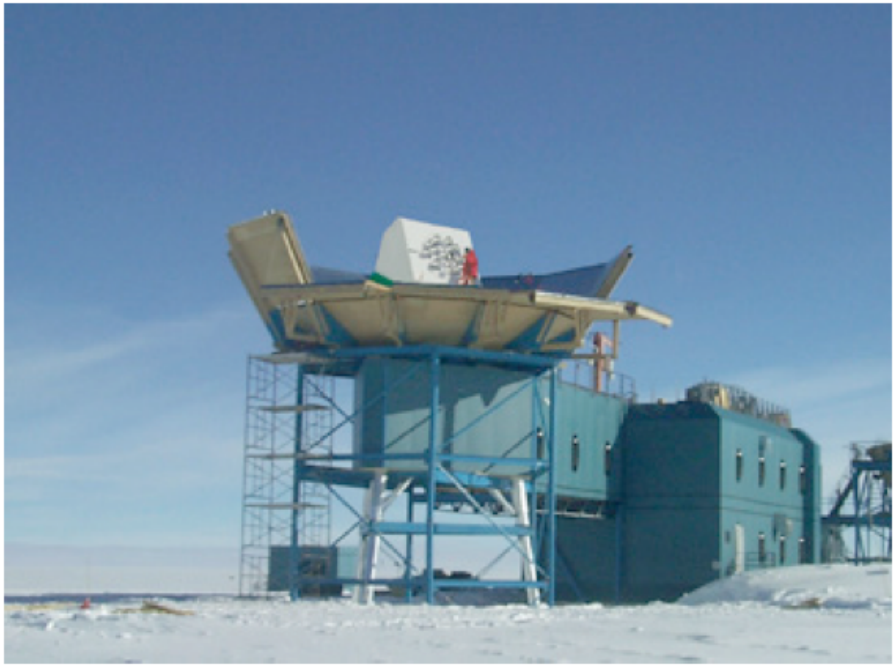

DASI in South Pole

CBI in Atacama desert

Few pictures

Bolometer experiments

ACBAR

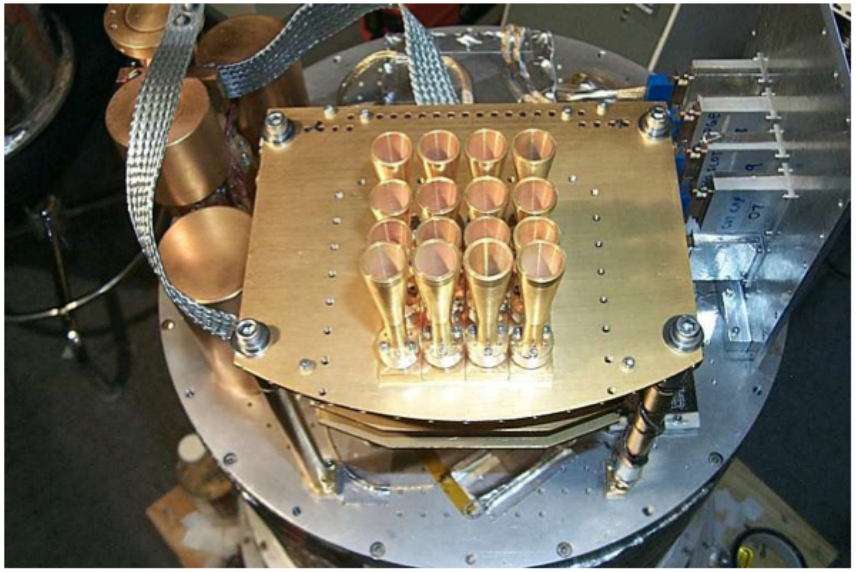

Boomerang